Phil. Trans. R. Soc. Lond. B **298**, 309–354 (1982) [309]
Printed in Great Britain

THE BRAIN OF THE HONEYBEE *APIS MELLIFERA*. I. THE CONNECTIONS AND SPATIAL ORGANIZATION OF THE MUSHROOM BODIES

BY P. G. MOBBS

Department of Zoology and Comparative Physiology, Queen Mary College, Mile End Road, London E1 4NS, U.K.

(*Communicated by J. Z. Young, F.R.S.* – *Received* 23 *October* 1981)

[Plates 1–11]

CONTENTS

The mushroom bodies of the bee are paired neuropils in the dorsal part of the brain. Each is composed of the arborizations of over 17×10^4 small interneurons of similar architecture called Kenyon cells. Golgi staining demonstrates that these neurons can be divided into five groups distinguished on the basis of their dendritic specializations and geometry.

The mushroom body neuropils each consist of a pair of cup-shaped structures, the calyces, connected by two short fused stalks, the pedunculus, to two lobes, the α- and β-lobes. Each calyx is formed from three concentric neuropil zones, the basal ring, the collar and the lip. The calyces are organized in a polar fashion; within the calyces each of the five categories of Kenyon cell has a distribution limited to particular polar contours. The dendritic volumes of neighbouring Kenyon cells arborizing within each individual contour are greatly overlapped. Fibres from groups of neighbouring cells within a calycal contour are gathered into bundles that project into the pedunculus, each fibre dividing to enter both the α- and β-lobes. The pedunculus and the lobes are conspicuously layered. Kenyon cells with neighbouring dendritic fields within the same calycal contour occupy a single layer in the pedunculus and lobes. Thus the two-polar organization of the calyces is transformed into a Cartesian map within the pedunculus, which continues into the α- and β-lobes.

The calyx receives input fibres from both the antennal lobes and the optic neuropils. The branching patterns of these cells reflect the polar organization of the calyces as their terminals are restricted to one or more of the three gross compartments of the calycal neuropil. The course of these tracts and the morphologies of the fibres that they contain are described.

Cells considered to represent outputs from the mushroom bodies arborize in the pedunculus and α- and β-lobes. Generally the arborizations of the output neurons reflect the layered organization of these neuropils. Fibres from the two lobes run to the anterior median and lateral protocerebral neuropil, and the anterior optic tubercle. Additionally there is an extensive network of feedback interneurons that inter-

connect the α- and β-lobes with the ipsi- and contralateral calyces. Many individual neurons have branches in both the α- and the β-lobes and in the pedunculus. The pathways and geometries of the fibres subserving the two lobes are described. The hypothesis of Vowles (1955) that the individual lobes represent a separation of sensory and motor output areas is shown to be incorrect.

The anatomy of the bee's mushroom bodies suggests that they process second-order antennal and fourth- and higher-order visual information. The feedback pathways are discussed as possible means of creating long-lasting after-effects which may be important in complex timing processes and possibly the formation of short-term memory.

1. Introduction

The mushroom bodies or corpora pedunculata are structures found in all insect brains so far examined, and have also been described in many Crustacea and Annelida. The mushroom bodies were the first internal division of the insect brain neuropil to be distinguished. Dujardin (1850) in his 'Mémoire sur le système nerveux des insects' compared them, because of their lobula and folded appearance, to the convoluted surface of the human brain. He regarded them as the 'corps d'intelligence' of the insect.

In most insects the mushroom bodies are paired structures lying on either side of the brain's midline, occupying a large part of the protocerebral volume. The mushroom bodies consist of three major divisions; an upper cup-shaped part called the calyx, a stalk or pedunculus, and the lobes. The lobes represent either a bipartite or a tripartite division of the pedunculus, and are referred to as the α-, β-, and γ-lobes. Of insects with γ-lobes so far examined, only flies (Strausfeld 1976) and moths (Pearson 1971) have been described in detail. Each body consists of the compacted arborizations of many thousands of similar interneurons called Kenyon cells (K cells) after their discoverer (Kenyon 1896), which have their dendrites in the calyces, and single long projection fibres that run through the pedunculus and then divide sending a branch forward into the α-lobe and ventrally into the β-lobe. Kenyon pointed to an apparent similarity between the dendritic geometry of the K cells and the Purkinje cells of the vertebrate cerebellum. Such a comparison has also been suggested by Strausfeld (1976) and Schürmann (1974).

There is a considerable volume of literature concerning the anatomy, physiology and control of behaviour associated with the corpora pedunculata. This wealth of detail is available because of the conjecture that surrounded the association of these neuropils with 'intelligence' or the complexity of instinctive behaviours. Stimulation experiments (Huber 1955, 1959; Rowell 1963*a*; Elsner & Huber 1969; Otto 1971; Wadepuhl & Huber 1979) reveal that current injected into various areas in and around the mushroom bodies can result in the production of entire and complex motor patterns, suggesting the possibility that the bodies select and coordinate these patterns. Lesions in the area of the calyces (Howse 1974) produce the apparent disinhibition of competitive reflexes, results interpreted as supporting the hypothesis that the mushroom bodies are responsible for the selection of motor patterns and their assembly into behavioural sequences.

Anatomical investigations have produced widely different pictures of the connections and possible functions of the mushroom bodies. Vowles (1955), in common with Kenyon (1896), shows connections of the optic lobes and the antennal lobes with the calyces of the bee. Weiss (1974), however, concluded from a detailed examination of the cockroach brain that the mushroom bodies are centres for the processing of olfactory and gustatory inputs alone, a view supported by the studies of the fly by Strausfeld (1976) and of the locust and cockroach by Ernst *et al.* (1977). Howse (1974), in a study of the relative volumes of the mushroom bodies in

different insect species, suggests that insects with highly developed visual memories have rather different calycal structure to those that do not. He points out that certain regions of the calycal wall are well developed in species such as the cockroach and that these areas are subserved by olfactory and gustatory inputs. In contrast, he suggests, in the social and subsocial Hymenoptera that have visual and olfactory memories, calycal areas associated with visual inputs are well developed. From Howse's work it would appear reasonable to suggest that the different reports concerning the nature of the connections of the mushroom bodies may simply be related to the primarily olfactory role of these neuropils in some insects and the additional visually mediated memory present in others. The possible association of olfactory memory in Hymenoptera with the mushroom bodies has been demonstrated by Menzel *et al.* (1974) and Erber *et al.* (1980) in a series of intriguing experiments that utilized miniature cooling probes to interfere with the memory storage process. The existing accounts of the structure of insect mushroom bodies suggest that the bee calyx may differ in its neuroanatomy from that of locusts and crickets.

In his study of the bee brain Vowles (1955) described numerous tracts that connect the corpora pedunculata to other brain regions that he defined as either sensory or motor areas. On the basis of his study of the projections of tracts to and from the calyces and lobes, Vowles developed a model of mushroom body function in which the calyces represent regions of multimodal input and integration and the lobes are zones from which the output is disseminated. Schürmann (1970, 1972, 1973, 1974) has performed elegant electron microscope analyses of the synaptic organization of the mushroom bodies of crickets and bees. His results confirm Vowles's (1955) suggestion that the calyces largely represent an input area while the α- and β-lobes are outputs. Vowles suggested that the α-lobe is concerned mainly with cells sampling activity across the lobe and projecting to sensory regions while the β-lobe has motor and premotor associations in which extrinsic fibres sample activity in small, closely associated bundles of Kenyon neurons. He suggested that such a system of connections may represent a feedback loop in which the state of implementation of motor activity is relayed back from the α-lobe to sensory neuropils which pass corrective signals into the calyx altering or 'remedying' the error in the output. In such a feedback system the mushroom bodies would also be responsible for the selection and control of behaviours, as suggested by Huber's (1959, 1960) experiments. Vowles's claim that the α-lobe has sensory connections and the β-lobe motor connections has not been supported by Goll (1967) or Pearson (1971), who could not demonstrate such specific associations in the ant and the sphinx moth respectively.

Weiss (1974), incidentally to his anatomical study, laid down rigorous criteria for the analysis of fibre tracts and connections. He suggested that earlier descriptions of the connections of the corpora pedunculata failed to demonstrate the penetration of fibres into the structures that they were purported to connect.

The account presented here attempts to describe the three-dimensional organization of the mushroom bodies in the bee in relation to the geometries of their constituent neurons. The α and β lobes and the connections of the calyces are re-examined on the basis of the criterion that actual penetration of fibres into the neuropils concerned must be demonstrated. The possible functional roles of the mushroom bodies of the bee are considered in relation to their structure, connections and known physiology, and evidence drawn from the locust and the cricket as well as the bee is presented supporting the view that the mushroom bodies are involved in timing

operations that may be important in the formation of behavioural sequences. In the bee the possible role of the structures is discussed in relation to the formation of memory.

2. Methods

Worker bees were captured at the hive entrance and decapitated, and a small window was cut over the brain, between the antennae, the compound eyes and the ocelli. Then either whole heads were fixed in alcoholic Bouin solution (after the technique of Gregory (1970)) or the mouthparts were removed and the upper part of the head was dropped into one of the Golgi mixtures described below.

Bouin-fixed material was embedded in wax by a rapid schedule similar to that described by Weiss (1972). Sections, 10 μm in thickness, were cut from the blocks in the three major planes, vertical, horizontal and sagittal (see figure 1). The sections were then stained either by the Rowell (1963*b*) lutidine–silver stain at pH 8.5 or by Gregory's modification of the Bodian technique. Neither method produced consistent results despite considerable care to standardize procedures. For the Bodian method this may have been caused by the use of different Protargols owing to difficulty in obtaining any particular brand or by inconsistencies in the composition of the fixative (see Gregory 1980). Both techniques are capable of good results, although the excellence of some Bodian preparations made this the method of choice.

For Golgi staining the Colonnier modification of the Golgi rapid method was used (Colonnier 1964). Head capsules were immersed in a 1:3 mixture of electron microscope grade 25 % glutaraldehyde with 2.5 % potassium dichromate solution. After 1 week the material was transferred to 0.75 % silver nitrate solution for 1 day or until such time as it was to be dehydrated and embedded in Epon–Araldite (Taab Laboratories).

The Kopsch (1896) method which utilizes formaldehyde in place of glutaraldehyde did not produce the consistent impregnations free from artefactual precipitates that the Colonnier method did. In contrast, however, Kenyon's (1896) modification of the Kopsch technique, employing 5 % potassium dichromate in a 4:1 ratio with formaldehyde, produced a number of useful preparations marred only by occasional light specklings of precipitate within the blocks.

A fourth Golgi technique (Ribi 1976) was also employed. Heads were fixed in 2.5 % glutaraldehyde and 2 % paraformaldehyde in Millonig's phosphate buffer (pH 7.2) at 4 °C for 4 h. They were then transferred to a solution containing 1 % osmium tetroxide, 2 % potassium dichromate and 2 % D-glucose, titrated with potassium hydroxide to pH 7.2, and post-fixed in the dark at room temperature for up to 24 h. Finally the preparations were placed in 0.75 % silver nitrate solution for 1 or 2 days. This technique proved particularly powerful for, in contrast to other methods, it often impregnates small numbers of large fibres, sometimes delineating their entire course. The Colonnier and Kopsch techniques, while usually impregnating many small-diameter fibres in their entirety, seldom stain large cells and if such neurons are stained they are usually only partially impregnated. As a result of the probablistic nature of the Golgi process and the tendency to stain some neurons partially it was found necessary to examine very large numbers of preparations and relate the results of non-random staining techniques such as Bodian silver and Wigglesworth ethyl gallate to the fibre patterns and pathways revealed by Golgi impregnation.

To produce Araldite blocks to be cut at thicknesses of 50 μm or more it was necessary to pass

the heads through an ascending series of resin–propylene dioxide solutions over a period of not less than 3 days. A number of resins were tried, the most successful of which was TAAB (TAAB Laboratories). Large blocks were produced which were clamped directly in the chuck of a

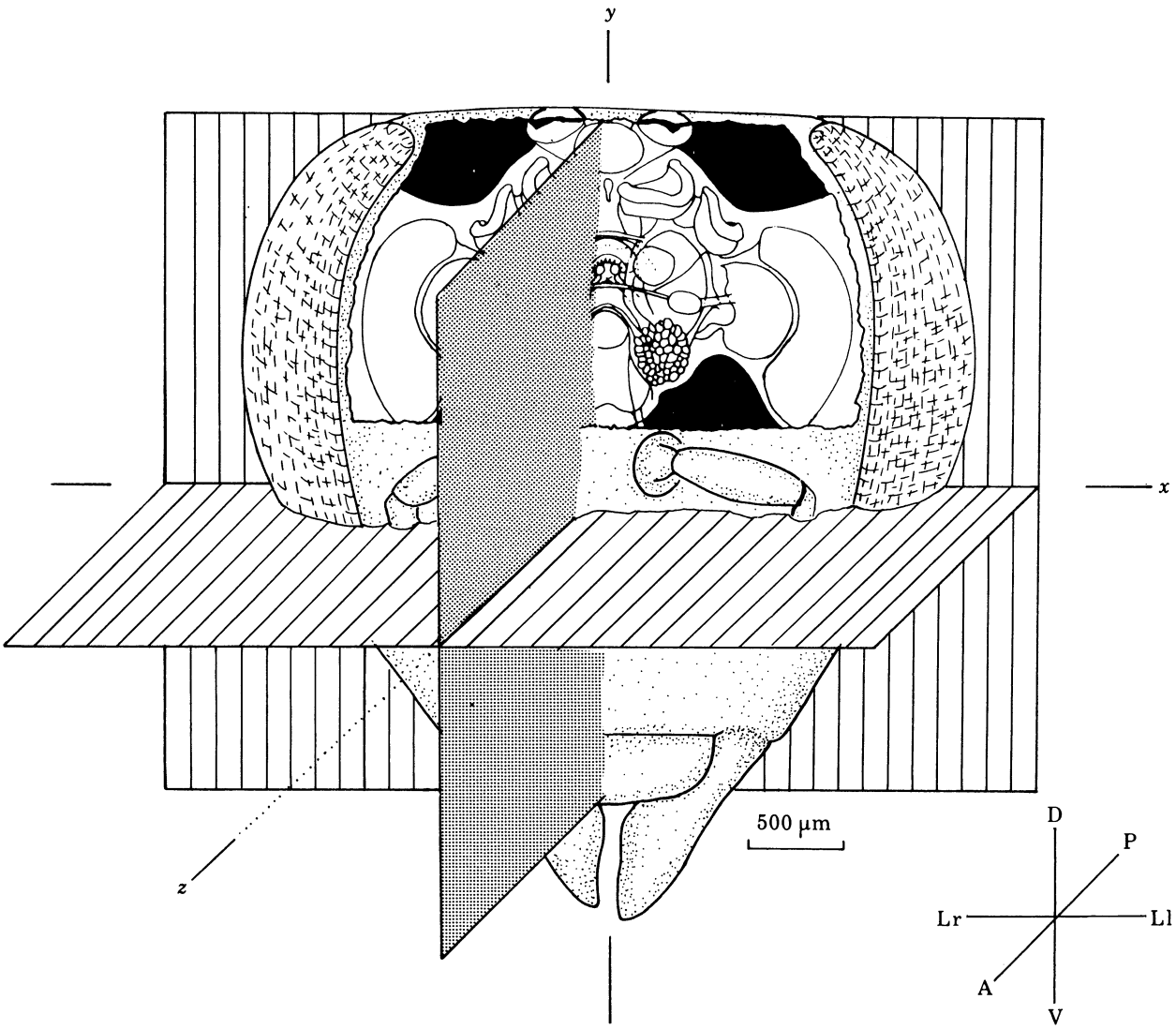

FIGURE 1. Diagram drawn to scale to illustrate the main section planes, with respect to the head's axes, used in the histological preparations. Sections cut in the *xz* plane are referred to as horizontal, those cut in the *xy* plane as vertical, and those cut in the *yz* plane as sagittal. The inset illustrates the use of the terms left and right lateral (Lr, Ll), anterior (A), posterior (P), dorsal (D) and ventral (V), with respect to the bee head.

rotary microtome placed 100 cm or so from a small electric fire or a 250 W infrared bulb. Sections were cut between 50 and 150 μm in thickness and mounted under Araldite by heating to 60 °C with weights on the cover glasses. The weights ensured that the sections were reasonably flat for later photographic procedures and drawing.

Approximately 500 brains were usefully stained by silver and Golgi techniques. The success rates were about 50 % for the Golgi methods (the Colonnier method being nearer 90 % successful) and 30 % for the reduced-silver stains. Many of the silver preparations were aban-

doned only because sections tended to lift from the slides, a tendency reduced by a 1 % nitrocellulose coating, a process that unfortunately reduces contrast owing to staining of the cellulose itself.

A few brains were stained with ethyl gallate by Wigglesworth's (1957) method. This technique, in which osmium-fixed material is soaked in saturated ethyl gallate to render a blue–black stain, produced excellent results if the bee brains were pre-fixed in Karnovsky's fixative. The blocks produced were so brittle as to require embedding in Steedman's (1947) ester wax and sectioning with a supremely sharp knife. Sections were cut between 1 and 7 μm thick, affixed to slides, dewaxed in xylene and mounted under balsam.

Diagrams of pathways to and from the mushroom bodies are based upon reconstructions from serial sections stained with reduced silver made with a Zeiss Photomicroscope III equipped with a drawing tube. The tracing of these pathways was facilitated by initial reconstructions made from Nomarski interference micrographs of serial 50 μm Araldite sections. Sections for this purpose were cut from whole heads, dissected, embedded and sectioned as described above for Golgi staining, but fixed in a 1:3 solution of 25 % glutaraldehyde in 0.1 M cacodylate buffer (pH 7.3). Individual Golgi-stained neurons were drawn with the aid of a drawing tube. Neurons passing out of a single section were reconstructed by matching the cut ends of the cells, a process aided by registering the edges of the Araldite section with a low-power drawing of the previous section.

3. Results

3.1. *The gross architecture of the mushroom bodies*

(i) *Introduction*

The mushroom bodies dominate the midbrain of the bee and represent 10 % of the total worker bee brain volume (see figure 3, plate 1) (i.e. 0.132 mm^3 out of the total brain volume of 1.32 mm^3). Mushroom bodies of drones are considerably smaller, 74 % of the volume of the worker bee. Their volume of 0.098 mm^3 represents 1.2 % of the drone's total brain volume of 7.84 mm^3. The comparatively huge volume of the drone brain is attributable to the massive development of the retina and underlying optic neuropils. As a result of the increase in optic lobe volume the drone brain contains in total many more nerve cells than does the worker brain Witthöft (1967) estimates that the drone brain contains some 1 210 000 neurons, 360 000 more than the worker brain with only 850 000 nerve cells. Despite the smaller total number of neurons, the worker's brain contains 340 000 K cells compared with 295 000 cells in the drone's mushroom bodies. Each mushroom body consists of a pair of elongated cup-like neuropilar structures, the calyces, with the concave surface of the lateral calyx orientated dorsolaterally and the median calyx dorsally (figure 3). The long axis of both calyces' assymetries runs anteroposteriorly. The bases of the cups are attached to short stalks, which fuse to form the pedunculus. This extends ventrally and divides to give rise to the α- and β-lobes. The β-lobe continues ventrally and the α-lobe extends frontally. The three-dimensional shape of the structures is best appreciated by reference to a model (figures 4, 5, plate 1).

Each mushroom body is formed from the many thousands of small intrinsic interneurons, the K cells. The shape of the mushroom bodies reflects the geometries of the individual K cells (figure 2), each of which has its cell body and dendritic arborization in the calyx. From the calyx each K cell sends a long projection into the pedunculus that divides into two branches which enter the α- and β-lobes.

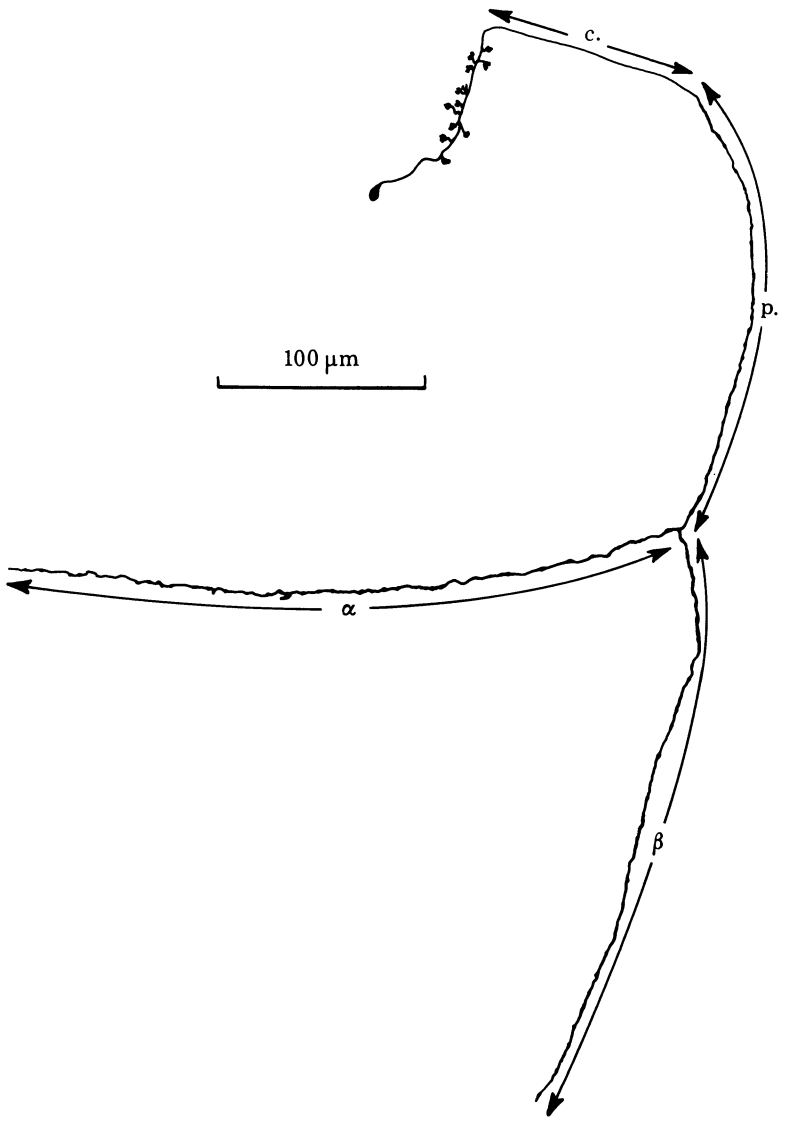

FIGURE 2. Drawing of a K cell (type KV) stained by the Golgi–Colonnier technique. The cell body lies beneath the collar zone of the calyx in which the cell's dendritic arbors lie. The unblebbed length of cell (c.) lies within a ray over the calycal surface. The length p. lies within the pedunculus and the lengths α and β within the α- and β-lobes respectively.

(ii) *The calyces*

The cups of the calyces are filled dorsally with K cell bodies (figure 3) which can readily be divided into two groups on the basis of their diameters. The inner group, the shape of which resembles a cone with an oval base, consists of smaller cells (diameter 4–5 μm). This inner cone is invested with a layer of larger-diameter cells (6–7 μm), which fills the remaining space and spills over the edge of the lip of the cup. A third group of small cells (diameter 4–5 μm) covers the entire undersurface of the calyx in a layer one to three cells thick.

A vertical section through the brain about the axis of the pedunculus shows that the calycal

neuropil can be divided into three regions, the lip, the collar and the basal ring (figures 3; 6, 7, plate 2; 9, plate 3). In sections stained with reduced silver, there is no distinction in the affinity of the lip and the collar for silver, both appearing homogeneously stained, in contrast to the basal ring which is clearly more fibrous. Several authors (Trujillo-Cenoz & Melamed 1962; Howse & Williams 1969; Pearson 1971; Schürmann 1974) have suggested that the neuropil of

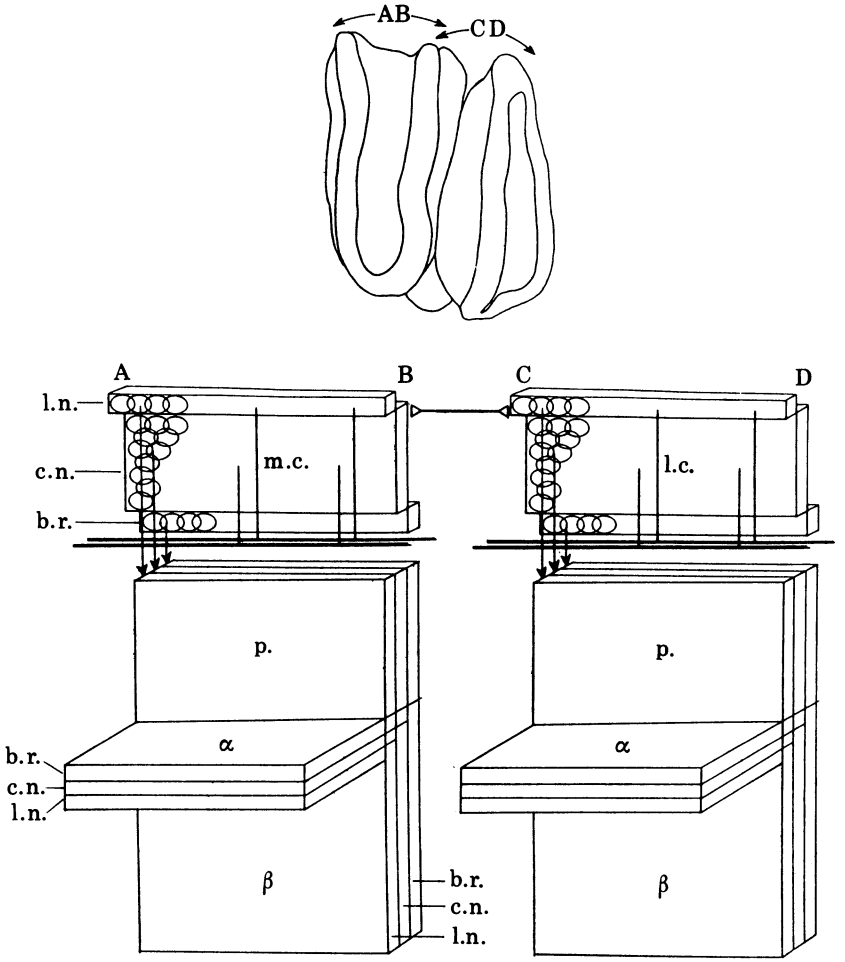

FIGURE 15. The calyces are unfolded diagrammatically to show them as part of a continuous series of linear arrays. The medial calyx (m.c.) and the lateral calyx (l.c.) unfold from the points arrowed and the polar coordinates of the calyces are transformed to Cartesian coordinates with the pedunculus (p.) and α- and β-lobes.

The lateral and median calyces map from A to B and C to D respectively and at the conjunction of the two peduncular stalks the pedunculus and the α- and β-lobes map the calyces as continuous sheets from A to D. After the division of the pedunculus to form the α- and β-lobes the calycal zones map into the α-lobe with the basal ring (b.r.) at the dorsal surface, the collar (c.n.) placed medially, and the lip (l.n.) ventrally. In the β-lobe the basal ring is the most posterior sheet; the collar fibres are located centrally and the lip fibres anteriorly.

the calyces is glomerular (more correctly microglomerular). Howse & Williams suggested that in Hymenoptera only the neuropil of the basal ring is glomerular while the remainder of the calyx is aglomerular. The Bodian preparations made for this study show that the entire calycal neuropil is finely glomerular (figure 9), but the glomeruli of the basal ring are more pronounced than those of the rest of the calyx. The electron microscope studies of Trujillo-Cenoz & Melamed (1962) and Schürmann (1974) suggest that the glomeruli are the sites of association between a

number of postsynaptic elements represented by the K cells and presynaptic blebs presumed to originate from efferent extrinsic neurons.

The K cell dendrites forming the lip arise from the population of larger cell bodies within the cup and around the lip. The collar contains the projections of large K cell bodies within the cup and those of small K cells clothing the undersurface of the collar zone. The basal ring draws its volume from the population of small cell bodies that occupy the central regions of the cup and also from small K cells located on the underside of the calyx about the basal ring. The neurites from the K cells find their way to their dendritic arborizations in the calyx via irregular paths and do not present any obvious pattern.

(iii) *Projections from the calyces to the pedunculus and lobes*

Horizontal sections across the calycal surface demonstrate that there is a highly ordered and regular arrangement of the K cell projections into the pedunculus. The peduncular projections of the Kenyon neurons form discrete rays, each formed from neurons with neighbouring arborizations in the calyx (figures 6; 7; 8, 11, plate 3). The three major divisions of the calyx are reflected in the organization of the pedunculus, the rays from each calycal zone amalgamating within the origin of the pedunculus to form curved bands (figures 6; 7). Each point within a peduncular band represents a particular area within the calyx and each band maps a contour within the calyx parallel to its circumference. The bands from the paired calyces fuse within their common pedunculus and homologous bands come together to form contiguous sheets of fibres. The banding pattern is maintained from its origin in the pedunculus through the peduncular division into the α- and β-lobes (figures 10, 12, 14, plate 3).

The calyces can be considered as a series of concentric contours whose polar coordinates map into the Cartesian space of the pedunculus and lobes (figure 15). The transformation between the polar and Cartesian maps is brought about by the existence of 'break points' in the polar

---

Description of plate 1

Figure 3. Bodian-stained 10 μm vertical section through the brain 320 μm from the anterior surface. Three divisions of the two calycal neuropils (m.c., l.c.) can be distinguished and are shown in detail in figure 9. The two peduncular stalks (p.) fuse above the fingers of neuropil (arrowed) extending out of the plane of the photograph to form the α-lobe. The median peduncular stalk (right) shows the characteristic three bands derived from the three calycal zones. The lateral peduncular stalk (left) sectioned through the most anterior of the peduncular layers is characteristically traversed by a weft of extrinsic neuron dendrites. Three of the major tracts to the calyces are shown, the anterior superior optic tract (a.s.o.t.), the lateral antenno-glomerular tract (l.a.g.t.) and the median antenno-glomerular tract (m.a.g.t.).

Figure 4. A frontal view of a wax reconstruction of the mushroom bodies showing the major divisions of the neuropil, the median calyx (m.c.), the lateral calyx (l.c.), the pedunculus (p.) and the α- and β-lobes (α, β).

Figure 5. A dorsal view of the same wax model as in figure 2, showing the elongation of the calyces along the anteroposterior axis. Note that the lateral calyx (l.c.) is more folded than the median calyx (m.c.).

Description of plate 2

Figure 6. The right median calyx (m.c.) and the lateral calyx (l.c.) viewed in a horizontal silver-stained section. Note the evolution of rays (arrowed) from K cell processes of the lip zone (l.n.). The basal ring (b.r.) of the median calyx is sectioned at its lateral edge. In the lateral calyx, rays (arrowed) from the lip are visible passing over the surface of the collar neuropil (c.n.). The large fibres at the medial posterior edge of the calyces are part of the ocellar tract (o.t.).

Figure 7. Horizontal silver-stained section from the same brain as figure 6, but 50 μm deeper. The collar and basal ring neuropils can be seen in the median calyx. Three major bands have evolved in the pedunculus (p.) from the amalgamation of rays from the K cells of the lip (1), collar (2) and basal ring (3).


l.n.
m.c.
oc.
c.n.
l.n.
l.c.
l.n.
b.r.
c.n.
b.r.
c.n.
p.
b.r.
l.n.
p.
c.b.
c.n.
b.r.
a.s.o.t.
β
l.a.g.t.
3
m.a.g.t.
100 µm

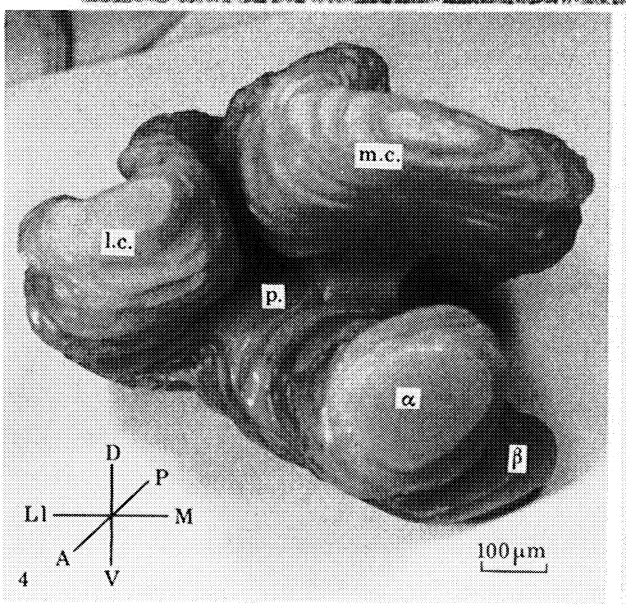
m.c.
l.c.
p.
α
β
D
P
Ll
M
A
V
100 µm
4

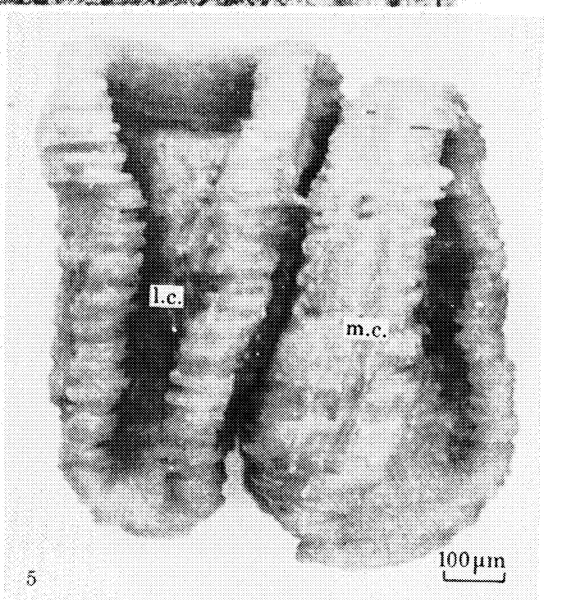
l.c.
m.c.
100 µm
5

(*Facing p.* 318)

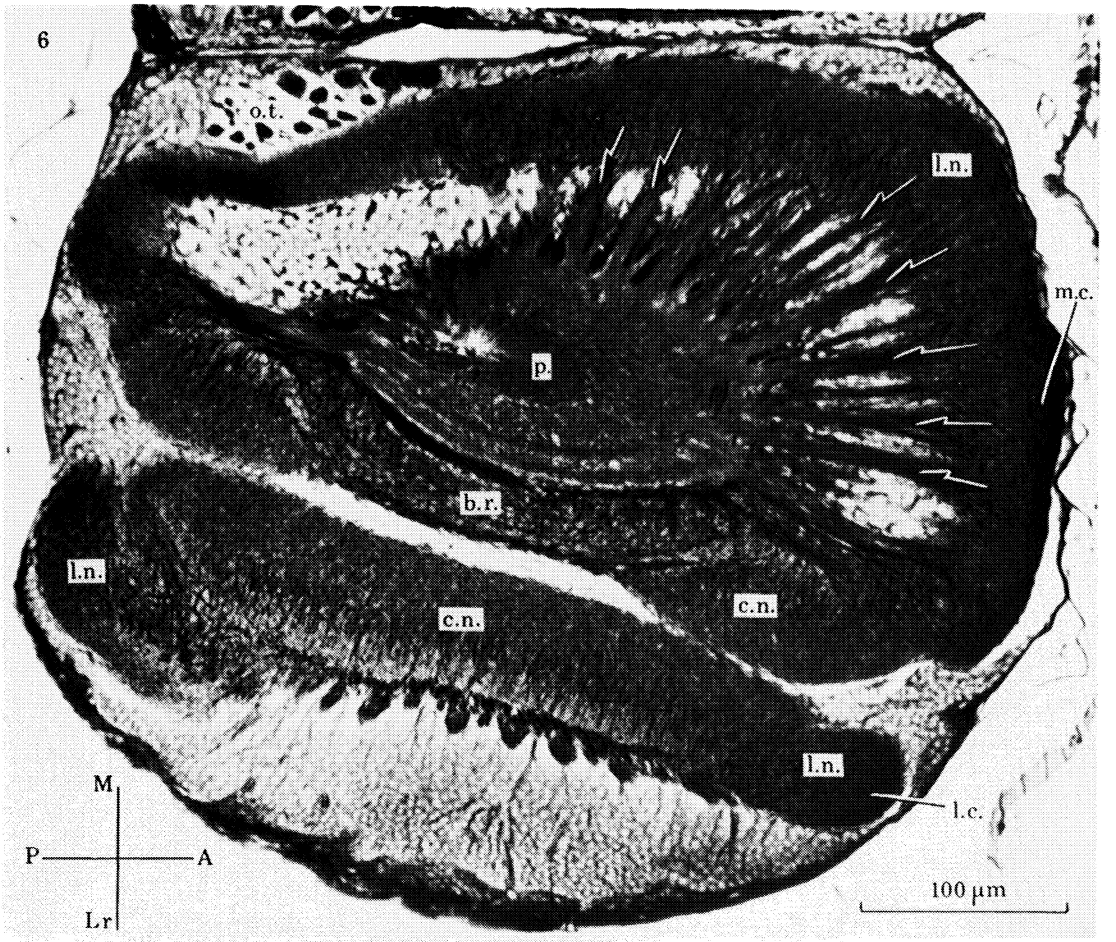
6
o.t.
l.n.
m.c.
p.
b.r.
l.n.
c.n.
c.n.
l.n.
l.c.
M
P
A
Lr
100 μm

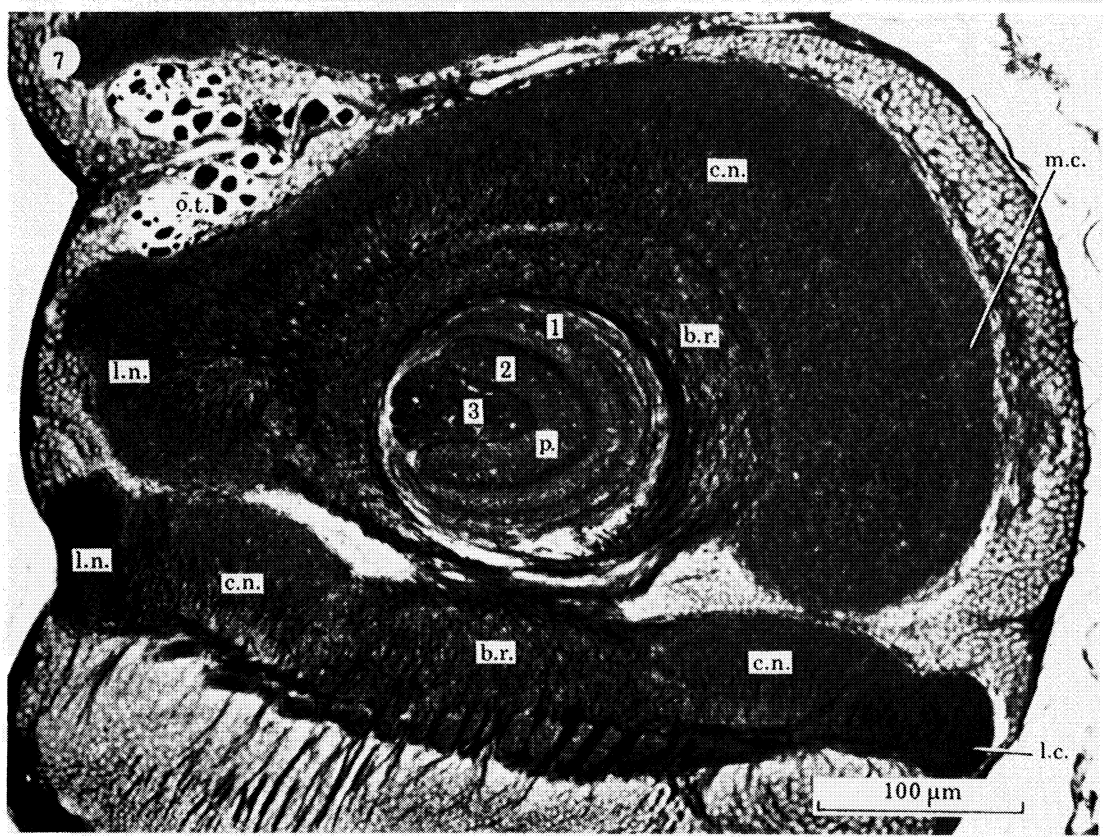
7
c.n.
m.c.
o.t.
1
b.r.
l.n.
2
3
p.
l.n.
c.n.
b.r.
c.n.
l.c.
100 μm


8
100 µm


o.r.t.
i.r.t.
9
50 µm

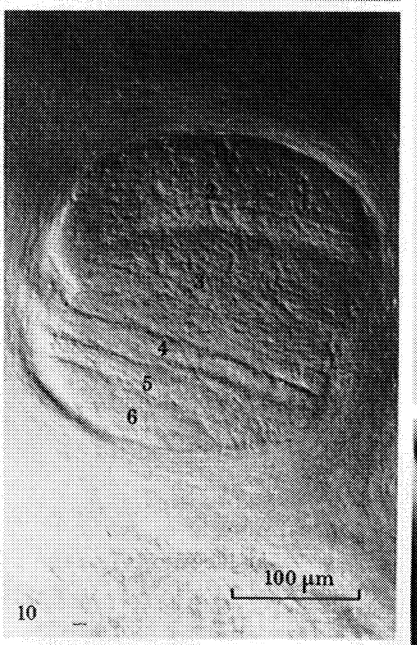
4
5
6
100 µm
10


50 µm
11

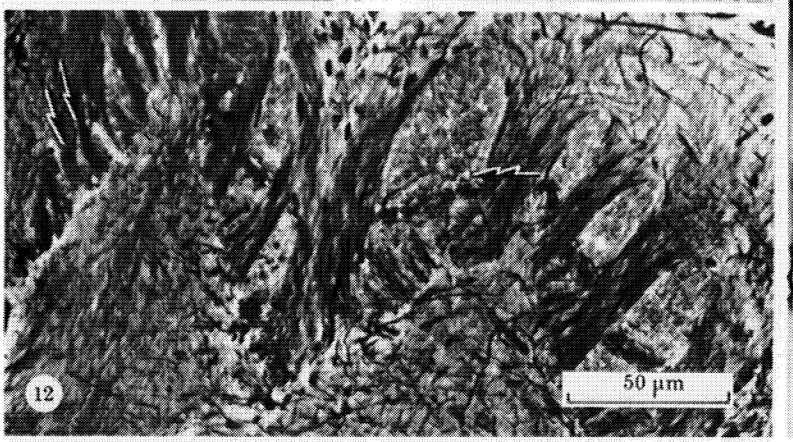
12
50 µm

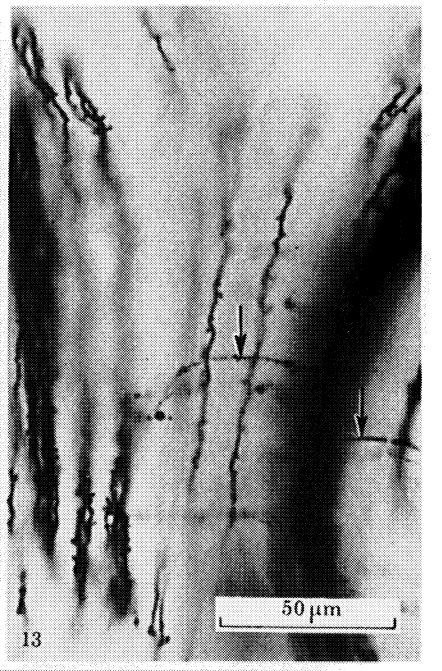
50 µm
13

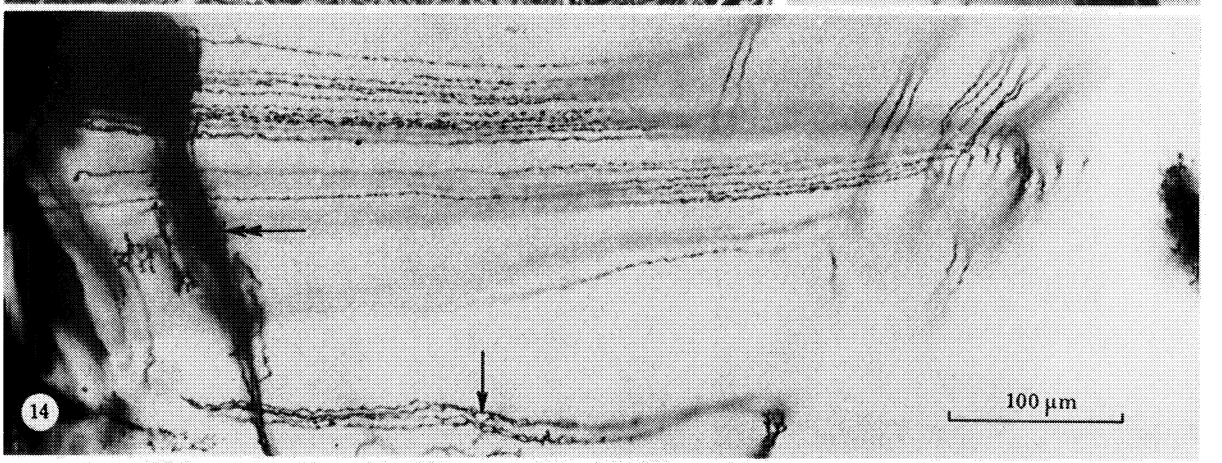
14
100 µm

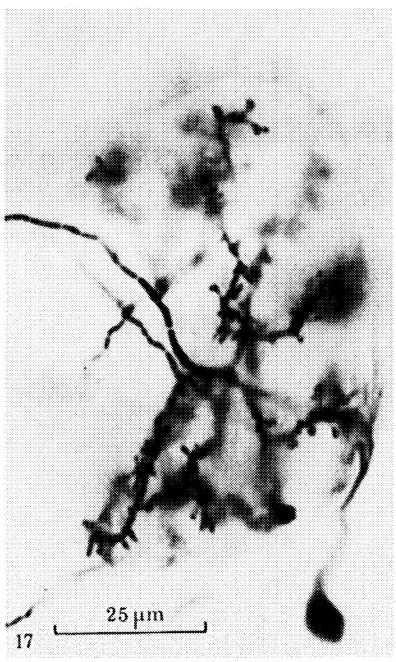
25 µm
17

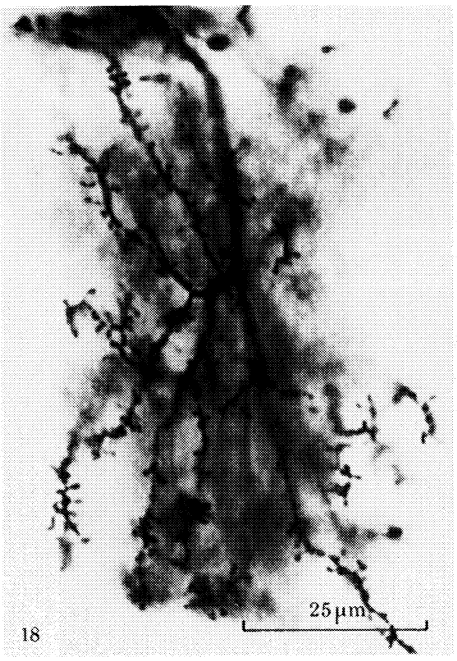
25 µm
18


25 µm
19

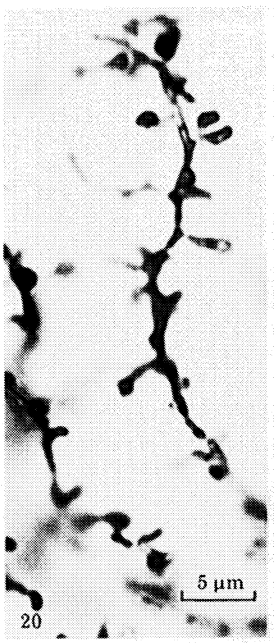
5 µm
20


25 µm
21

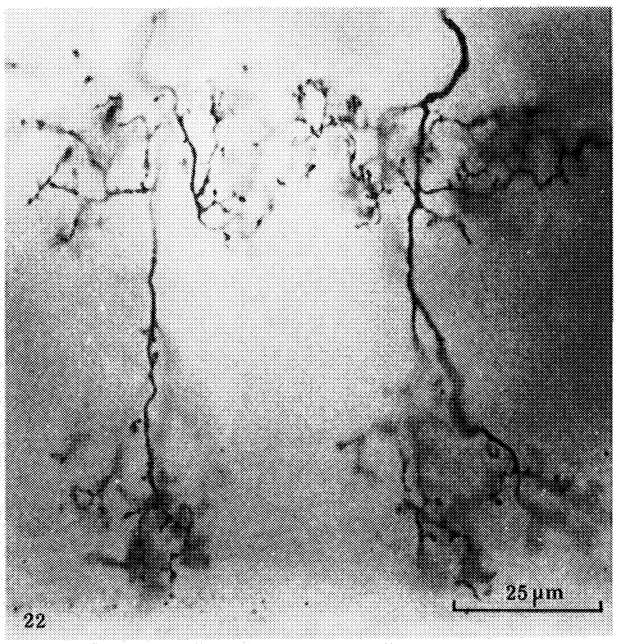
25 µm
22


25 µm
23

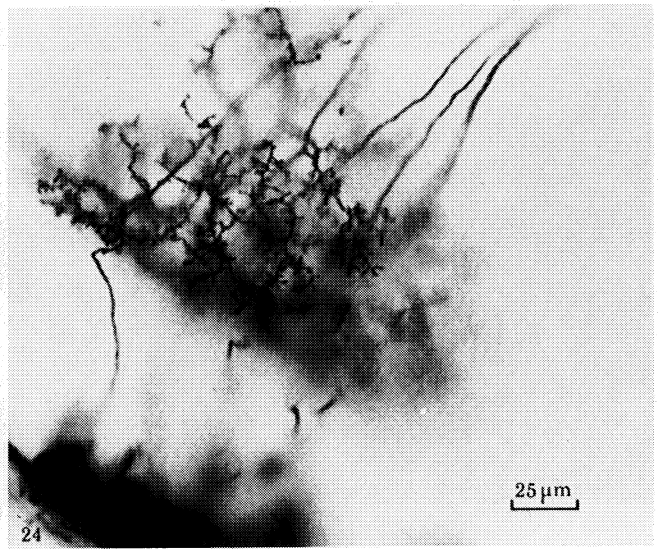
25 µm
24

contours' projections into the pedunculus that are located at the rear of each calyx. Each contour is represented as a horseshoe-shaped band at the top of the pedunculus that subsequently flattens into a bar.

Layered organizations within hymenopteran mushroom bodies have been described by Jonescu (1909) and by Howse (1974) in the bee brain and also by Goll (1967) in the ant. Jonescu figures the layers in his illustrations of the calyx and pedunculus. Howse correctly inferred from his own preparations that the bands within the pedunculus and α- and β-lobes are derived from the neuropil zones of the calyx but confusingly misrepresents the orientation of the bands and the shape of the mushroom bodies. Goll describes four locations for the K cell bodies surrounding the calycal neuropils in the ant. He shows that in the ant brain the polar organization of each of the calyces is maintained within the pedunculus and the α- and β-lobes.

Description of plate 3

Figure 8. Horizontal silver-stained section showing rays (arrowed) from the basal ring running around and over those of the lip and collar zone, the K cell fibres of which have amalgamated with the lip ray fibres running beneath those of the collar rays. Compare with figure 7.

Figure 9. Silver-stained vertical section through the lateral wall of the median calyx. Faint microglomeruli can be discerned throughout the wall's neuropil. Four tracts of fibres can be distinguished, the inner ring tract (i.r.t.), the outer ring tract (o.r.t.), input extrinsic fibres from the i.r.t. to the lip (single-headed arrow) and extrinsic fibres from the α- and β-lobes (double-headed arrow).

Figure 10. Nomarski interference photograph of a whole-mounted cleared brain viewed frontally, showing six layers in the α-lobe (numbered dorsal to ventral).

Figure 11. Golgi–Colonnier mass impregnation of a group of sparse spiny K cells, showing the gaps (single-headed arrow) between the fibres through which the collar and basal ring rays pass. The soma (double-headed arrow) of the sparse spiny neurons lies in the central cone of small cell bodies.

Figure 12. Silver-stained vertical section showing fingers of K cell processes within the pedunculus pushing through overlying layers to form the α-lobe. At this point the fibres previously running in a sheet form discrete bundles (single-headed arrows) that amalgamate to re-establish the peduncular organization within the α-lobe. Note layering in the larger groups of α-lobe processes (double-headed arrow).

Figure 13. A Golgi–Colonnier preparation sectioned vertically, showing fibres from KI and KII cells in the initial part of pedunculus bearing dendritic knobs and spines and extending horizontal processes (arrowed).

Figure 14. A Golgi–Colonnier preparation sectioned sagitally revealing the precisely parallel nature of the K cell processes within the α-lobe. The spined and knobbed fibres at the bottom of the lobe (single-headed arrow) originate from the lip, the remaining blebbed fibres from the collar and basal ring. A small banded neuron can be seen to arborize in the middle and upper part of the lobe (double-headed arrow).

Description of plate 4

Figure 17. A dense spiny lip K cell (KI) at the edge of the lateral calyx with its cell body located beneath the calyx.

Figure 18. A typical dense spiny collar K cell (KII).

Figure 19. A pair of unusual small-field dense spiny K cells with 'clawed' projections (arrowed).

Figure 20. Spiny projections typical of KI and KII neurons.

Figure 21. A group of 'clawed' KV cells in the collar.

Figure 22. A pair of bistratified sparse spiny KIII cells in the collar.

Figure 23. A group of KIV cells arranged around the inner ring tract of the basal ring.

Figure 24. Type KI neurons in the lip viewed in a horizontal section to show the overlapping of near-neighbour dendritic fields.

3.2. *Intrinsic neurons*

(i) *The Kenyon cell morphologies*

K cells all have approximately the same total path length (900 μm) within the pedunculus and lobes. They also share certain geometric features: each arborizes only in one region of the tripartite calyx and then extends a projection into the pedunculus, which divides, passing into

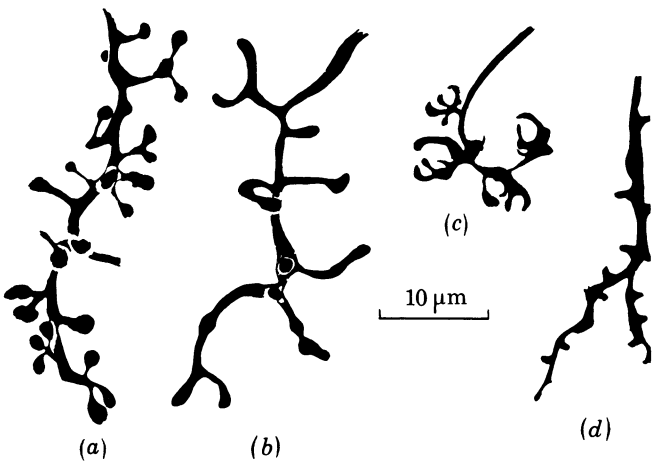

FIGURE 16. Scale drawings of the four types of dendritic specializations of the K cell arborizations in the calycal neuropils. (*a*) Dense spiny dendrites typical of K cell types I and II. (*b*) Sparse spiny dendrites of type KIII neurons. (*c*) 'Clawed' dendrites of type KV neurons. (*d*) 'Lumpy' dendrites of the small-field type KIV neurons.

both α- and β-lobes (figure 2). All K cells thus have λ-shaped projections within the ventral neuropils of the mushroom bodies.

K cells can be divided into subclasses on morphological grounds. The cell body can be either directly attached to the primary dendritic segment of the calycal arborization (Ka cells), or isolated from it by a neurite connected to the peduncular projection in the immediate vicinity of the calycal dendritic field (Kb cells). The K cells are described below on the basis of further subdivision according to their dendritic specializations within their calycal fields. Four types of specialization are encountered: dense spiny dendrites, sparse spiny dendrites, clawed, or bunched, dendrites, and small-field 'lumpy' dendrites (figures 16; 20, plate 4). As suggested by the internal spatial organization of the mushroom bodies and the distribution of K cell somata, the various zones of the calyx are composed of the dendritic arborizations of specific types of Kenyon neurons (figure 29). Only the dense spiny Ka cell type is encountered in the lip, while the collar contains both dense spiny Kb and bunched Ka cells. The basal ring contains both sparse spiny Kb neurons and bunched Ka and Kb cells. However the features used to establish the categories above do not always define specific identified classes of Kenyon interneurons.

The K cell categories described below have been Golgi-stained by a number of different procedures. Different staining schedules favour the staining of particular morphologies. The Colonnier process, for example, frequently reveals cell types KI and KII but seldom stains KIII neurons. In contrast the Kenyon–Kopsch technique most frequently stains KIII cells and

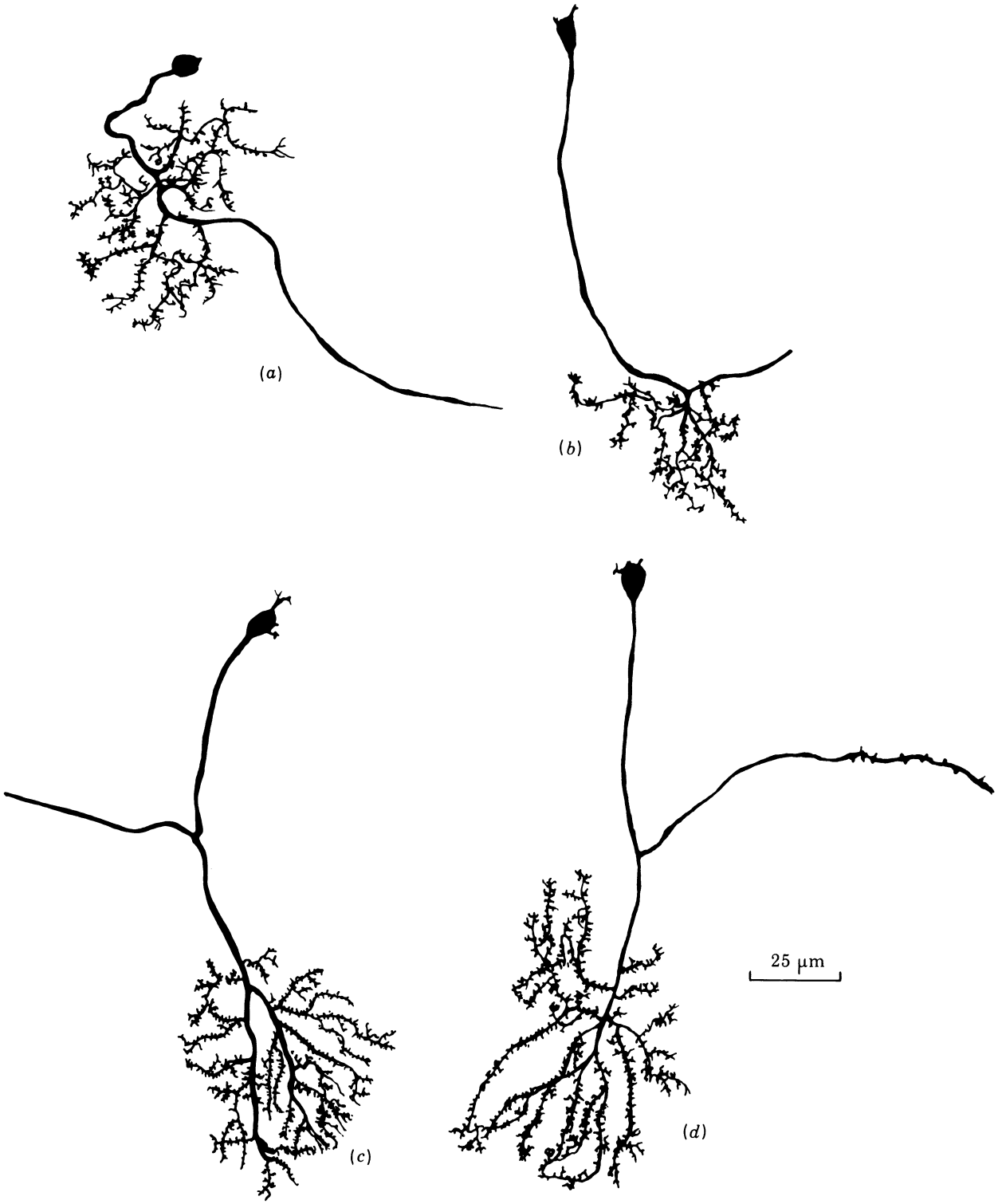

FIGURE 25. Scale drawings of dense spiny K cells. (*a*) A typical spherical-field K I cell in the lip zone. (*b*) A small-field K II neuron from the border between the collar and the basal ring. (*c, d*) K II neurons in the mid-collar.

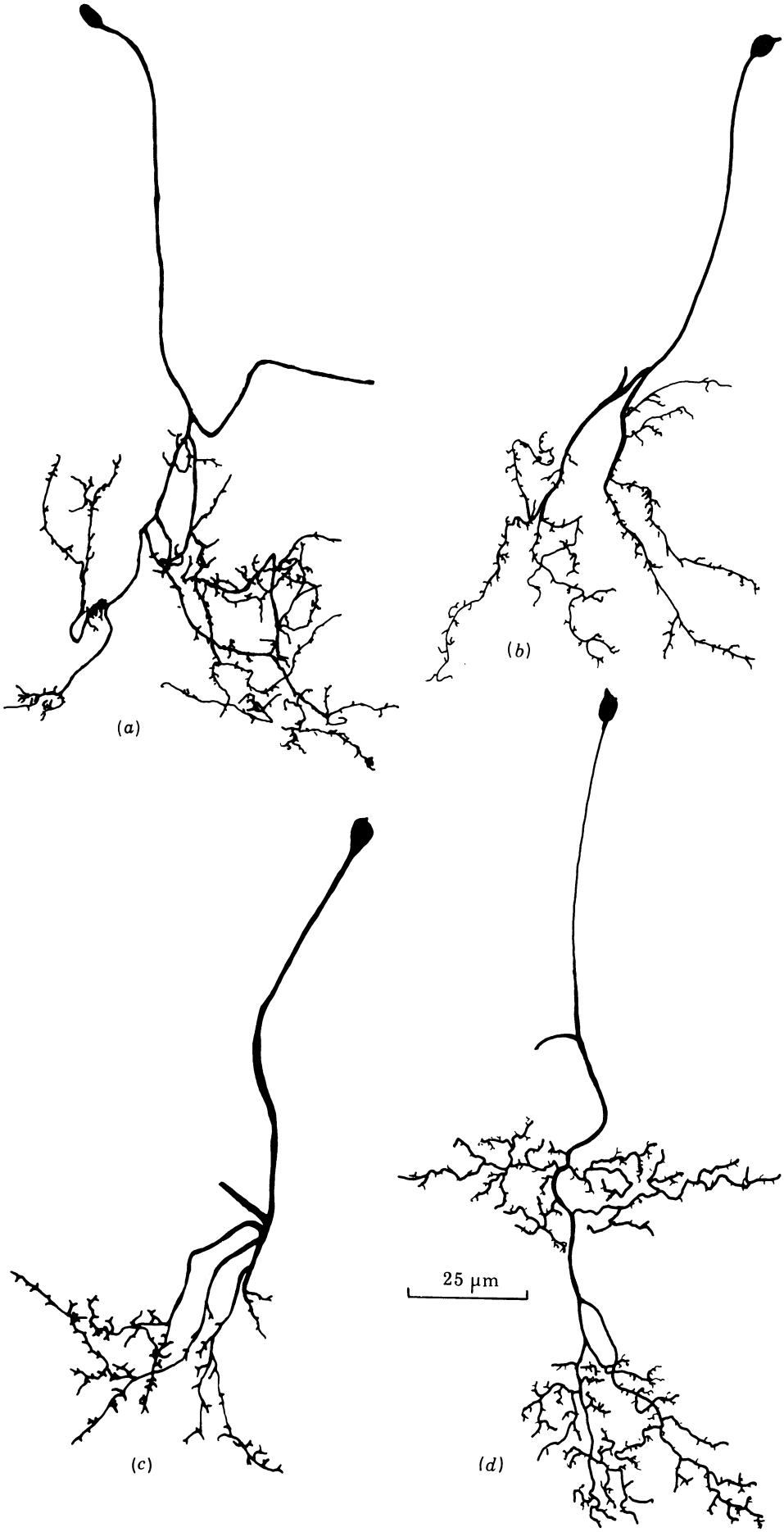

FIGURE 26. Drawings of sparse spiny KIII cells in the basal ring. (*a*, *b*) KIII cells arborizing throughout the depth of the basal ring. (*c*) KIII neuron branching in only the upper part of the basal ring. (*d*) Bistratified variant of the KIII cell type.

stains KI and KII with less regularity. The selective nature of the Golgi process has been noted by several authors and in particular Strausfeld (1976) comments on the probability of staining particular columnar neurons within the eye of *Musca*. As a result of the probablistic nature of the Golgi staining process it is impossible to determine the relative numbers of each of the cell types described below. For example, figure 19, plate 4, shows two K cells of similar morphology that were encountered in only a single preparation, yet they are probably present

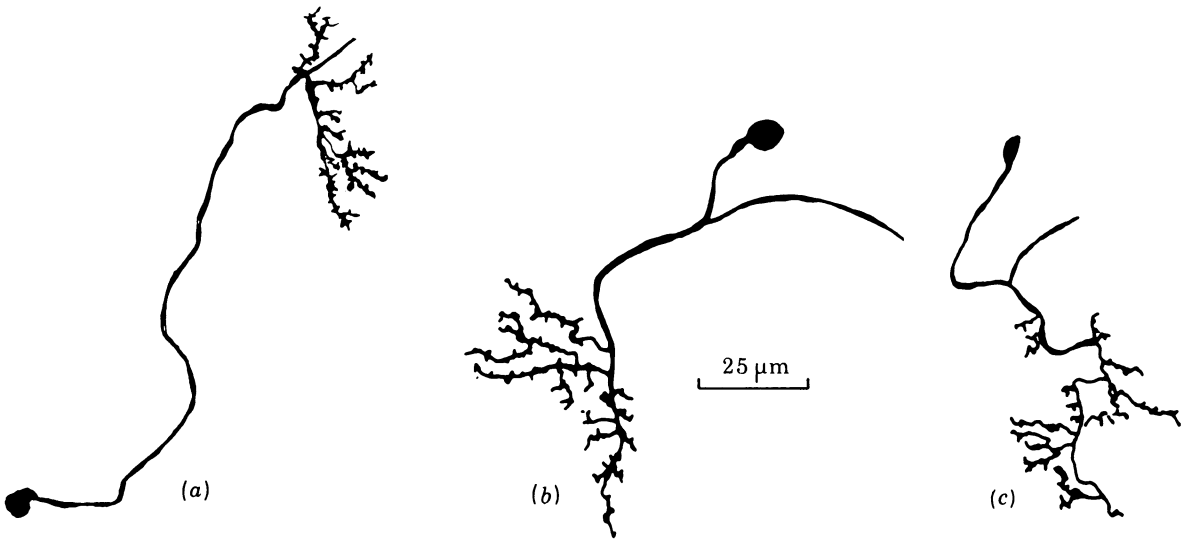

FIGURE 27. Drawings of KIV neurons in the basal ring: (*a*) from a contour occupied by the outer ring tract and (*b*, *c*) from a contour occupied by the inner ring tract.

in quite large numbers in the bee calyx but are seldom seen because they show a reduced tendency to be impregnated.

KI neurons are found exclusively in the lip zone. All KI neurons have very similar spherical dendritic fields approximately 75 μm in diameter with dense spiny endings (figures 17, plate 4; 25). The cell bodies of these neurons are directly added to the primary dendritic segment and are distributed around the lip neuropil, spilling over from the outer group of K cell soma into the region below the lip. While there is some variation in the branching patterns of KI neurons they probably represent a single morphological class.

KII neurons are Kb cells found exclusively within the collar zone. Their cell bodies occupy positions in the outer group of K cell somata. KII dendritic fields are roughly cylindrical in shape, about 60 μm in diameter; they branch through the entire depth of the collar neuropil (figures 18, plate 4; 25). Golgi stains reveal considerable variation in the precise branching pattern. In regions of high curvature of the calycal surface the KII fields tend toward a more flattened form and near the boundary with either the lip or the collar neuropil they are often of rather irregular shape (figure 25). In addition to these major variations in field shape the density of spines, the length of the spine shaft and the head volume vary between KII cells. Similar minor variations in KI cell dendritic morphology were observed. Goss *et al.* (1980) suggest that such variation is associated with the behavioural development and cumulative experience of individual bees.

KIII neurons are Kb cells found exclusively in the basal ring zone. Their cell bodies are located in the central group of K cell somata. KIII cells are represented by a number of different morphological classes within each of which there is considerable variation (figure 26). KIII dendritic fields frequently approximate cones or truncated cones with basal diameters of about 50 μm, occupying the entire depth of the calycal neuropil. Two other field shapes were sometimes encountered, both with stratified dendrites. The first of these is a bistratified neuron

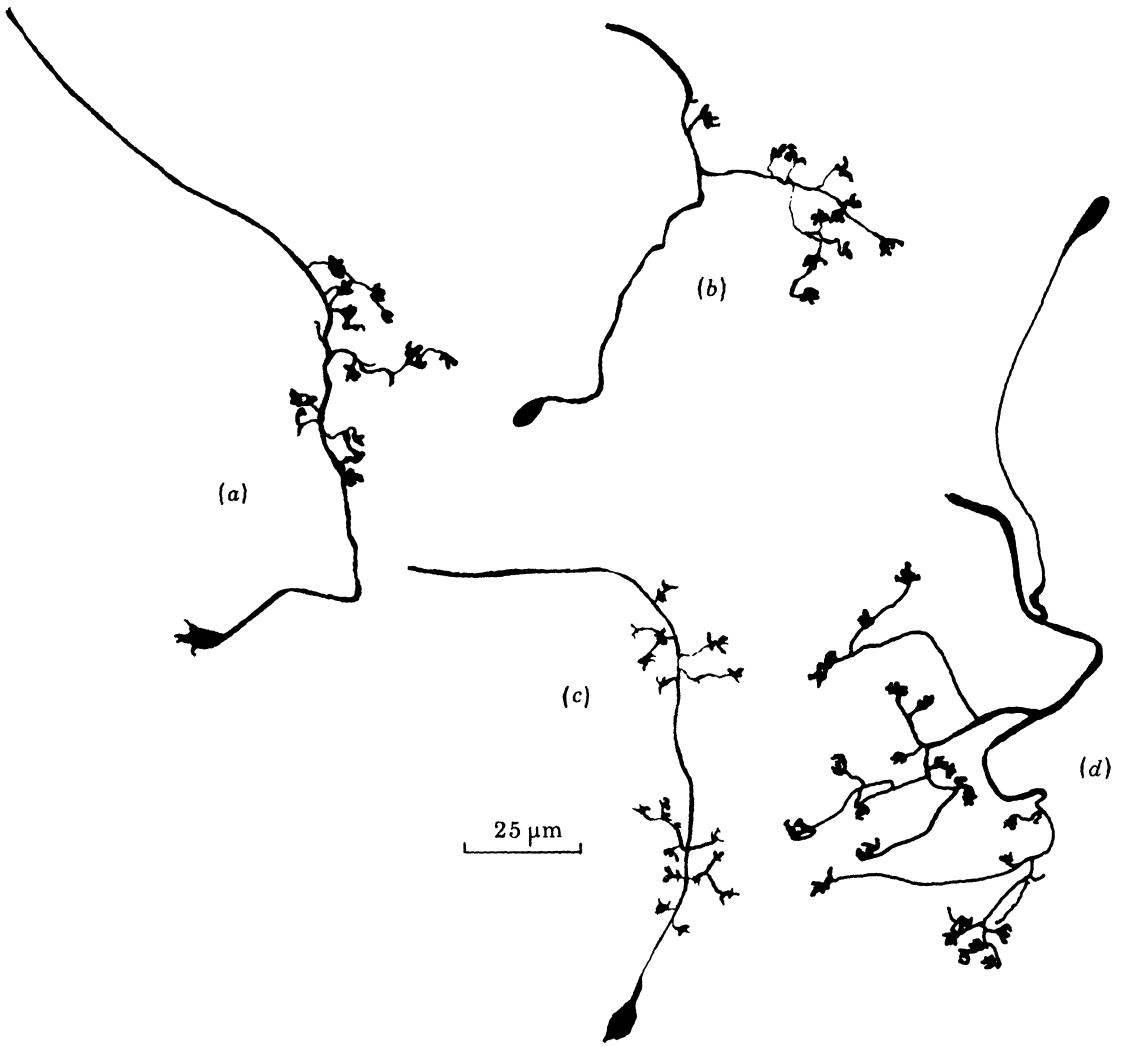

FIGURE 28. Drawings of variations of the KV 'bunched' cell type. (*a*) Neuron located on the lip margin of the collar. (*b*) Neuron with neurite running through the collar but with dendrites located in the basal ring. (*c*) Neuron arborizing within the basal ring. (*d*) Bistratified variant from the basal ring.

with a superficial field on the calycal surface and another in the ventral half of the neuropil (figure 22, plate 4). The second type has a small conical dendritic field that is restricted to either the upper or the lower half of the basal ring. All KIII neuron geometries have sparse spiny dendrites that can, despite variations in spine density, always be distinguished from the much more densely spined branches of KI and KII cells.

KIV neurons can be either Ka or Kb cells and are found exclusively within the basal ring

neuropil. Their cell bodies are found either in the central group of K cell soma or beneath the basal ring neuropil on the undersurface of the calyx. KIV cells are typified by their very restricted dendritic fields usually extending over less than 30 μm (figures 23, plate 4; 27). The dendrites of these cells do not extend throughout the basal ring and are restricted to the contours within the neuropil occupied by the two tracts that encircle it (the inner and outer ring tracts).

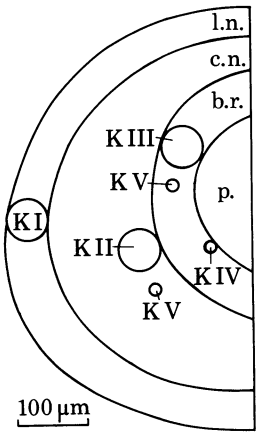

FIGURE 29. Diagram to show the regional distribution and relative average dendritic field diameters of K cell types I–V. A half-median calyx is shown artificially flattened by plotting the half circumference of sections from the wax model shown in figures 2 and 3 for different points along the anteroposterior axis Note that in the lip and basal ring some K cell fields fill the neuropil.

K V neurons can be either Ka or Kb cells and are found within both the collar and the basal ring neuropils. Their cell bodies can be located either above the calycal neuropil in the central group of K cell somata or below it. KV cells exhibit a great variety of branching patterns (figures 21, plate 4; 28). The form of the dendritic field cannot be related to the position that the cell occupies within one or other of the calyces, or to the Ka or Kb attachment of the cell body, or to the location of the cell soma. The different KV morphologies all share the same curious 'bunched' or 'clawed' type of dendritic specialization. While mass Golgi impregnation demonstrates that KI–IV cells have heavily overlapped dendritic fields, KV cells tend to stain in isolated groups, perhaps suggesting that they penetrate the matrix of the calyx at intervals.

(ii) *K cell projections within the pedunculus*

(*a*) *Individual K cell morphologies*

The first 50 μm of the peduncular length of KI and KII fibres are covered with dendritic knobs and spines (figure 13, plate 3). The remainder of their length and the entirety of the KIII–V fibres are irregularly blebbed with occasional spines (figure 14, plate 3). The peduncular projections of KIII–V are of a slightly smaller average diameter (0.2 μm) than those of KI and KII (0.3 μm). Mass Golgi impregnation reveals the presence of blebbed collaterals from a small proportion of KI and KII cells projecting laterally up to 50 μm within the pedunculus (figure 13). The K cells remain parallel in their course through the pedunculus and the α- and β-lobes. K cell projections within the pedunculus show a marked tendency to stain together as bundles, the fibres within each bundle arising from Kenyon neurons of the same geometry that occupy neighbouring and overlapped areas within an individual calycal zone.

(*b*) *Spatial organization of K cell projections*

Golgi stains in which large numbers of a particular K cell type are stained demonstrate that KI–V cells are distributed throughout 360° of the calycal contours. I have been unable to demonstrate the restriction of any one type of K cell to a particular sector of the calyx in the manner described by Strausfeld (1970) for *Vespa germanica* and other Hymenoptera. Mass Golgi

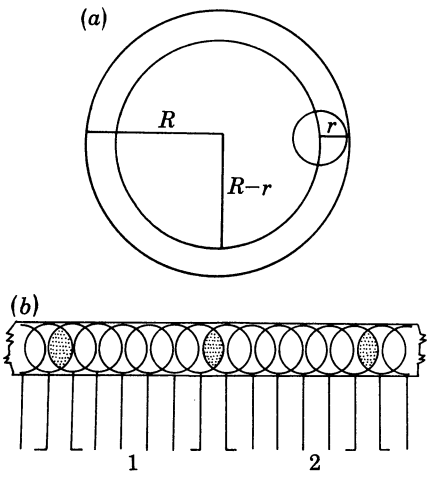

FIGURE 30. Diagram (not to scale) to illustrate the shared volume of domains in a calycal organization based on groups of neighbouring dendritic fields. (*a*) A collar domain in which *R* is the domain radius, dependent on the degree of overlap between neighbouring cells and their number, and *r* is the dendritic radius of an individual K cell. The collar neuropil is several KII dendritic fields deep and thus shared volume surrounds each domain. (*b*) Two neighbouring lip domains (1, 2). As the lip neuropil is only a single KI dendritic field wide the shared volume (shaded) is dependent only upon the number of cells within the domain. Shared volume will be present at either end of the domain.

impregnation of K cells of the same class lying in the same calycal zone shows that the neurons share a large part of their dendritic volume with their immediate neighbours (figure 24, plate 4). Neighbouring neurons of the same morphological class bundle to form rays over the calycal surface that continue as discrete bundles within the pedunculus. The integrity of the bundle is maintained throughout its course through the pedunculus and the α- and β-lobes. Mass Golgi impregnation confirms the impression gained from silver stains that the K cells' peduncular projections form sheets within the ventral mushroom body neuropils that represent Cartesian maps of the polar distribution of the different K cell types within the calycal neuropils (figure 15).

The degree of dendritic overlap between neighbouring K cells with projections in the same bundle depends upon the geometry of the neurons and upon precisely which two neurons within the bundle have been stained. The degree of overlap of neighbouring KI, KII or KIII cells varies between 50 % and greater than 90 %. The large shared volume of the K cells' calycal dendritic fields may in part explain the variability in the morphology of individual cells, as the precise spatial organization of one neuron's arborizations within the group may be of little importance. The tendency of K cells to stain as bundles and the extent of the overlap of neighbouring dendritic fields in the calyx suggests that the map of the calyx in the pedunculus and α- and β-lobes is based upon groups of neurons rather than individual cells. This view is supported by electron microscope evidence that shows groups of Kenyon cells wrapped together

in ensheathing glia (Maynard 1967; Mancini & Frontali 1967) and connected together by reciprocal synapses (Schürmann 1974).

Each bundle of Kenyon axons can, therefore, be considered to represent a domain within the calyx that overlaps other domains to an extent dependent upon the degree to which individual Kenyon cells' dendrites share calycal volume, the spatial organization of the domain, and the number of cells within any one domain (figure 30). Within the lip zone where only K I cells are found the domains are one dendritic field deep and the degree to which each domain overlaps the next can be approximated by considering the lip as a cylinder. The fraction of each domain's volume that is shared is then simply $2/N$, where N is the number of fields in the domain. Within the basal ring and collar the situation is complicated by the presence of more than one type of K cell with different field shapes and sizes. In the collar, which is up to five K II cell fields deep, domains also overlap in a complex but regular manner. An estimate for shared domain volume can be calculated for K II cells by considering the shared area around the edge of a domain of radius R. The proportion of the volume that is shared is given by $R^2-(R-r)^2/R^2$, where r is the radius of the K II cell dendritic field. Figures of 1 and 5 % respectively for the shared percentage domain volumes for neighbouring bundles of K I and K II cells, that assume approximately 200 cells per domain, illustrate the increased independence of K cell domains compared to individual neurons.

(c) Layering pattern within the pedunculus and lobes

In sections of the head of the pedunculus within the calyx three stratifications of the neuropil can be resolved. Each of these strata is derived from a different calycal zone. Sections stained with ethyl gallate, or with reduced silver methods, and cut from the α-lobe show a more complicated banding pattern that changes with depth. This changing banding pattern can be observed by optical sectioning of whole-mounted and cleared brains with a Nomarski interference microscope. Clear correspondence in the pattern of banding observed by the different staining and microscopical techniques can be demonstrated. For example silver stains stain one band in the α-lobe (band 2) particularly densely (figures 58; 60, plate 9) and this band can be found in an equivalent position in both ethyl gallate sections and Nomarski preparations (figures 10; 49, plate 7). Silver-stained sections parallel to this band, and Golgi preparations, show that the increased affinity of the layer for silver is due to the presence of numerous large extrinsic cell branches that run within it. Golgi and silver stains suggest that it is the pattern of extrinsic cell dendrites that produces the complex banding pattern observed in ethyl gallate sections. This complex pattern that changes with depth is a reflection of the underlying layered organization of the K cell fibres themselves.

Comparison of Golgi, silver and ethyl gallate material shows that the three basic layers that represent the lip, the collar and the basal ring are further subdivided into layers that represent each of the different geometric classes of K cell present within individual calycal zones. Thus the lip which contains only K I cells is represented by a single layer while the collar containing K II and K V neurons produces two strata. The basal ring contains K III, K IV and K V cells and produces four strata because the K V cells map two separate contours within the zone. This organization results in the production of seven individual strata.

At the point of peduncular division neighbour to neighbour relations are disrupted by the formation of the α-lobe from fingers of K cell fibre branches that push through the more anterior peduncular layers (figure 12). Within these fingers the stratification pattern of the pedunculus is maintained. K cell bundles seen in Golgi stains at the peduncular division never

cross but maintain their strict side-by-side order re-establishing the peduncular order within the α-lobe by fusion of the fingers of fibres (figure 14). Fibres in the most posterior part of the pedunculus run to the most dorsal part of the α-lobe and the most posterior part of the β-lobe. The result of the peduncular division is to establish a map in which the basal ring is represented by the upper α-lobe and the posterior β-lobe, the collar represents the central regions of both lobes and the lip represents the ventral part of the α-lobe and the anterior region of the β-lobe (figure 15).

The β-lobes meet below the central complex and in some silver preparations a region can be distinguished where the fibres in the two lobes are apparently confluent. Golgi impregnations show that K cell fibres do on occasion run into the opposite β-lobe although they never penetrate it by more than a few tens of micrometres. It is not clear whether this is a common occurrence or an abnormality.

(d) Comparative aspects of K cell morphology and organization

The K cell dendritic morphologies described here are similar in several respects to those described in other insects. Strausfeld (1976) points out that species representing the Coleoptera, Lepidoptera, Orthoptera and Hymenoptera all possess dense 'spiny' and 'clawed' K cell morphologies. Frequently the arrangement of the cell bodies of the different K cells is one in which the somata are displaced in radially arranged groups about the peduncular axis. Goll (1967) describes three basic classes of K cells in several species of *Formica*, two with dense 'spiny' dendrites and one with bunched endings, which have a differential distribution within the calyces and whose cell bodies occupy four distinct rind zones. Unlike in the bee the calycal zones of ants are represented within the pedunculus and lobes as concentric groups of fibres rather than as linear sheets. The result of this arrangement in ants is the continued separation of fibres from each calyx and a maintenance of the calycal polar organization within the pedunculus and lobes. In this respect it is interesting that Vowles (1954) found that the effects of destroying a single calyx in ants depended upon which of the paired calyces was damaged. In locusts a single calyx is subdivided into anterior and posterior lobes that form separate projections in the mushroom bodies' ventral neuropils (Williams 1972; Mobbs 1978; Ernst *et al.* 1977). Schürmann (1973) describes the formation of separate zones within the calyces and the α- and β-lobes of the cricket brain by different K cell types. The arrangement in the mushroom bodies of *Sphinx lingustri* appears rather different to that in other insects, with fibres at the origin of the pedunculus weaving about one another (Pearson 1970). It is interesting to note that in the *Sphinx* moth Pearson describes the formation of discrete bundles of K cell fibres which are twisted together. Fibres cross within a bundle but do not leave its confines. She states that individual bundles can be derived from K cells in both calycal cups. The situation in the fly *Musca* appears to bear some similarity to that found in the honeybee, with three calycal zones that Strausfeld (1976) refers to as axial, collar and lip zones. The arrangement of K cell types within the pedunculus and α-, β- and γ-lobes of *Musca* has not been described.

3.3. *Extrinsic neurons*

(i) *Inputs to the calyces*

The undersurfaces of the calyces are clothed in fibres derived largely from tracts running to them from the antennal lobes and the compound eyes. The origins and courses of pathways to the bee's calyces have been described by Kenyon (1896), Jonescu (1909), Jawlowski (1958) and

Vowles (1955). Vowles provides descriptions of some ten input tracts while Kenyon, Jonescu and Jawlowski describe up to six. The description presented here in general accords with that of Kenyon who demonstrates three tracts (the antenno-cerebral tracts O_1, O_2, O_3) running from the antennal lobe and one (the anterior superior optic tract, u.t.2g) from the compound eye. Kenyon additionally describes two other tracts, one visual, the posterior superior optic tract (u.t. 3g), and one of indeterminate origin, the dorsoventral tract (d.v.). Like Kenyon I have been unable to demonstrate with certainty any projections of the posterior superior optic tract within the calyces. In the silver preparations produced for this paper I have been unable to locate a tract that *penetrates* the calyces that can be equated to Kenyon's dorsoventral tract although along the line he describes there is a *fascicle* of descending cell neurites which may be equivalent to it. In addition to the fibres of these input pathways the calyces are penetrated by a number of single neurons from the tangled neuropils of the anterior lateral and median protocerebrum. Feedback neurons running from the α- and β-lobes form a further calycal input; these are considered in § 4.4.

The terminology used in this account differs from that of Kenyon in the following respects. The antenno-cerebral tracts O_1, O_2 and O_3 are referred to here as the median, mediolateral and lateral antenno-glomerular tracts (the m.a.g.ts, m.l.a.g.ts and l.a.g.ts respectively). Kenyon's term for the optic tract to the calyx, the anterior superior optic tract, has been retained but his abbreviation u.t.2g has been changed to a.s.o.t.

(*a*) *The antenno-glomerular tracts*

The median antenno-glomerular tract (*m.a.g.t.*) consists of many hundreds of fibres, the majority of which are gathered from the core of the glomerular neuropil of the antennal lobe (figures 31, 40). Bodian silver stains show that fibres are also gathered into this pathway from the dorsal lobe and the suboesophageal (s.o.g.) neuropil. The precise origin of the s.o.g. fibres remains obscure, but perhaps represents chemosensory input from the mouthparts. From their origin in the antennal lobes the tracts turn medially and posteriorly, running over the posterior surfaces of the β-lobes. The tracts continue parallel to the midline, running either side of the central complex. At the level of the ventral noduli each tract branches, giving rise to the m.l.a.g.t. The m.a.g.t. continues dorsally and then turns sharply outwards to meet the median calyx (figure 31). Within the network of fibres about the calyx the m.a.g.t. axons branch and send projections into each of the calyces that run around the inner margins of the basal rings (figure 40). These divisions of the m.a.g.t. are described below as the inner ring tracts (i.r.ts). The fibres of the m.a.g.t., having branched into the i.r.ts of both calyces, loop laterally and ventrally, and most terminate in a small area in the lateral protocerebrum at the base of the lobula. A few axons continue ventrally within the l.a.g.t. and, remarkably, return to the antennal lobe.

The median lateral antenno-glomerular tract (*m.l.a.g.t.*) at its point of division from the m.a.g.t. turns sharply laterally and then passes dorsally to meet the mushroom bodies behind the two calyces.

The lateral antenno-glomerular tract (*l.a.g.t.*) fibres pass posteriorly from the antennal lobe, running as a distinct bundle through the origin of the m.a.g.t., and then loop laterally, paralleling the lateral protocerebral continuation of the m.a.g.t. to the lobula (figure 31). The l.a.g.t. enters the plexus of axons about the calyces and then branches into the i.r.ts of both calyces. The majority of the l.a.g.t. fibres simply end here (figures 40; 42, plate 6) but a few have been

followed into the m.a.g.t., possibly representing the axons previously described that loop back to their point of origin in the antennal lobe. The cell bodies of all the a.g.t. fibres lie within the rind of the antennal lobes.

(*b*) *The anterior–superior optic tract* (*a.s.o.t.*)

The a.s.o.t. consists of hundreds of fine fibres (mostly less than 1.5 μm), that are gathered from the anterior surfaces of the medulla and lobula. Most of the fibres in this tract are derived

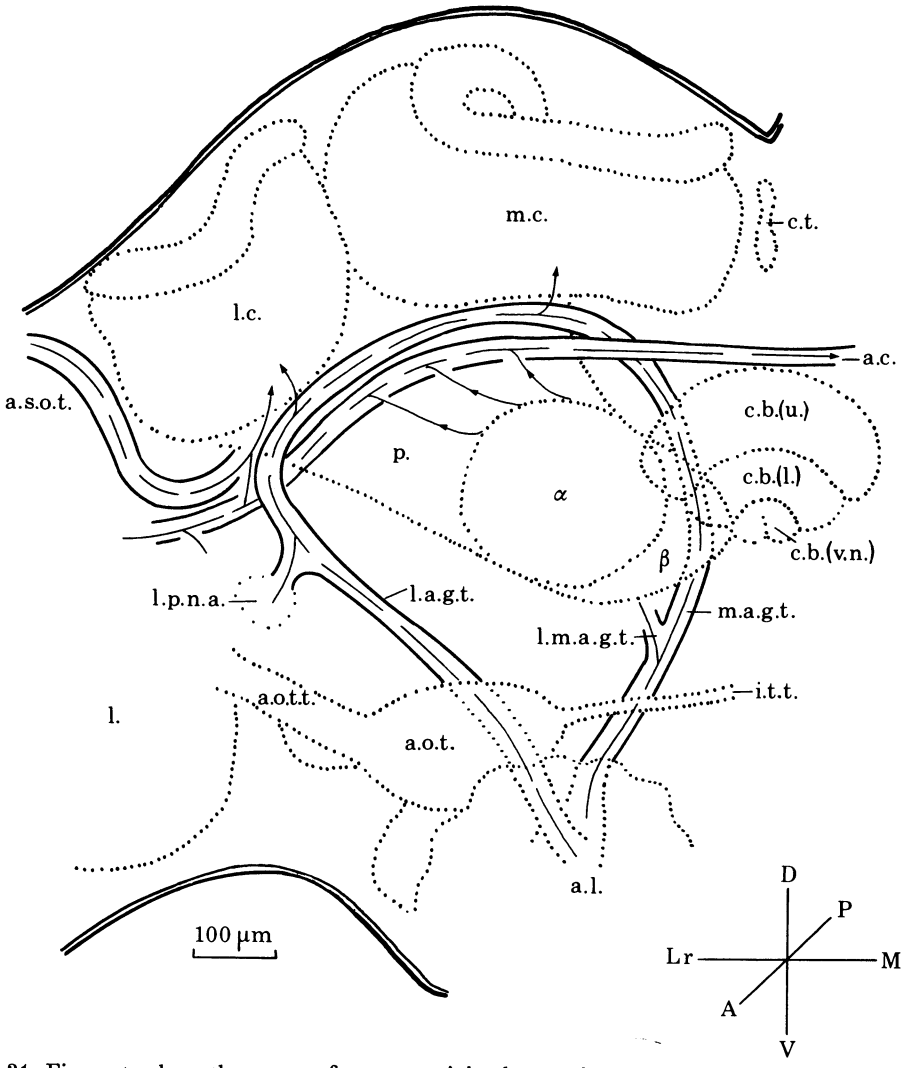

FIGURE 31. Figure to show the tracts of sensory origin that project to the calyces. Diagrammatic anterior view of a half brain drawn to scale.

from the stratifications of the medulla below and including the serpentine layer, and also from the outer columnar layers of the lobula's neuropil. From the dorsomedial edge of the lobula the tract traverses the short distance to the lateral calyx, where the fibres enter the calyces' external fibre plexus (figures 31; 41, plate 6). The fibres then branch into each of two outer ring tracts (o.r.ts) that delimit the outer edges of the basal rings of the calyces. The cell bodies of the a.s.o.t. neurons are gathered in a discrete group on the median dorsal edge of the lobula.

(c) Antenno-glomerular tract (a.g.t.) neurons and the anatomy of the antennal lobe

The antennal lobe is a highly structured and compartmentalized macroglomerular neuropil. The dendrites of the a.g.t. neurons reflect the organization of the olfactory and gustatory receptor terminals but it is not currently possible to relate individual a.g.t. neuron geometries to the structure of the antennal lobe. The honeybee's antennal neuropils have been the subject

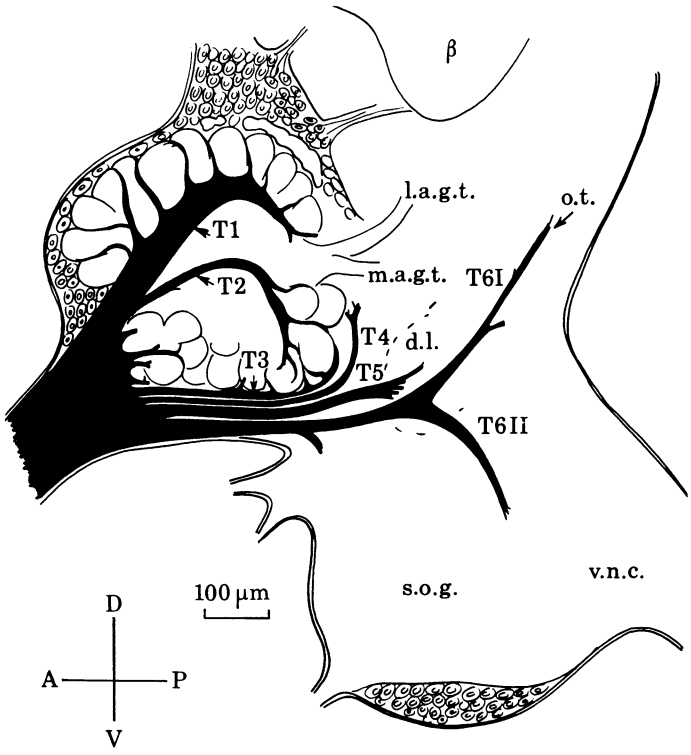

FIGURE 32. Diagrammatic sagittal view through the antennal lobe. See text for description and abbreviations.

of three recent studies by Pareto (1972), Suzuki (1975) and Satzinger (1980). The nomenclature of Suzuki is adopted here. In the following description the results of Suzuki from Procion yellow iontophoresis of the whole antennal nerve are related to Golgi and reduced-silver preparations.

The antennal lobe is a spherical neuropil consisting of a central feltwork of fibres, receptor axons and interneurons, intrinsic and extrinsic to the lobe, including those of the m.a.g.t. and l.a.t.g., and a radially and peripherally distributed series of glomerular spheres (figures 33, 34, plate 5). The antennal nerve of the bee is roughly divided into two strands (figure 32). The dorsal strand, presumed to consist of chemosensory receptor axons, projects mainly into the glomerular neuropil of the antennal lobe. The ventral strand, of presumed mechanosensory and motor neuron axons, passes largely into an area of neuropil behind the antennal lobe, the dorsal lobe.

Three bundles of fibres can be traced into the antennal glomeruli: T1, T2 and T3. T1 and T2 enter the glomeruli via the central feltwork while T3 penetrates them from the periphery of the antennal lobe. T1 terminates in the glomeruli located in the dorsal part of the lobe. Suzuki (1975) describes T2 as entering a single large glomerulus but in silver stains it is clear that this comparatively small bundle projects to a series of glomeruli located medioventrally.

A fourth bundle, T4, runs around the antennal lobe's ventral margin with T3 but continues into a small neuropil located at the rear of the lobe. Two bundles, T5 and T6, project to the dorsal lobe. The T5 neurons all appear to terminate in this neuropil while some of those of T6 continue through the lobe, dividing to form two groups, T6I and T6II. T6I projects posterodorsally to terminate in close proximity to the large neurons from the ocelli located on the protocerebral posterior slope. T6II turns posteroventrally from the dorsal lobe and runs into the suboesophageal ganglion, passing toward its midline to meet the T6II bundle from the opposite side of the brain. The distribution of these divisions of the antennal nerve is illustrated in figures 32–34.

Each antennal lobe contains approximately 100 glomeruli. The glomeruli are clearly not functionally equivalent as they receive input from distinctly different divisions of the antennal nerves' receptor fibre complement. On the basis of Golgi-stained receptor axons the glomeruli can be divided into at least five distinct types (figures 36, plate 5; 39). The majority of terminals in the dorsolateral glomeruli innervated by T1 are of the branched varicose type 1 illustrated in figure 39*a*. Glomeruli near the point of entry of the antennal nerve receive simple and frequently unbranched finely blebbed terminals (type 2). A more diffuse type of ending (type 3) can be found in some more centrally located areas. The glomeruli innervated by T3 are characterized by a fourth kind of receptor terminal with branched and sparsely blebbed dendrites. A fifth type of receptor terminal found within smaller ventrally located areas is heavily blebbed with very fine interconnecting segments, between the swollen regions. Generally glomeruli receive only one kind of terminal and these end in just a single glomerulus. However, occasional biglomerular endings are encountered (see figure 39*f*).

Interneurons of several different kinds have projections within the antennal lobes. The most readily identified and frequently encountered type are those connecting the antennal lobes to the calyces via the a.g.ts (figure 40). These cells have globular dendritic fields often appearing almost a solid ball because of the density of their branches within a glomerulus (figures 37, 38, plate 5). Some of these antenno-glomerular tract interneurons have branches in several glomeruli located in different regions of the antennal lobe, but the type most commonly encountered in Golgi preparations have uniglomerular terminals. Neurons with these characteristics are assumed to carry information to the calyces and represent primary antennal interneurons. A second type of fibre with projections in the a.g.ts is also encountered although rather less frequently than the primary antennal interneurons described above. These fibres are of smaller diameter than the a.g.t. primary interneurons and always arborize around several glomeruli with rather sparse blebbed endings. These neurons are centrifugal elements

---

DESCRIPTION OF PLATE 5

FIGURE 33. Silver-stained sagittal section of the antennal lobe.

FIGURE 34. Silver-stained sagittal section 50 μm lateral to that in figure 33.

FIGURE 35. Golgi–Kopsch-stained multiglomerular intrinsic interneuron within the antennal lobe.

FIGURE 36. Golgi–Colonnier preparation of antennal lobe showing T1 to dorsal glomeruli and T5 to the dorsal lobe. Note single terminal (arrowed) in T3 running around antennal lobe neuropil.

FIGURE 37. Golgi–Colonnier stain of the biglomerular ending of an a.g.t. neuron. Note position of cell body (arrowed) in peripheral rind of antennal lobe.

FIGURE 38. Golgi–Colonnier impregnation of an a.g.t. neuron uniglomerular ending in the antennal lobe, showing the high density of the dendritic arborizations.

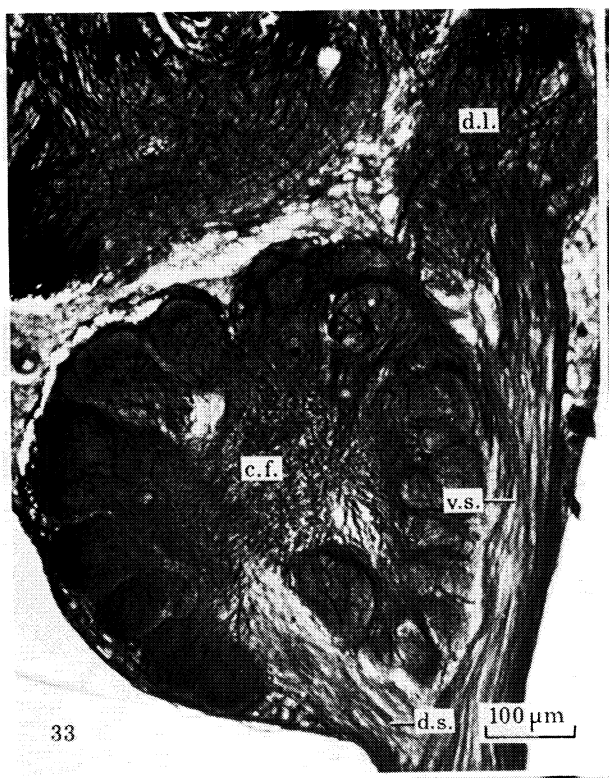

33

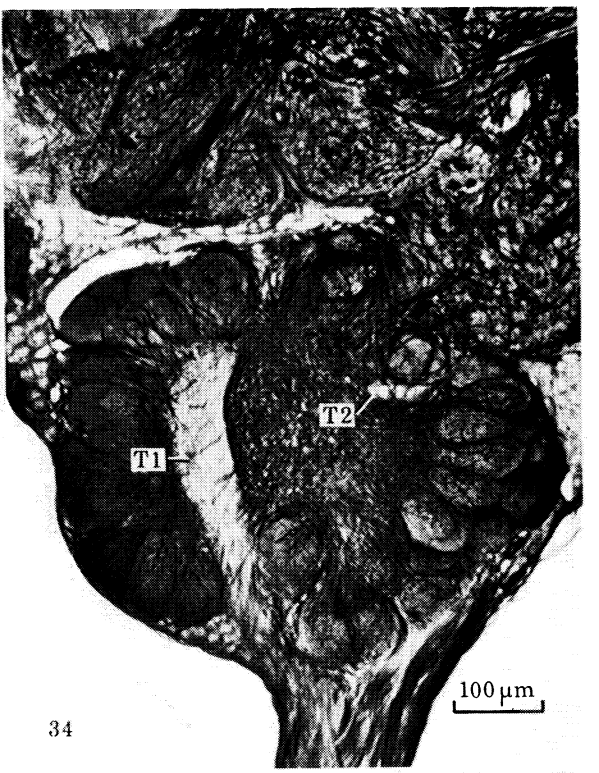

34

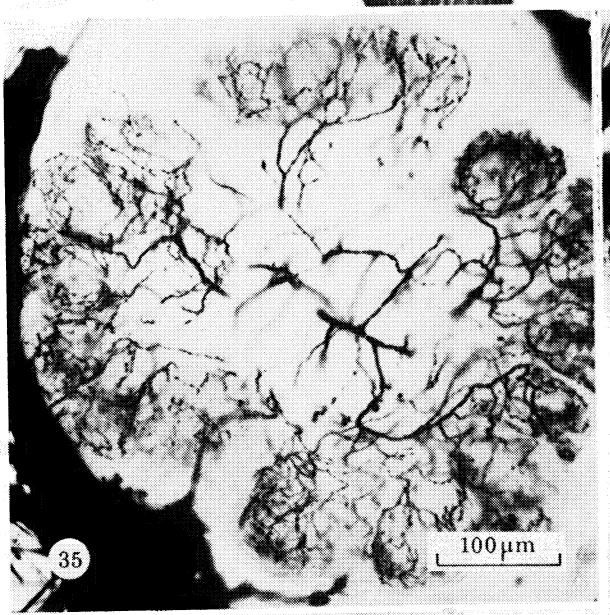

35

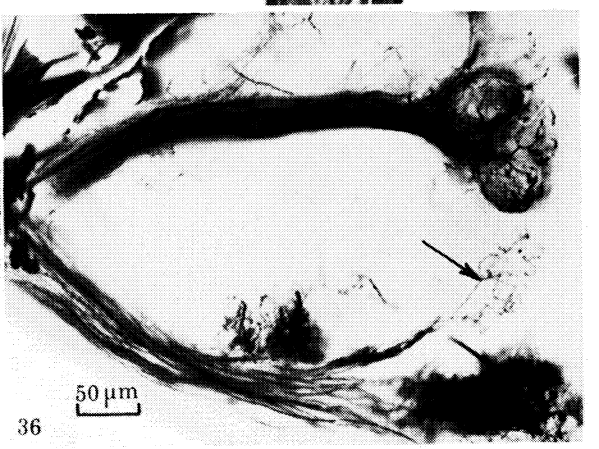

36

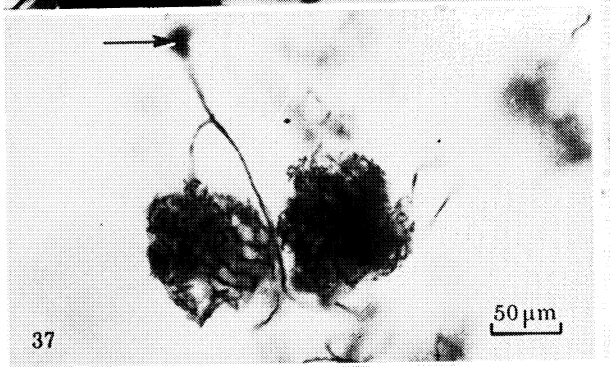

37

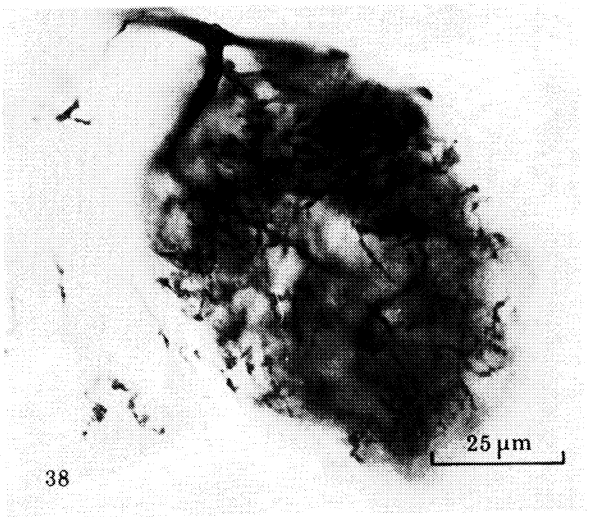

38

(*Facing p.* 332)

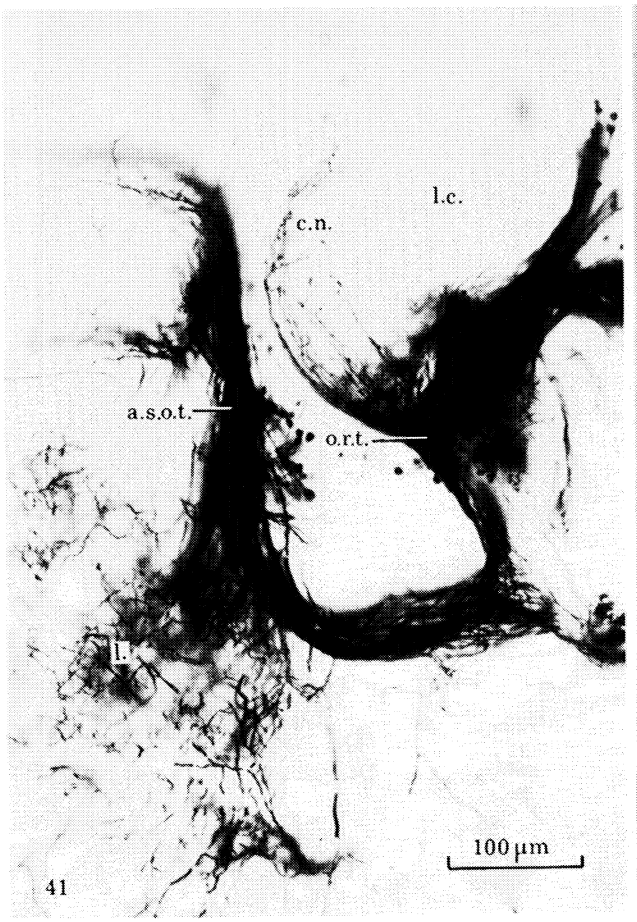
l.c.
c.n.
a.s.o.t.
o.r.t.
l.
100 μm
41

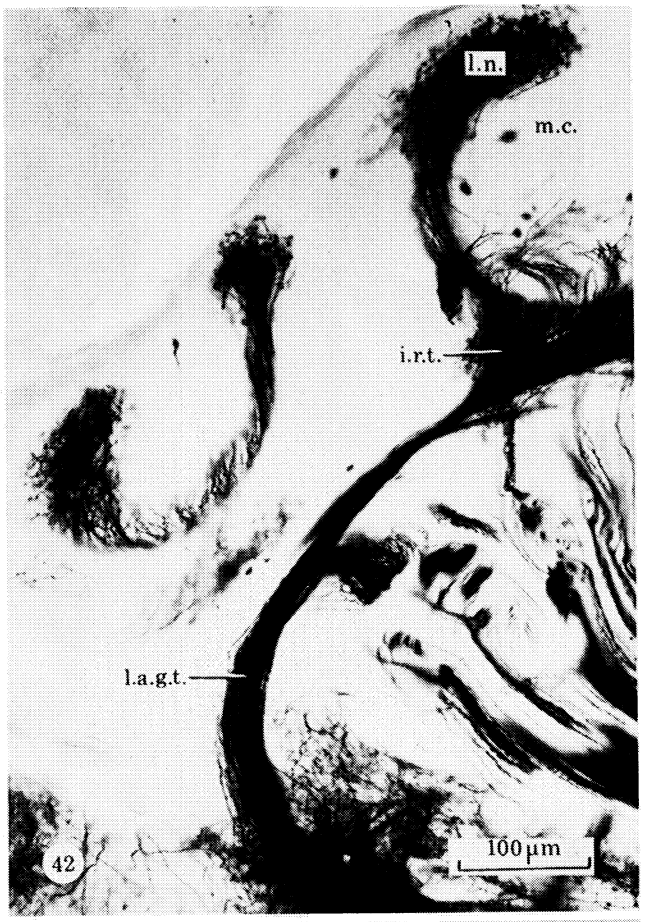
l.n.
m.c.
i.r.t.
l.a.g.t.
100 μm
42

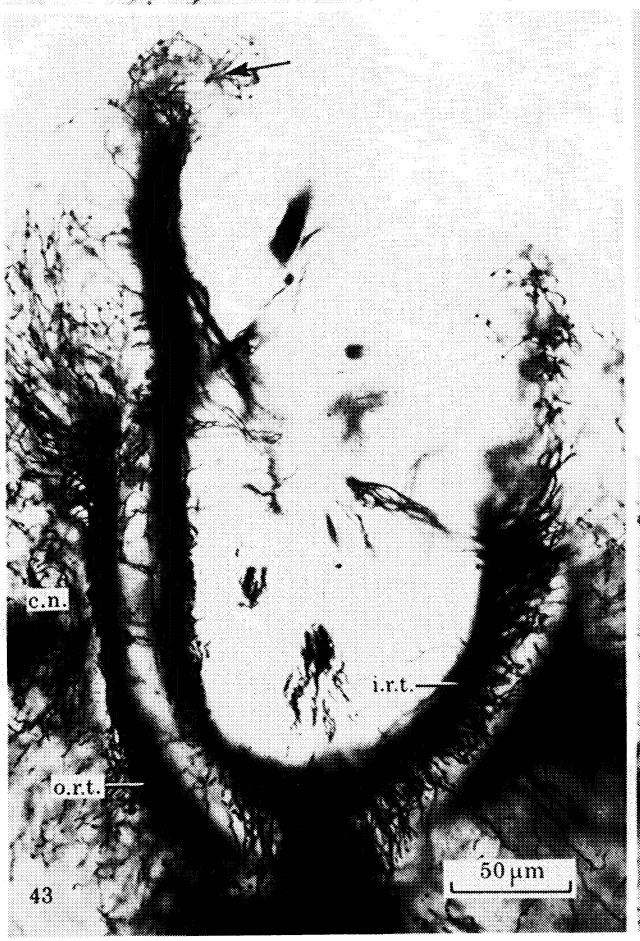
c.n.
i.r.t.
o.r.t.
50 μm
43

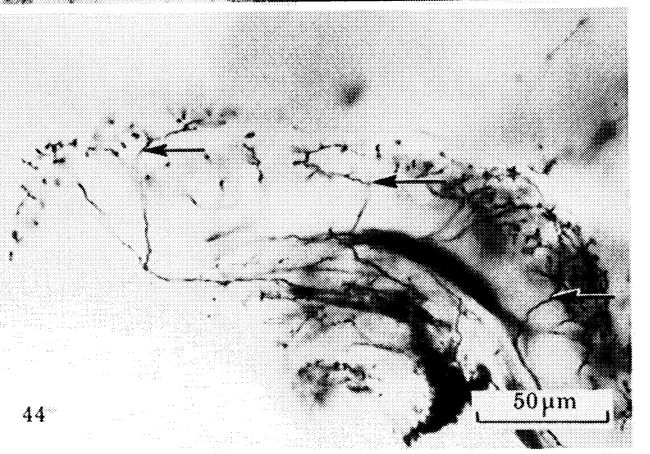
50 μm
44

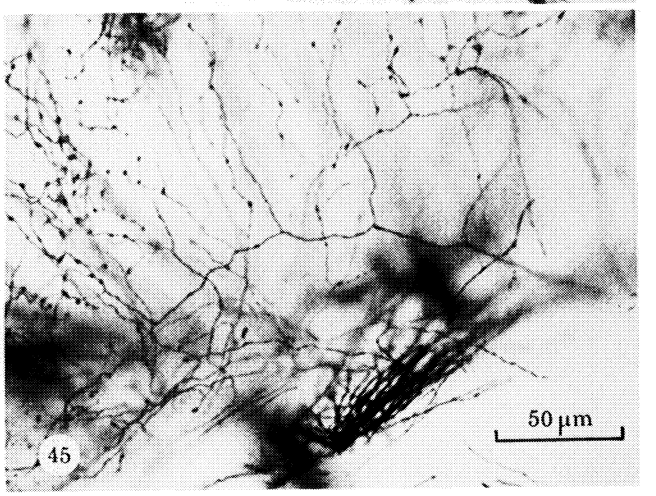
50 μm
45

running in the a.g.ts. They possibly originate from the calyces or pedunculus. In addition to neurons with projections in the a.g.ts there are several different fibre types whose branches are entirely restricted to the neuropil of the antennal lobe. Such antennal lobe intrinsic neurons always invade several glomeruli, often passing into 20 or more, which it is assumed they serve to connect (figure 35, plate 5). The cell bodies of both primary interneurons and intrinsic neurons are located in the rind of the antennal lobe. In common with Kenyon (1896) I am unable to find any evidence to suggest that there are any receptor fibres that terminate contralaterally in the bee's antennal lobes, in contrast to the situation in *Musca*, which has an interantennal commissure (Strausfeld 1976).

Witthöft (1967) estimates the total number of neuron cell bodies in the bee's deutocerebrum to be about 7000. As there are approximately 100000 axons in the antennal nerve about 30 receptor cells must converge onto each interneuron to the calyx, if only half the cell bodies counted by Witthöft are assumed to be those of intrinsic neurons. In the locust about 50000 receptor organs converge on 1200 a.g.t. neurons (Schürmann & Weschler 1970; Ernst *et al.* 1977). In both the bee and the locust convergence in the antennal lobe neuropil considerably reduces the number of transmission channels. However, as Schürmann & Weschler (1970) and Ernst *et al.* (1977) demonstrate with their anatomical studies the antennal lobe neuropil is a complex integrative area rather than a region for the simple addition of convergent inputs. Perhaps the most surprising aspect of the convergence of the receptor complement onto relatively few interneurons within the deutocerebrum is the subsequent divergence of the a.g.t. interneurons onto larger numbers of K cells within the calyx. If, however, the K cells are grouped into bundles that are functional assemblies, and many are involved in the processing of other modalities, there may in fact be a further reduction in the number of channels present in the a.g.t.

(*d*) *Input fibre arrangements within the calyces*

Fibres entering the calyces from the compound eye and the antennal lobes form two separate tracts, the inner and outer ring tracts, that encircle the bases of the calyces delimiting the inner and outer perimeter of the basal ring neuropil. Generally these fibres send projections into both median and lateral calyces, although occasionally cells projecting to a single calyx have been encountered (figure 40).

Description of plate 6

Figure 41 Golgi–Kopsch preparation of the lateral protocerebrum and part of the optic lobe sectioned vertically, showing the anterior superior optic tract (a.s.o.t.) running over the dorsal surface of the lobula (l.). Branches enter the lateral calyx (l.c.) and the axons continue to the median calyx. The cell bodies of the a.s.o.t. fibres are arrowed. Note that only the collar region (c.n.) contains a.s.o.t. arbors.

Figure 42. Golgi–Colonnier preparation of the lateral protocerebrum sectioned vertically, showing the lateral antenno-glomerular tract (l.a.g.t.). The point at which the tract branches to the lateral protocerebral neuropil area is arrowed. The inner ring tract (i.r.t.) is stained in the median calyx (m.c.). Note that only the lip zone contains l.a.g.t. arbors.

Figure 43. Horizontal section through the median calyx of a Golgi–Kopsch-stained brain. The inner ring tract (i.r.t.) and outer ring tract (o.r.t.) are heavily impregnated. Branches from the i.r.t. within the lip are arrowed. Branches from the o.r.t. radiate into the collar (c.n.).

Figure 44. Horizontal section through the median calyx of a Golgi–Ribi-stained brain. Fibres running in the mediolateral antenno-glomerular tract are stained within the basal ring. The arborizations of these cells (arrowed) lie athwart the zone occupied by the outer ring tract.

Figure 45. Sagittal section through the lateral calyx impregnated by the Golgi–Kopsch procedure. The branching points of a single outer ring tract neuron are arrowed. Note the blebbed endings.

FIGURE 39. Receptor endings in the antennal lobe drawn from Golgi–Colonnier and Kopsch preparations. (*a*) Type 1 ending in the dorsolateral part of the lobe subserved by T1. (*b*) Type 2 ending in the front glomeruli of the lobe. (*c*) Type 3 ending in the central feltwork. (*d*) Type 4 ending from the T3 division of the antennal nerve in posterior part of the lobe. (*e*) Type 5 ending in a medioventral glomerulus subserved by T2. (*f*) A biglomerular ending of a receptor in the T2 tract.

The outer ring tracts (*o.r.ts*) originate from the a.s.o.t. The fibres of the a.s.o.t. run around the basal rings of both calyces, sending numerous blebbed branches into the collar. In impregnations stained *en masse* with Golgi's method the collar appears to be randomly penetrated by a web of fine blebbed fibres (figures 41, 43, plate 6). Preparations in which single neurons can be

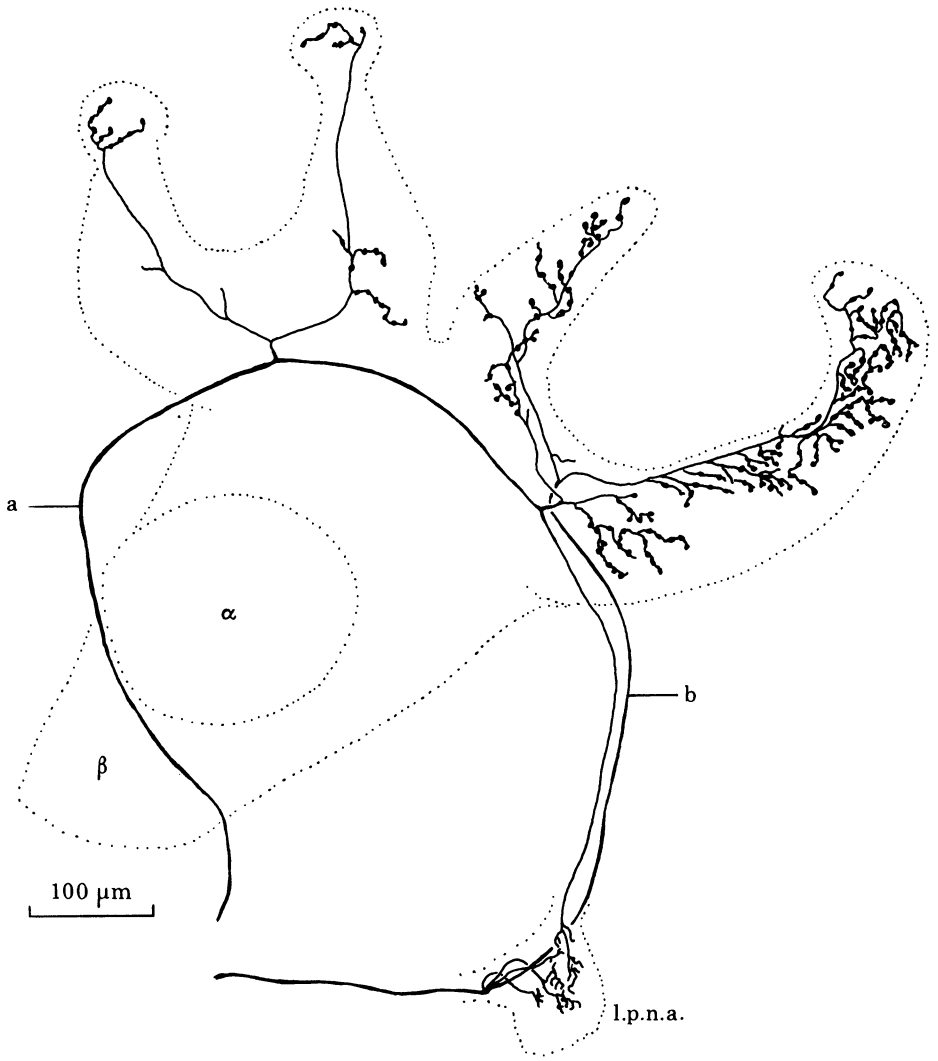

FIGURE 40. Reconstruction from a vertically sectioned Golgi–Kopsch preparation of two antenno-glomerular tract neurons. Fibre a, in the m.a.g.t., runs to both calyces while fibre b, in the l.a.g.t., arborizes only in the lateral calyx and has most of its branches restricted to the lateral part of the lip zone. Both fibres branch into the lateral protocerebral neuropil (l.p.n.a.). The antennal lobe dendrites were not stained.

resolved show that each fibre in its course within the o.r.t. radiates a series of branches rather like the spokes of a wheel from a central hub (figure 45, plate 6). Some short collaterals also project into the basal ring neuropil.

The inner ring tracts (*i.r.ts*). The a.g.t. fibres project into the calyces via the i.r.ts. These cells' blebbed projections enter the lip and radiate over the dorsal surface of the calycal neuropil (figure 42). The geometry of the a.g.t. neuron branches is very similar to that of the a.s.o.t. fibres with a characteristically spoked appearance. The basal ring also receives some short collaterals from a.s.o.t. fibres in the i.r.t. Some a.g.t. fibres also send projections into the initial

part of the pedunculus that branch in the regions where K I and K II cell types possess dendritic spines and knobs.

(*e*) *Distribution of inputs within the calycal zones*

As a result of the distribution of the fibre branches from the ring tracts within the calyx, the lip receives an input almost exclusively derived from the antenna while the collar derives a

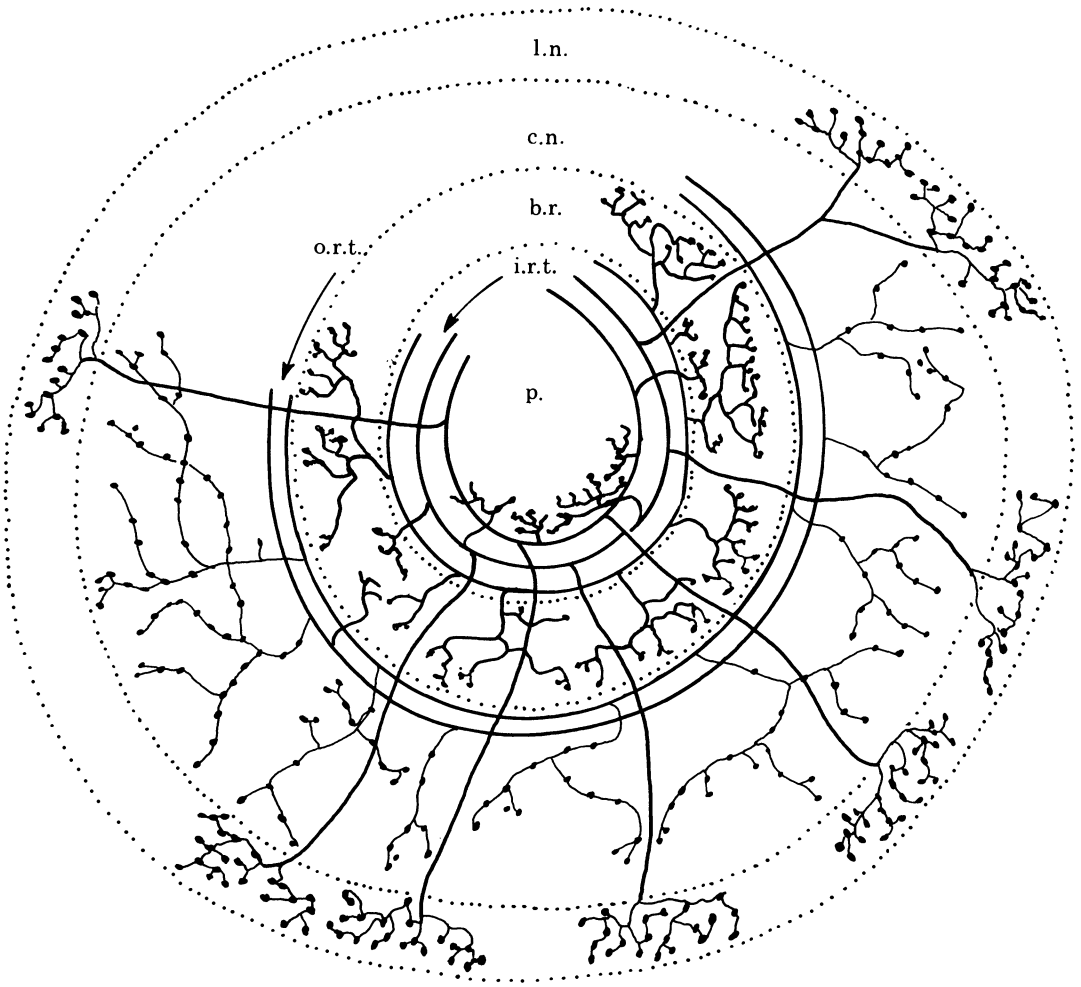

FIGURE 46. A diagrammatic representation (not to scale) of a median calyx to show the distribution of branches from fibres in the inner and outer ring tracts (i.r.t. and o.r.t.). Individual fibres running in the i.r.t. or o.r.t. have different branching patterns.

large part of its input from the compound eye. The basal ring, in addition to receiving input from collaterals of a.g.t. and a.s.o.t. fibres running to the lip and collar, also receives an exclusive input from some of the larger-diameter a.g.t. neurons (figure 44, plate 6). Individual a.s.o.t. and i.r.t. fibres within the calyces have radial branches that project to different sectors of the calycal zones' circumference (figure 46).

Individual receptors belonging to large chemoreceptive fields such as those found on insects' antennae may convey either highly specific information ('specialist' cells) or general information ('generalist' cells) concerning the nature of the stimulant chemical (Kaissling 1971). It is reasonable to speculate that the convergence of particular receptor terminal geometries within

the same glomerulus may represent the association of either 'specialist' fibres with identical responses or 'generalist' fibres with similar spectrums. An across-fibre analysis of information from 'generalist' fibres within one or more glomeruli might be expected to lead to rather more specific responses within following a.g.t. interneurons. Drongelen *et al.* (1978) point out the simple summation of unitary activity within receptors will also lead to an increased sensitivity

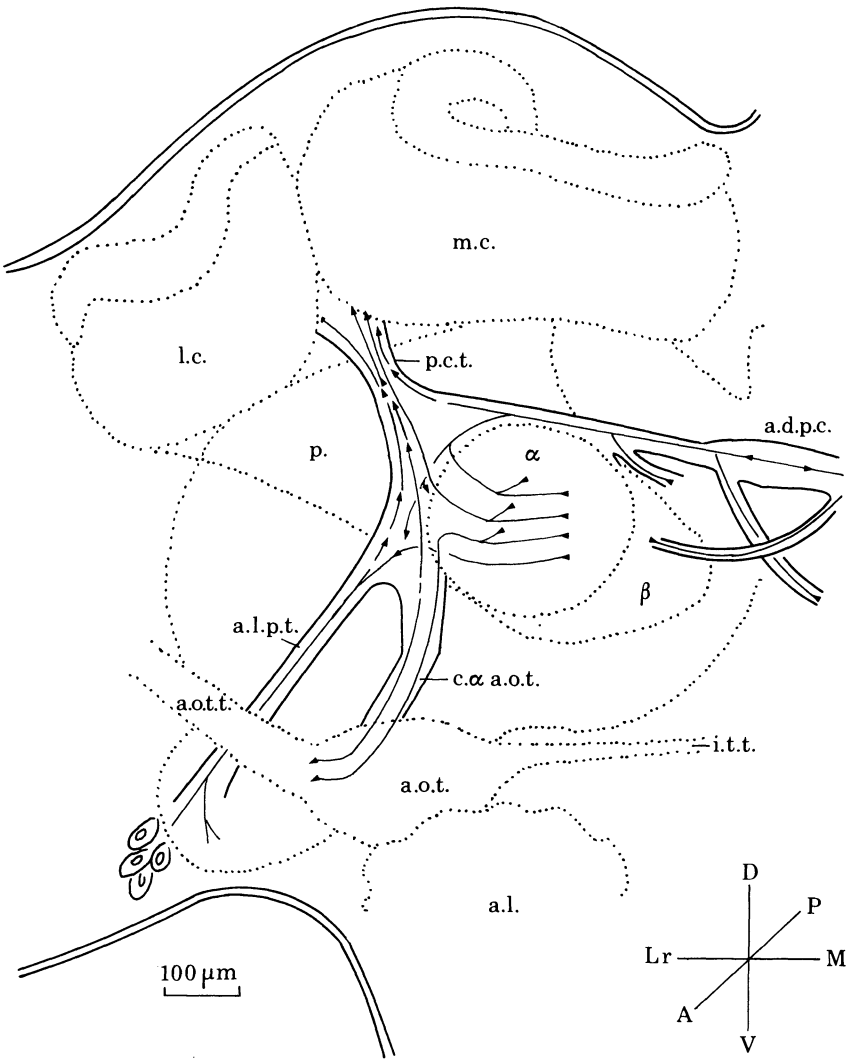

FIGURE 47. Output tracts subserving the α- and β-lobes. Diagrammatic anterior view of a half brain.

that will be dependent in degree upon the convergence ratio. A high convergence ratio has the theoretical disadvantage that the following neurons may be driven to physiological saturation at moderate concentrations, which may produce a requirement for feedback to prevent swamping of the system. The intrinsic neurons and neurons returning input to the antennal lobe from the calyces may act in part as an inhibitory network as well as part of a filtering and integrative system.

A representation of the pattern of activity within the a.g.t. neurons will be distributed across K cell dendrites of the lip and will be available to extrinsic neurons in the lip layer K cell

projections of the pedunculus and α- and β-lobes. The response characteristics of extrinsic chemosensory neurons will be dependent upon the geometry of their dendritic fields within the peduncular projections of lip K cells. Theoretically such extrinsic neurons have the capability to sample the activity induced in an area as small as a single K cell domain or as large as the entire volume of the lip. The number, density and distribution of the radial branches of the a.g.t. to the lip are such that even a single domain must receive input from more than one a.g.t. neuron. In terms of dendritic domains, information transfer to the lip can be viewed as a convergent process. The following section considers the architecture of the dendritic fields of output extrinsic neurons in the mushroom bodies. The significance of visual input to the calyces is considered in the final discussion.

(ii) *Output fibres*

(*a*) *Fibre tracts subserving the pedunculus and* α- *and* β-*lobes*

Tracing the tracts connecting the pedunculus and α- and β-lobes to other neuropil areas presents a number of problems. The pathways taken by fibre tracts do not necessarily mirror the connections of individual cells with processes within them. Rather, tracts may contain unique neurons with very different origins or destinations. The tracts reported here have been established as containing neurons running into the mushroom bodies and are mapped here to provide a framework into which individual neurons, perhaps stained intracellularly, can at some later date be fitted.

The pedunculus and lobes are wound about with fibres. Only a fraction of these neurons have projections that actually penetrate the mushroom bodies. Golgi and cobalt stains show that many of the encircling processes are neurites that, because of the volume of the mushroom bodies, take a rather indirect course to their cell bodies in the protocerebral rind. As a result it is often difficult or impossible reliably to follow single large neurons or small groups of fibres.

There are two major locations at which fibres leave the α- and β-lobes; one of these is situated on the α-lobes' lateral margin (the α-exit) and the other at the ventral median junction of the two lobes (the β-exit). At each of these two exit points fibres from several distinct tracts penetrate and run and divide within the mushroom body neuropils (figures 47; 48). The majority of these fibres are considered, because of their spiny dendrites and the available electron microscope evidence (Schürmann 1973), to represent the major outputs of the mushroom bodies.

(A) *The* α-*exit point* (located 95–140 μm from the surface of the brain) carries fibres from four tracts leaving the lobe (figure 47). These are described below:

(1) *The anterior dorsal protocerebral commissure* (*a.d.p.c.*). This tract largely originates from neurons with dendrites in the α- and β-lobes of the mushroom bodies in one half of the brain and connects the lobes with neuropils on the opposite side. In horizontal sections it presents a peculiar looped appearance in the median protocerebrum (figure 52, plate 8). Some of the fibres in this tract may serve to connect indirectly either the calyces or both the calyces and lobes, on one side, with the bilaterally symmetrical structures in the opposite half of the brain (figure 67, plate 10). Many, however, terminate in the anterior protocerebral neuropil and in the area around the opposite α-lobe.

(2) *The anterior lateral protocerebral tract* (*a.l.p.t.*). This tract runs from the α-lobe to the anterior lateral protocerebrum. It contains fibres that have dendritic fields in both the α- and the β-lobes. Some of these neurons have axons that project into the lateral protocerebrum via the a.l.p.t. while others have axons that run in the protocerebro-calycal tract (figure 51, plate 7) and collaterals and neurites in the a.l.p.t.

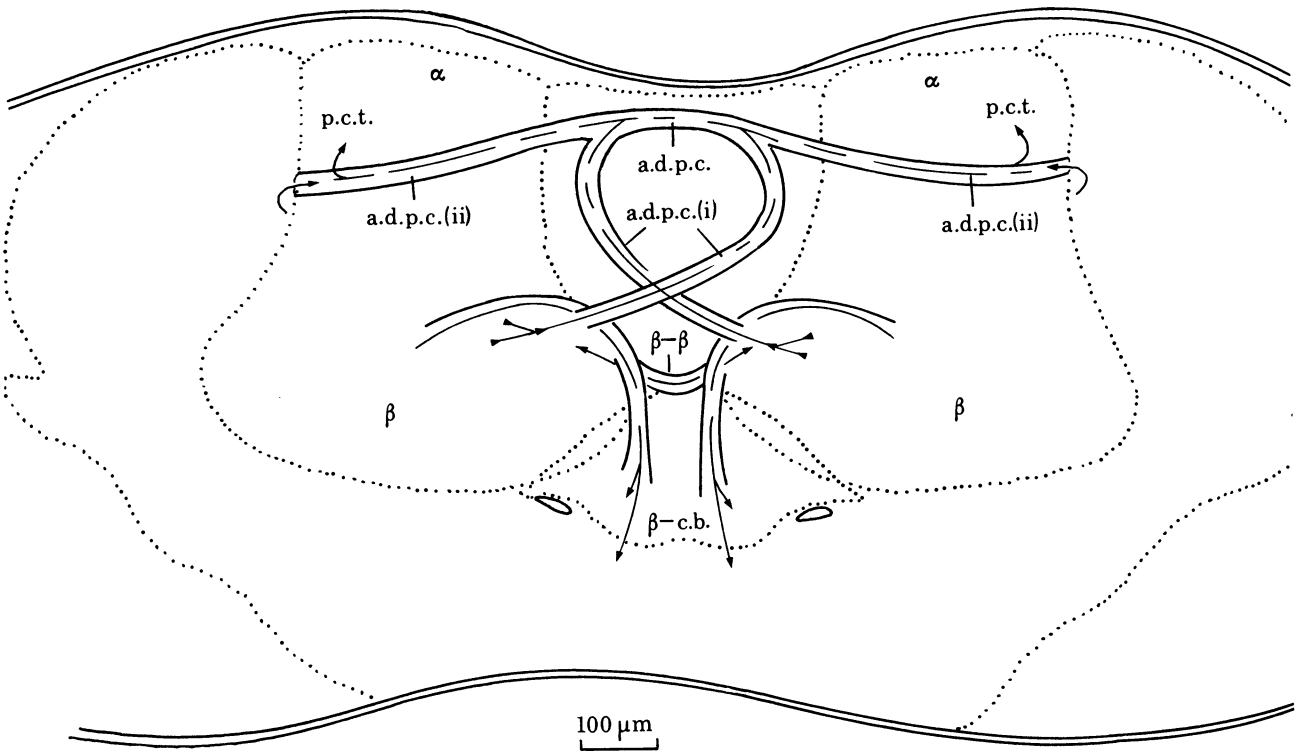

FIGURE 48. Output tracts subserving the α- and β-lobes. Reconstruction from a series of 25 horizontal sections 10 μm thick.

(3) *The α-lobe to anterior optic tubercle tract* (*α-a.o.t.t.*). This tract contains neurons with dendrites in both α- and β-lobes with axons that run into the anterior optic tubercle (a.o.t.). One of these fibres has arborizations in the lateral and median protocerebrum (figure 75). In addition the α-a.o.t.t. contains fibres that pass by the ipsilateral α-lobe and arborize in the lateral and median protocerebrum, some passing into the p.c.t.

(4) *The protocerebro-calycal tract* (*p.c.t.*). The p.c.t. is formed by the grouping together of fibres from a.d.p.c., a.l.p.t. and α-a.o.t.t. In addition it contains a considerable number of feedback neurons running from the α- and β-lobes into the calyces (figure 74). Together the four groups of fibres form a particularly obvious fascicle that passes under and between the two calyces. The p.c.t. divides about the two peduncular origins under each calyx, and fibres from it penetrate both the calyces and the pedunculus. Calycal input fibres within the p.c.t. arborize in the collar and lip. The collar processes of p.c.t. neurons can be readily distinguished from those of the o.r.t. as they penetrate the neuropil from above and are additionally particularly obvious in reduced-silver preparations because of the density with which they stain.

(B) *The β-exit point* (located 190–240 μm from the brain surface) carries fibres from three tracts (see figure 48). Additionally a single large fibre (diameter 10–15 μm) leaves the lobes accompanied by a number of smaller axons (figure 53, plate 8). The large cell's soma is located in the anterior rind just below the front of the α-lobe and has huge dendrites in both the α- and β-lobes themselves and the anterior median and lateral protocerebrum on either side of the α-lobe. The smaller cells' neurites form a group running into the anterior protocerebral rind alongside the large fibre. This group of neurites is in an equivalent position to that of Vowles' (1955) tract 10 which he describes as running from the 'antennal glomerulus' to the α-lobe. The three fibre tracts forming the β-exit point are listed below:

(1) *Anterior dorsal protocerebral commissure* (*branch* i). Immediately posterior to the point at which the single large fibre described above leaves the α- and β-lobes, branches of the a.d.p.c. form a conspicuous X-shaped chiasm (figures 54, 55, plate 8) as they run, from the α- and β-lobes, through the median protocerebrum, to the α-lobe and the neuropil around it, in the opposite half of the brain.

(2) *β-lobe to central body tract* (*β-c.b.t.*). Twenty or thirty fibres 6–8 μm in diameter leave the α- and β-lobes via the ventral median exit point and run *toward* the lower part of the central body (the fan-shaped body). They turn sharply posterior after leaving the lobes and run along the inner surface of the β-lobe.

(3) *β-lobe to β-lobe tract* (*β–βt.*). This is a small U-shaped tract that links the β-lobes on both sides of the brain just in front of the anterior neuropil of the central body (figure 54).

(*b*) *Isolated fibre groups penetrating the α-lobe* are found at several points along its length (figures 56–61, plate 9). The most anterior of these, 25–40 μm from the brain's surface, consists of fine fibres which ramify across the whole extent of the α-lobe (figures 47; 56) and enter a very superficial tract that runs across the midline from the lateral protocerebrum and then passes over the front face of the opposite α-lobe to enter the lateral, inferior and anterior protocerebral rind. Another small group of axons penetrate the α-lobe at a depth of 140 μm on its ventro-median margin; the group consists of four or five fibres, of diameter 5 μm or more, with branches that form flat tree-like patterns in the lower part of the lobe (figures 48; 59). The projections of these fibres outside the α-lobe have not been traced. A further bundle of five or six 5 μm fibres penetrate the α-lobe on its ventrolateral edge and extend branches up through the lobe from processes that traverse its diameter (figures 60; 61).

Description of plate 7

Figure 49. Ethyl gallate-stained vertical section through the α-lobe 100 μm from the anterior surface of the brain. Numerous processes can be seen to penetrate the lobe from its lateral margin and form horizontally oriented series of branches. Note the conspicuous banding of the lobe. Bands numbered as in figure 10.

Figure 50. Horizontal section from a Golgi-Ribi-stained preparation, showing two large fibres leaving the α-lobe on its lateral margin. These cells both run back through the α-lobe, branching in its dorsal layers, and then arborize within the posterior layers of the β-lobe. Figure 72 is a reconstruction of one of these fibres.

Figure 51. Vertical section from a Golgi–Ribi-stained preparation, showing three fibres that form part of the protocerebro-calycal tract between the α-lobe and the calyces, leaving the α-lobes laterally. The processes on the left of the α-lobe are projections of these cells running in the anterolateral protocerebral tract. Figure 73 is a reconstruction of a similar fibre from another preparation.

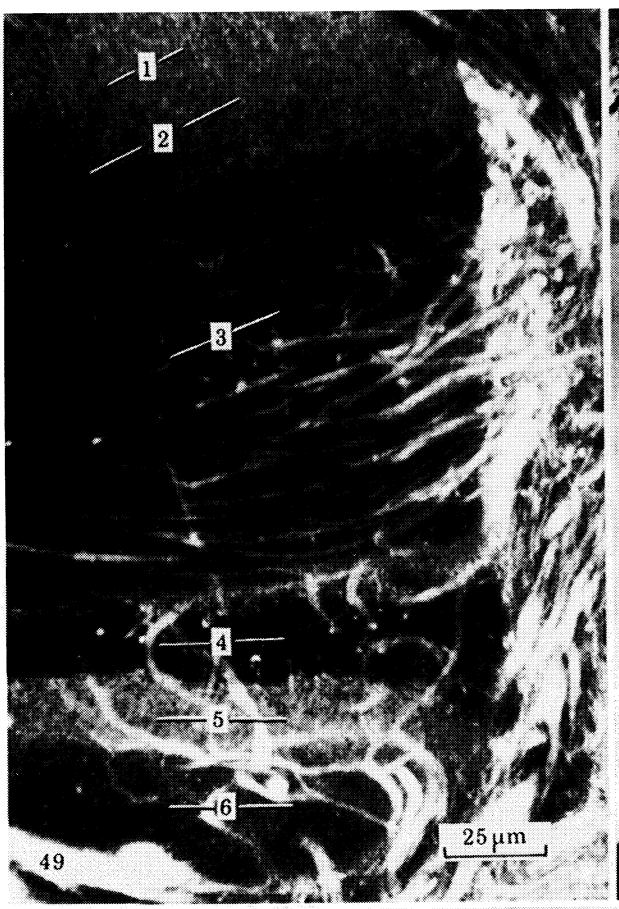

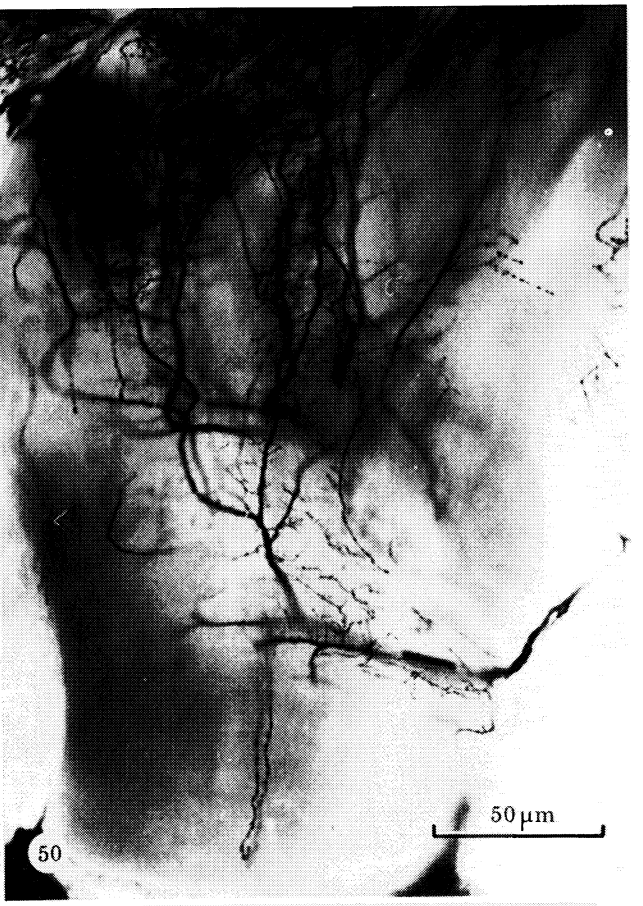

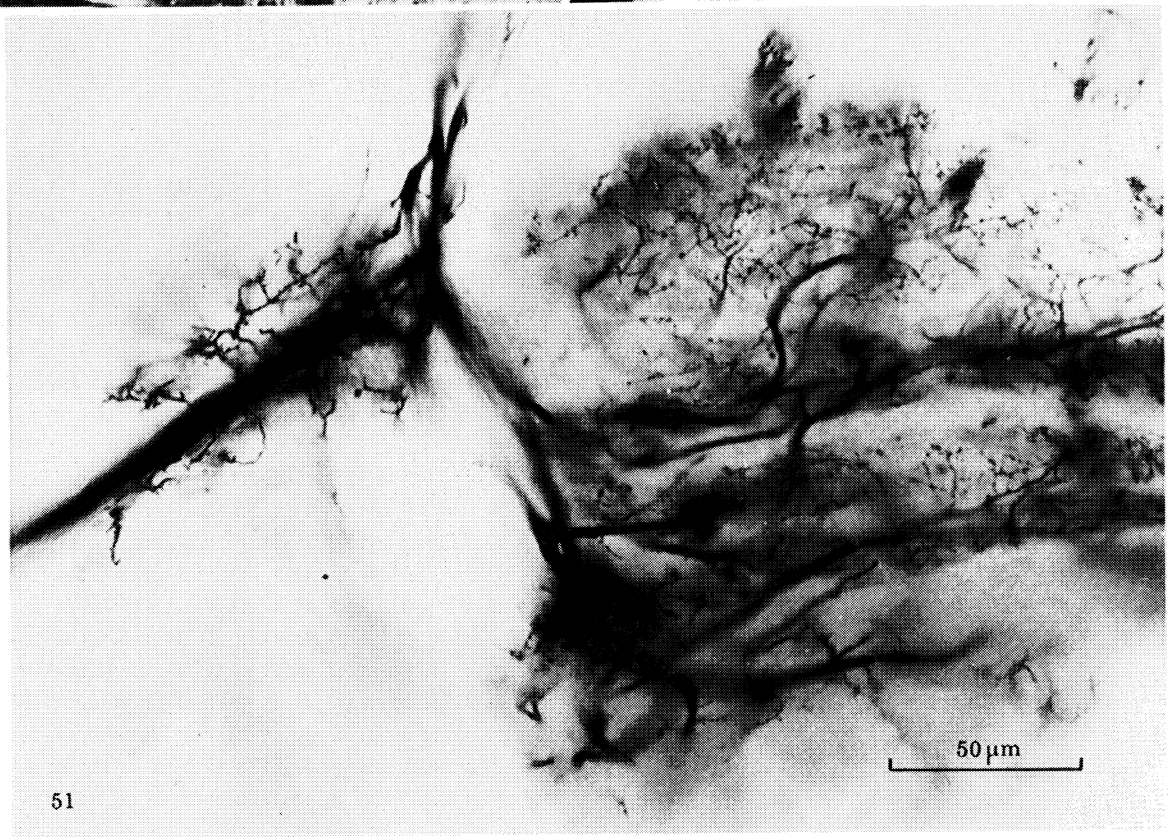

(*Facing p.* 340)

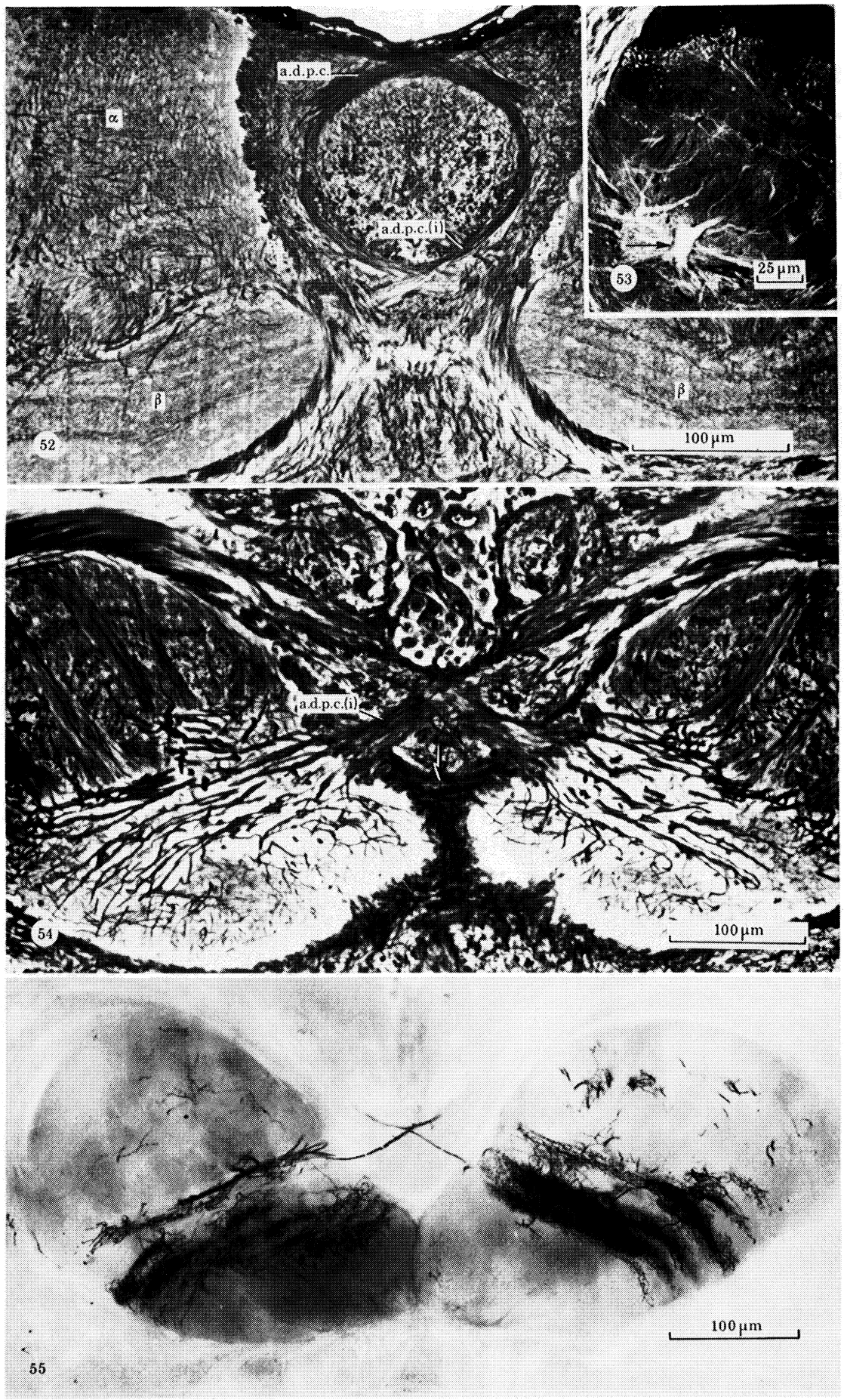
a.d.p.c.
α
a.d.p.c.(i)
β
52
100 μm
53
25 μm
β
a.d.p.c.(i)
54
100 μm
55
100 μm

Description of plate 8

Figure 52. Silver-stained horizontal section of the brain, showing the anterior dorsal protocerebral commissure (a.d.p.c.) in the median protocerebral neuropil between the α- and β-lobes (α and β). Note the striated appearance of the β-lobe.

Figure 53. Ethyl gallate-stained vertical section through the α-lobe 190 μm from the anterior surface of the brain, to show the entry of a single large fibre (diameter 15 μm) (arrowed).

Figure 54. Silver-stained vertical section, 220 μm from the brain's anterior surface, showing the chiasm of the tracts from the β-lobe to the anterior dorsal protocerebral commissure (a.d.p.c. (i)). Note the fibres joining the β-lobes (β–β) (arrowed).

Figure 55. Vertical section from a Golgi–Ribi preparation at the same level as figure 52. Two symmetrically displaced fibres in the anterior dorsal commissure are stained along with their lavered dendrites in the β-lobes.

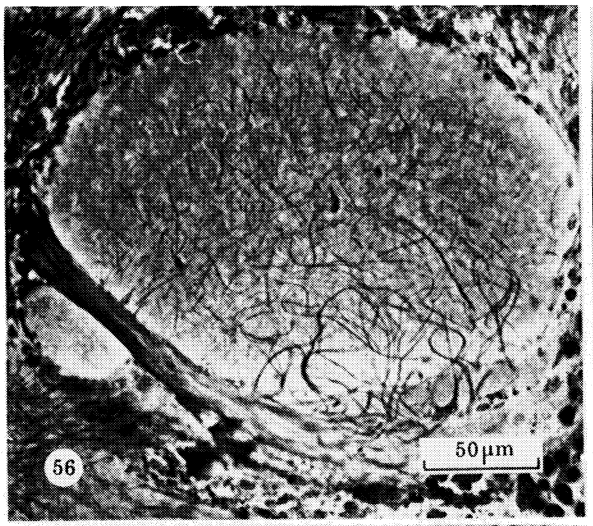
56
50 μm

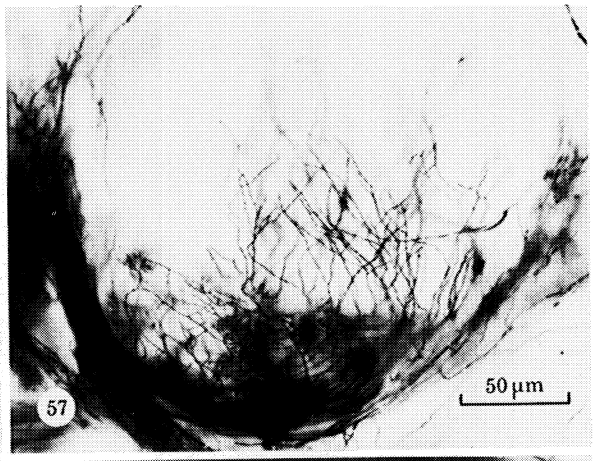
57
50 μm

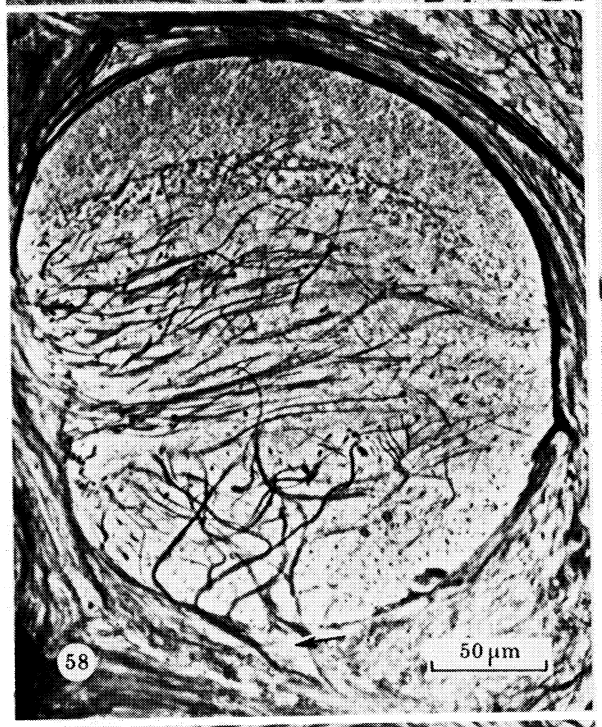
58
50 μm

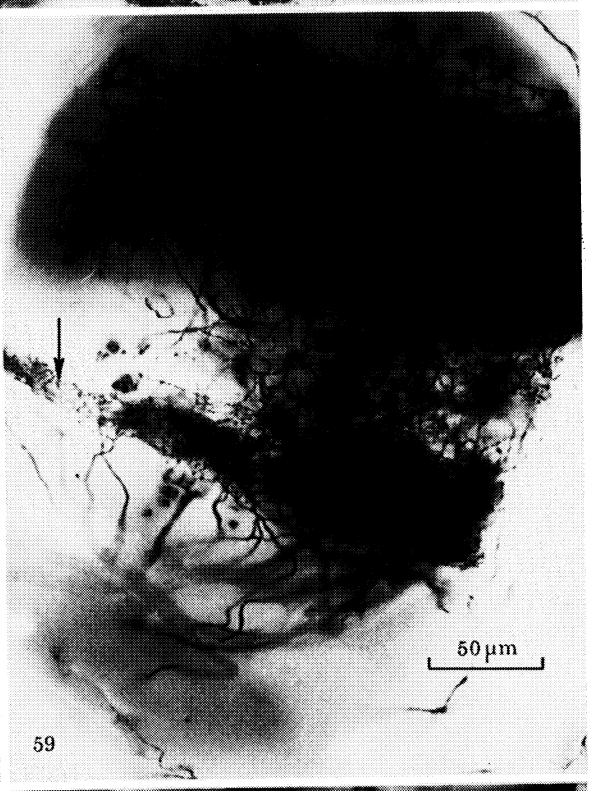
59
50 μm

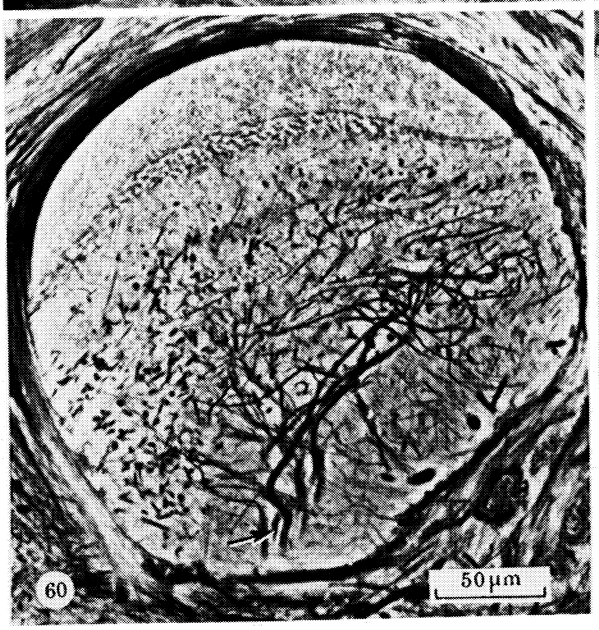
60
50 μm

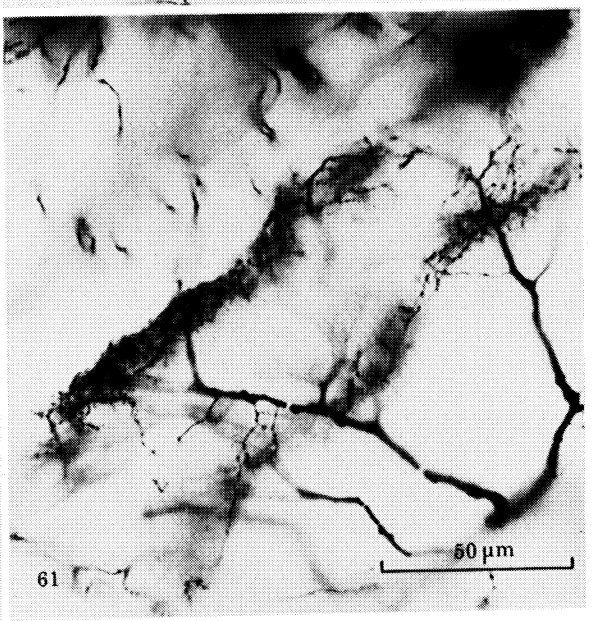
61
50 μm

Description of plate 9

Figure 56. Silver-stained vertical section through the α-lobe 32 μm from the anterior surface of the brain, showing some of the fine fibres that ramify throughout the lobe at this depth.

Figure 57. Vertical section showing Golgi–Colonnier-impregnated fibres ramifying through the α-lobe at the same level as in figure 56.

Figure 58. Silver-stained vertical section through the α-lobe at 140 μm from the brain's anterior surface. Note the fibre group (arrowed) and the fibrous layer near the lobe's dorsal surface.

Figure 59. Vertical section from a Golgi–Ribi preparation showing the same fibre group as in figure 58 giving rise to banded dendritic fields (arrowed).

Figure 60. Silver-stained vertical section through the α-lobe at 150 μm from the brain's anterior surface. Note the fibre group (arrowed).

Figure 61. Vertical section from a Golgi–Kopsch-stained preparation showing the multistratified banded dendrites of one of the cells in the fibre group shown in figure 60.

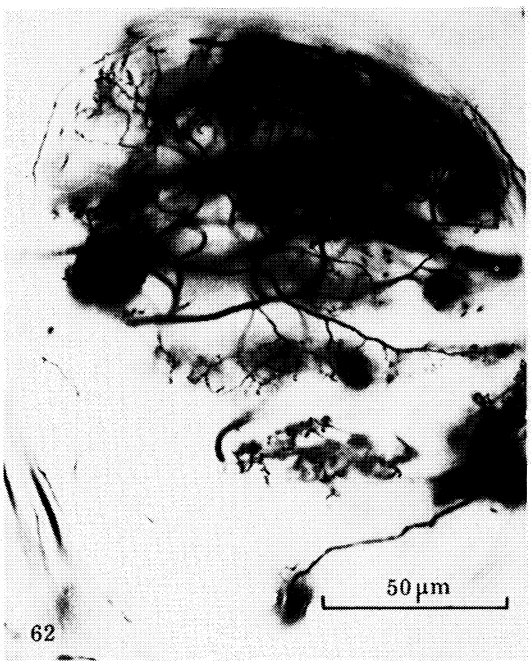
50 µm
62

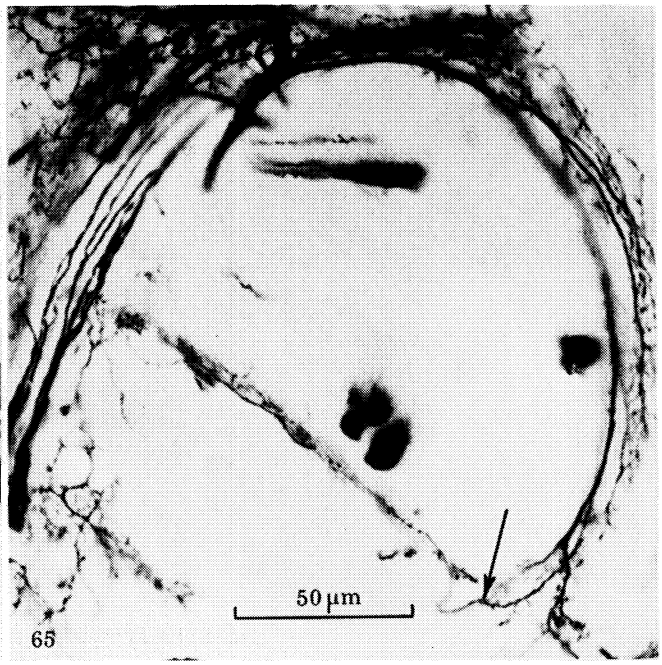
50 µm
65

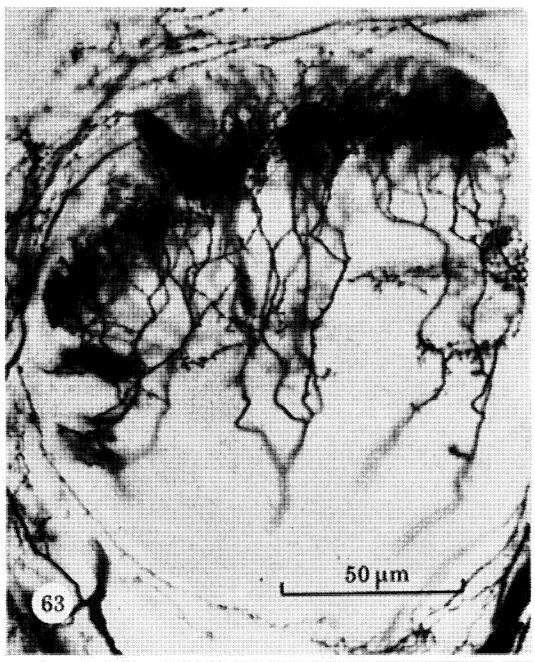
50 µm
63

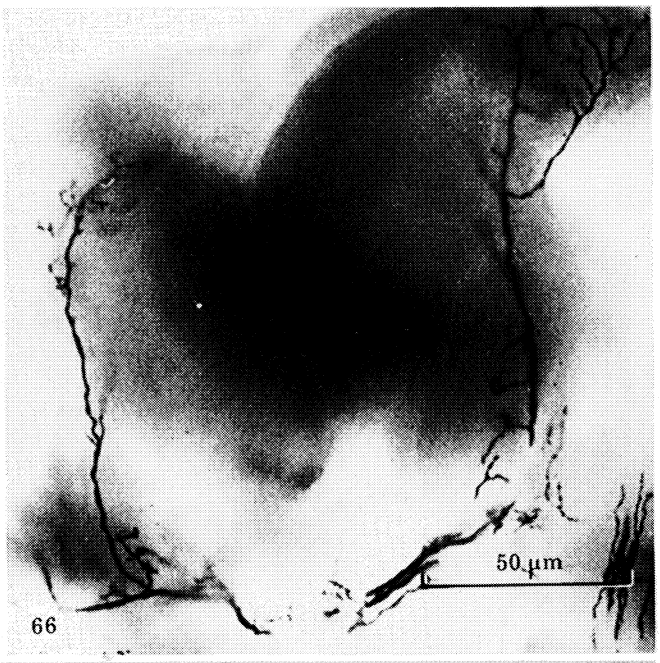
50 µm
66

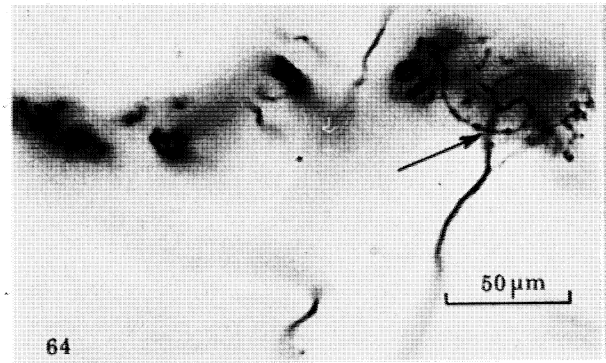
50 µm
64

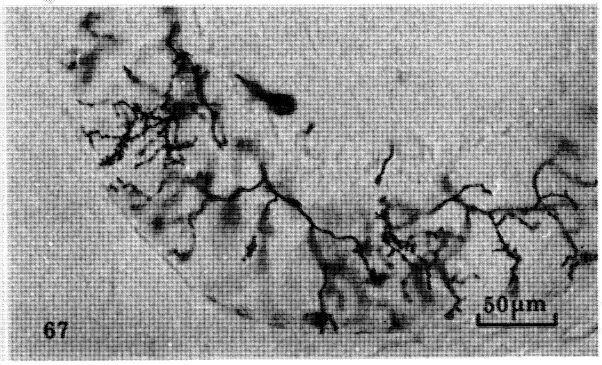
50 µm
67

Description of plate 10

Figure 62. Vertical section from a Golgi–Colonnier preparation through the α-lobe, showing multistratified banded dendritic fields of cells running to the lateral protocerebrum.

Figure 63. Vertical section from a Golgi–Colonnier preparation through the α-lobe, showing the stratified banded dendritic field of a small neuron running to the median protocerebrum.

Figure 64. Vertical section through the α-lobe from a Golgi–Colonnier preparation. The 'rosetted' ending of a small stratified banded cell is arrowed.

Figure 65. Vertical section through the α-lobe from a Golgi–Colonnier preparation. A large median protocerebral interneuron gives rise to a collateral (arrowed) that forms a small stratified banded dendritic field within the lobe.

Figure 66. Vertical section through the α-lobe from a Golgi–Ribi preparation, showing the calycal arborization of a feedback neuron from the protocerebro-calycal tract.

Figure 67. Vertical section from a Golgi–Kopsch preparation, showing the wide field endings of a neuron from the anterior dorsal protocerebral commissure in the collar zone of the medial calyx.


p.c.t.
a.c.
50 μm
68

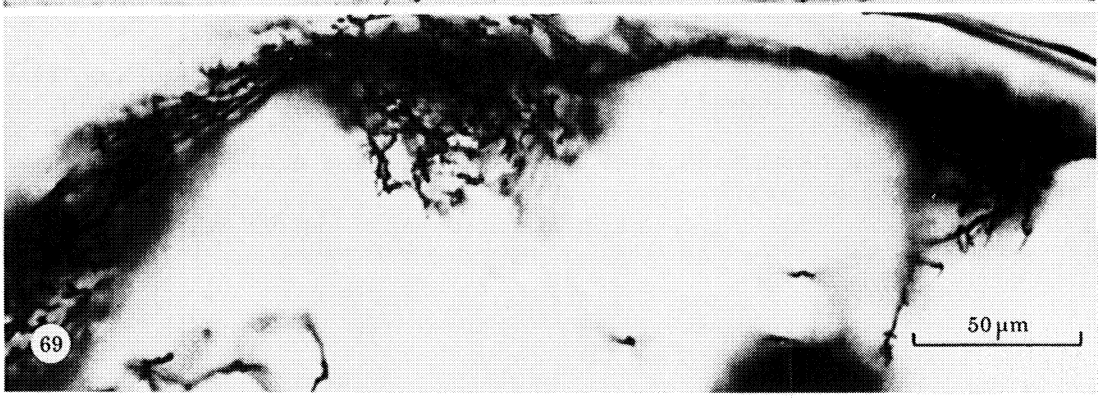
50 μm
69

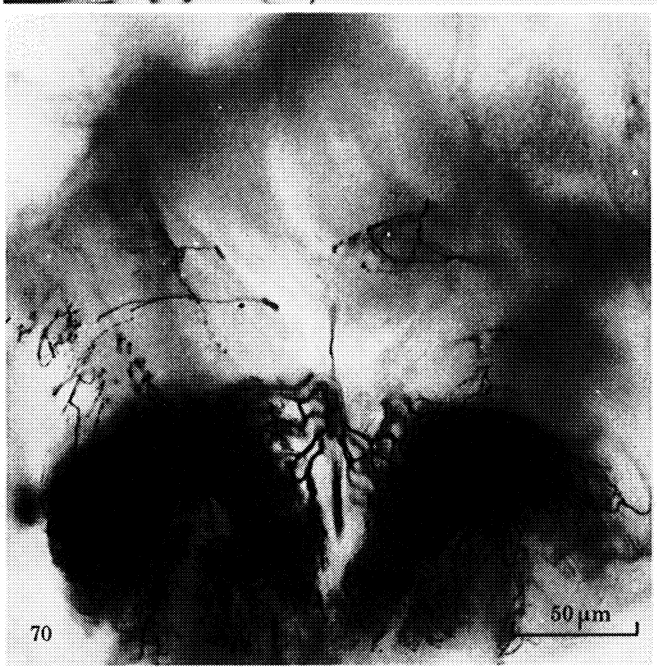
50 μm
70

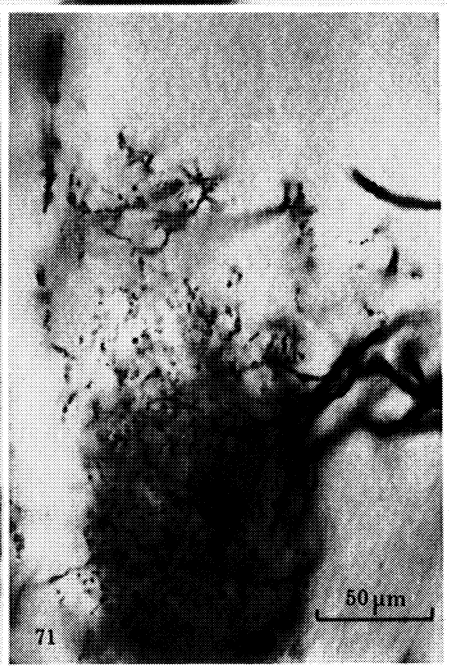
50 μm
71

(iii) *Individual fibre arrangements within the* α- *and* β-*lobes*

(*a*) *Large extrinsic neurons*

Particular extrinsic axons within both the pedunculus and the α- and β-lobes have branches restricted to various levels and depths. They can be divided into two types, stratified and unstratified.

Unstratified fields are encountered only in the first 50 μm of the α-lobe, where a small group of fibres with long unbranched processes ramify throughout all of the layering pattern visible in this region.

Stratified dendritic fields of two different kinds are encountered. One type forms narrow horizontal bands across the length of the K cells' peduncular projections (figures 61; 62, plate 10; 75). A second type produces sheets of dendrites running parallel to the K cell fibres over some distance (figures 50, plate 7; 72; 73). Many of the large cells that were Golgi-stained have several dendritic fields of both types with parallel endings in some K cell layers and banded terminals in others (figures 74; 75). Golgi stains confirm the impression gained from silver stains that many individual fibres arborize in both α- and β-lobes. Additionally some cells also branch in the pedunculus and the calyx.

Large fibres penetrating the α-lobe at its lateral exit point turn across the lobe before extending numerous major branches parallel to the K cells' peduncular axes, causing the fibrous appearance of the layer near the α-lobe's dorsal surface (figures 60; 62). The branches of these cells across the α-lobe account for its horizontally striated appearance in silver- and ethyl gallate-stained sections at depths between 84 and 140 μm (figure 49). At the junction of the α- and β-lobes these cells send collaterals both ventrally into the β-lobe and dorsally into the pedunculus. Fifteen cells, each with a unique geometry, but taking the course described above, have been stained. Some of these cells branch throughout a single α-lobe layer, then follow the layer through the peduncular division into the corresponding layer within the β-lobe and the pedunculus (figures 50; 72; 73). Others possess dendritic branches running through the α-lobe forming a parallel sheet in one layer, and then branching in the β-lobe and pedunculus to form conspicuous bands of dendrites at different levels and depths within the neuropil. Stratified extrinsic neurons branching at different points dorsoventrally and at different depths anteroposteriorly present a distinctive stepped appearance (figure 75). Some of the large cells stained could be traced from the protocerebro-calycal tract into the calyces via the i.r.ts, where their distinctive thick blebbed branches penetrate one or more of the calycal zones from the dorsal surface of the neuropil (figures 66, plate 10; 74). Others of these neurons extend branches from the ring tracts into the pedunculus.

Description of plate 11

Figure 68. Vertical section from a Golgi–Ribi-stained preparation, showing fibres in the anterior commissure (a.c.) with collaterals that arborize in the pedunculus. The protocerebro-calycal tract is visible above the commissure.

Figure 69. Vertical section from a Golgi–Colonnier-stained preparation, showing a small fibre in the anterior commissure arborizing among the fibres running over the peduncular surface and arborizing in the pedunculus at intervals.

Figure 70. Vertical section from a Golgi–Ribi preparation, showing a set of intrinsic anaxonal fibres and their dense dendritic fields within the pedunculus.

Figure 71. Detail illustrating density of spined dendritic endings of the anaxonal neurons shown in figure 70.

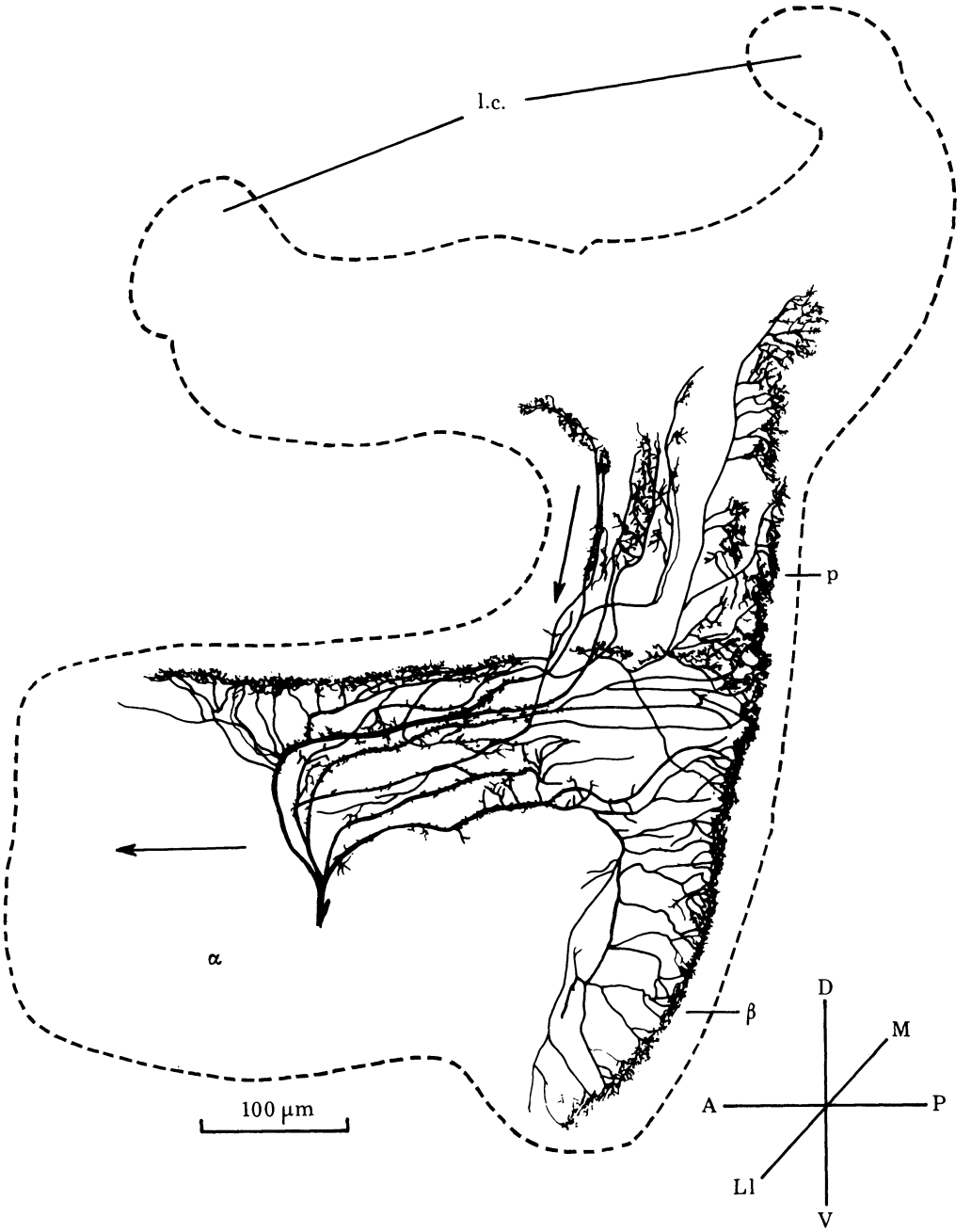

FIGURE 72. Reconstruction of a Golgi–Ribi-stained neuron that leaves the α-lobe on its lateral margin and runs through to the β-lobe. The cell arborizes within the same layers of K cells in the dorsal part of the α-lobe as it does in the posterior β-lobe. The long axis of the K cell peduncular projections are shown by arrows.

Individual fibres of the a.d.p.c. leaving the α- and β-lobes at the point of peduncular division have arborizations in both the α- and the β-lobes. These neurons have a similar range of branching patterns to those leaving the α-lobe at the lateral exit point described above. A curious feature of some of the a.d.p.c. fibres, and some of the stratified cells leaving the lateral margin of the α-lobe, is the reduction in the spacing between successive dendritic stratifications.

In a single instance it was possible to follow the axon of a stratified a.d.p.c. neuron from the α- and β-lobe to the calyx on the opposite side of the brain, where it terminated in heavily blebbed endings within the collar. Within the α- and β-lobes fibres of the p.c.t. and a.d.p.c. are

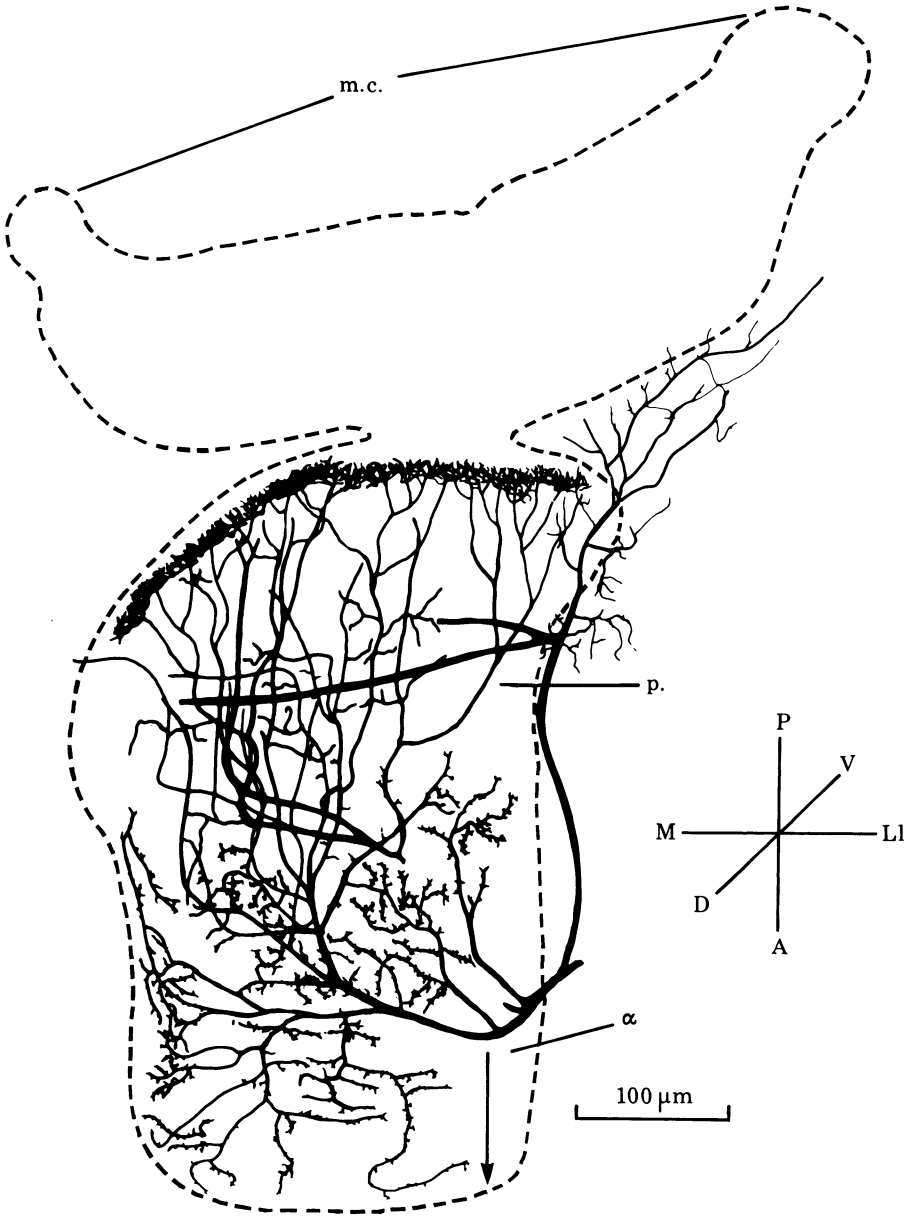

FIGURE 73. Reconstruction of a Golgi–Ribi-stained neuron leaving the α-lobe laterally and arborizing extensively within the dorsal layers of the α-lobe and the posterior layers of the β-lobe. The long axis of the K cell projections is indicated by an arrow in the α-lobe and projects perpendicularly from the page in the β-lobe. Note projection external to the mushroom body neuropil to fibre weft beneath the calyces.

heavily spined, suggesting that they are postsynaptic within these neuropils. These fibres of the p.c.t. and a.d.p.c. represent feedback loops from the ipsilateral and contralateral α- and β-lobes to the calyx.

Unfortunately none of the fibres linking and α- and β-lobes to the central body (β–c.b.t.)

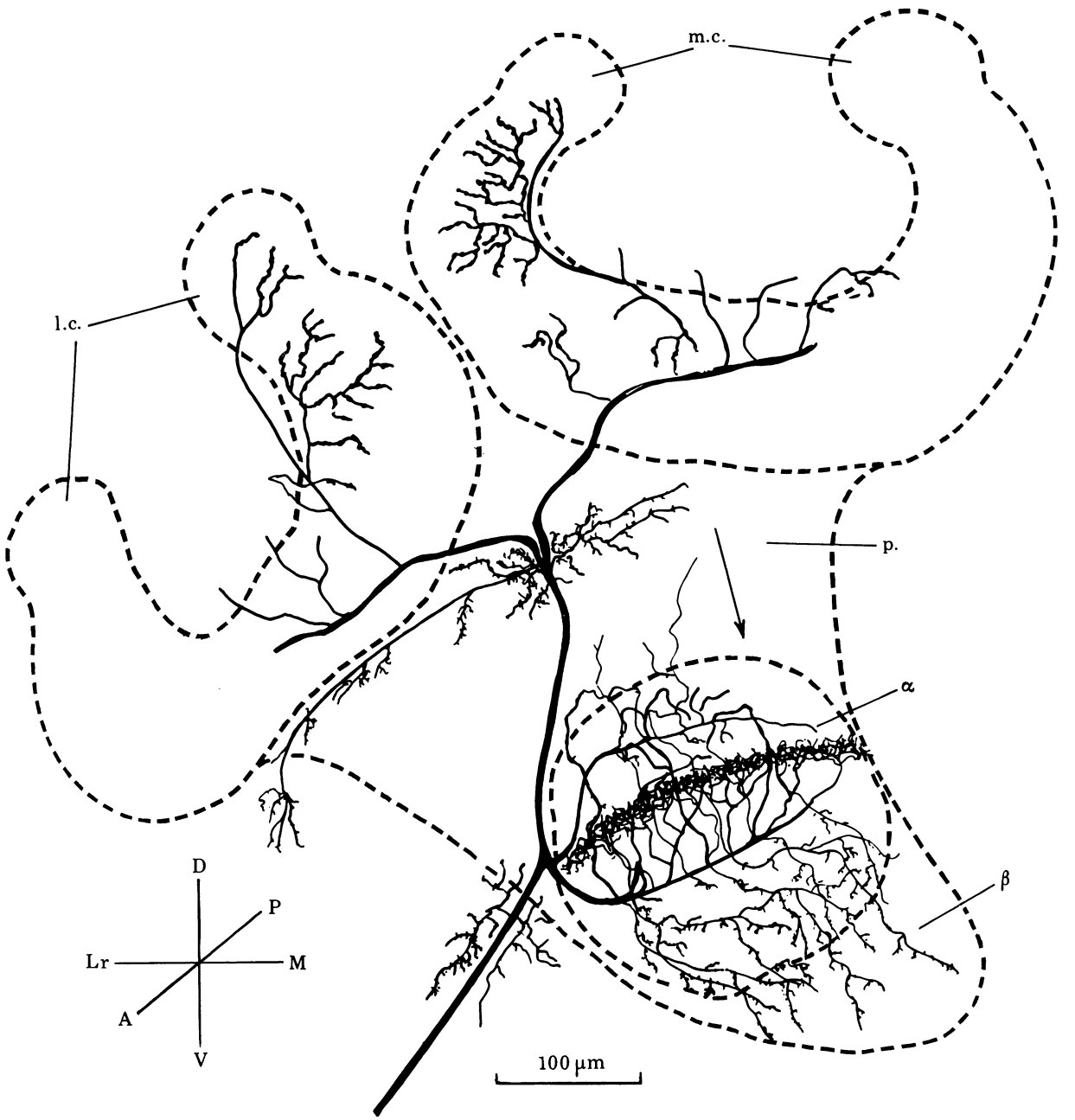

FIGURE 74. Reconstruction of a Golgi–Ribi-stained neuron running between the α- and β-lobes and the calyx via the protocerebro-calycal tract. Note the banded dendritic field in the α-lobe, the parallel field in the β-lobe, and the projection into the fibre weft beneath the calyces. The long axis of the K cells in the pedunculus and β-lobe is indicated by an arrow and projects perpendicularly from the page in the α-lobe.

were completely stained. The impression gained from silver stains and partial Golgi impregnations is that these cells have fan-shaped arborizations in the lower part of the central body and both parallel and banded endings in the lobes. However, in the absence of more conclusive evidence this connection is best regarded as tenuous.

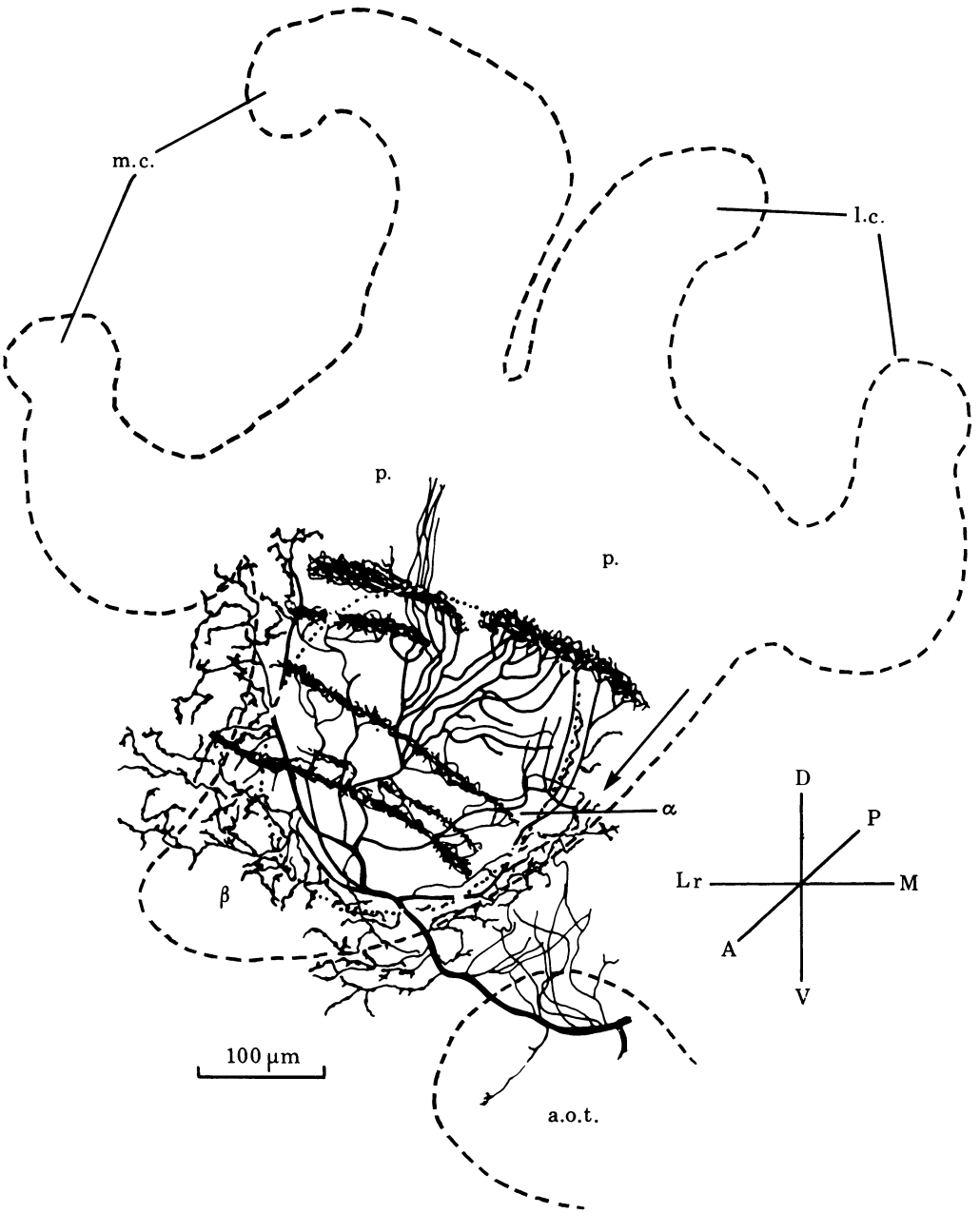

FIGURE 75. Reconstruction of a Golgi–Ribi-stained neuron running from the α- and β-lobes to the anterior optic tubercle (a.o.t.). Note the multistratified banded terminals in the β-lobe in the median protocerebrum. The K cell's long axis in the pedunculus is indicated by an arrow.

(*b*) *Small extrinsic neurons*

Silver stains show that a large proportion of the output fibres of the mushroom bodies are of small diameter. Unfortunately very few of these fibres were Golgi-stained completely by any of the techniques used in this study. It was clear from a number of preparations that small dendritic branches within the mushroom bodies derived from partial impregnation of much larger cells (figure 65, plate 10). Although few small fibres stained completely it was often

possible to correlate the Golgi-stained neurons with fibre groups found in silver stains (figures 56–61). Small neurons were traced into the tangled neuropil of lateral and median protocerebrum (figure 63, plate 10) but no details are available with regard to their specific associations. The basic configuration of the small cells' dendritic fields is similar to those of the large neurons described above, with most of the arborizations stratified; however few small cells were found running into the β-lobe or arborizing within both lobes. Small fibres in the anterior commissure (figures 68, 69, plate 11) running around the pedunculus were stained that possess projections into the fingers of K cell fibres that form the α-lobe. The arborizations of these cells form discrete bunches of dendrites along the length of the fibres as they pass around the pedunculus. Neurons running in this commissure also send collaterals into the collar via the o.r.t.

(*c*) *Anaxonal neurons*

In addition to neurons running within distinct tracts external to the mushroom bodies, a set of anaxonal fibres was stained that arborize solely within the mushroom body neuropils. Each of these cells branches in both halves of the pedunculus. The neurites from the two arborizations take a distinctive path to their somata in the posterior protocerebral rind, running beneath the calyces between the two peduncular halves before they fuse above the α-lobe. The arborizations of these cells lie just below the calyx with huge stratified fields within some layers and narrow parallel fields in others (figures 70, 71, plate 11). Each major branch collects from several subfields and sends collaterals both within the pedunculus and along its external surface to the calyx where they terminate in blebbed endings in all three calycal zones.

(*d*) *Feedback loops to the calyces*

Feedback loops form a distinctive feature of the organization of the extrinsic neurons of the mushroom body. All of the tracts running from the lateral exit point of the α-lobe contain fibres that send projections back into the pedunculus and calyces. Fibres in the protocerebro-calycal tract connect the calyces and pedunculus directly with the α- and β-lobes. Homberg & Erber (1979) have recorded and stained four neurons running in the p.c.t., and shown them to have a feedback function. The neuroanatomical study presented here suggests that such feedback fibres are present in considerable numbers and that numbers of other potential loops exist.

The a.d.p.c. connects the calyces and α- and β-lobes of one side of the brain with the bilaterally symmetrical neuropils on the other. This pattern of connection may represent a further series of feedback loops involving the K cells of both mushroom bodies. In the locust and cricket potential feedback fibres have been observed in a tract that runs between the α-lobe and the calyx similar to those described above (personal observation; Wadepuhl 1980). The γ-tract in the Lepidoptera (Pearson 1971) forms a potential feedback pathway from the γ-lobe to the calyces. Pearson however suggests that the direction of conduction in the γ tract is away from the calyces.

Other tracts associated with the mushroom bodies can also be considered as part of a series of longer feedback pathways involving sensory neuropils. The fibres connecting the α- and β-lobes to the a.o.t. may form part of such a long loop in which output from the lobes is fed into the optic neuropils via the anterior optic tubercle tract, to the lobula and returned to the calyces via the a.s.o.t. This circuit would be comparable to that formed by efferent and afferent fibres within the m.a.g.t. and l.a.g.t., looping information back into the calyces via the antennal

lobes. The significance of the direct and indirect feedback pathways is considered in the discussion.

4. Discussion

4.1. *Models of mushroom body function*

Vowles (1964) developed a model of mushroom body function in which the K cells act as part of a series of reafferent loops. In this model the calyces receive input from the sensory centres and the α-lobe sends an output back to them. The β-lobe receives a copy of the information sent to the α-lobe and provides an input to the motor centres. The loops between the sensory centres and the mushroom bodies, he argues, serve to correct the motor output of the β-lobe for the prevailing, sensory input. I am unable to confirm the anatomical basis required for Vowles's model. There is no evidence to suggest that the β-lobe has specific motor, and the α-lobe specific sensory, connections. Indeed it seems most unlikely because many of the α- and β-lobe output neurons have dendrites in *both* lobes. Further, no direct pathways to the antennal and mouthpart motor neuropils within the brain exist, and cobalt infusion into the ventral nerve cord shows that none of the large (presumed directly) premotor descending interneurons of the dorsal median longitudinal tract of the thoracic ganglia have dendrites in the mushroom bodies.

The present study has confirmed Vowles's (1964) suggestion that the mushroom bodies have reafferent connections. These connections consist of two types, direct feedback inputs from the α- and β-lobes to the calyces, and possible indirect open loops in which output from the mushroom bodies is fed from the lobes to sensory neuropils that have inputs to the calyces. The latter connections form the major output pathways of the mushroom bodies. However, a large proportion of the single neurons that do not form part of distinct tracts represent potentially unlooped output pathways, as do fibres from the α and β exits that end in the anterior median protocerebral neuropil around the α-lobe and in the lateral protocerebral neuropil. A functional model of the mushroom bodies must necessarily explain their known behavioural roles, these patterns of connection and the spatial organization of intrinsic and extrinsic neuron geometries

4.2. *Spatial organization*

The projection of K cells into the pedunculus and lobes produces a polar to Cartesian transformation. This transformation can best be explained by the requirement to fit a linear array of cells into a small space. If the two paired calyces were not arranged as four separate polar neuropils a length of 5.4 mm would be required instead of 1.7 mm. The pairing of the calyces may also represent a solution to the most economic use of space. The organization of extrinsic neurons in the calyces suggests that an individual calyx is not a discrete compartment, for the majority of input fibres arborize within both calyces. Output fibres have not been observed to arborize within just half of the K cell layer in the pedunculus and lobes as one might expect if individual calyces were functional compartments.

Figure 15 shows the calyces unfolded as a series of parallel linear arrays. Within such arrays calycal extrinsic cells running in the ring tracts distribute information, via their radial branches, to several areas along the length of one or more arrays. As shown in §4.3, ring tract neurons are not all (geometrically) equivalent, for they originate in specific glomeruli within the antennal lobe and from different areas within the optic neuropils and distribute their information differentially within the calyces. Calycal input activity is therefore expressed as a series of patterns across the calycal arrays.

It seems likely, because of the huge degree of overlap between neighbouring K cell dendritic fields within individual calycal zones, that the functional unit of the mushroom bodies is a bundle of K cells rather than a single K cell. Probably many K cells pool their information by forming a bundle of fibres that represents a more discrete, but coarser, unit of the calycal output image. Support for the concept that assemblies of K fibres, forming calycal domains, are the functional unit, comes from the clear bundling of the cells within the calyx and the presence of some extrinsic neurons with 'rosetted' endings in the α- and β-lobes that appear suited to sampling activity within fibre bundles (figure 64, plate 10). In addition the electron microscope studies of Schürmann (1974) show repeated reciprocal synapses between neighbouring K cell projections along their length. The extent of such synaptic coupling, and its inhibitory or excitatory nature, remains to be investigated. Excitatory coupling would serve to pool information in groups of linked K cells further to the pooling already achieved by virtue of dendritic overlap in the calycal array. Inhibitory coupling would produce a sharpening effect highlighting activity in the most active fibre within the group. The grouping and coupling of K cells in bundles may be important in the suppression of synaptic noise. Excitatory coupling will reduce temporally uncorrelated noise, while inhibitory coupling will reduce correlated noise.

The calycal zones into which input neurons project depend upon the modality of their origin. The anatomical techniques used in this study have shown a restriction of chemosensory input to the lip zone and optic input to the collar, the basal ring appearing to receive both these inputs. Erber's (1978) and Vowles's (1964) recordings show that in addition tactile stimulation of both the abdomen and antenna can elicit electrical responses in the calyces. While calycal inputs show a distinct zonation, local circuits and feedback neurons may produce some subdivision and/or mixing of the input modalities.

4.3. *Behavioural roles*

Huber (1955, 1959, 1960), Elsner & Huber (1969), Rowell (1963) and more recently Otto (1971), Howse (1974) and Wadepuhl & Huber (1979) have examined the role of brain neuropils in the control of insect behaviour, using lesioning and stimulating techniques. The evidence of these experiments suggests that the mushroom bodies are responsible for the selection of different behaviour patterns. Momentary stimulation at a single locus in the mushroom bodies can elicit complex sequences of behaviour that include, in the cricket, foraging, digging and singing (Otto 1971).

The decision to implement a complex sequence of behaviours is unlikely to result from an instantaneous assessment of the sensory surround. It is possible that the looped circuits that are represented by the mushroom bodies play some part in storing a momentarily modifiable and multi-modal image of the surround on which such decisions could be based. The timing capabilities of parallel looped circuits could be used to sequence behavioural subunits in addition to forming a basis for the comparison of temporally disparate sensory inputs.

Young (1938), as a result of a study of learning in *Sepia*, suggested that reverberatory circuits may be involved in the formation of short-term memory. In this animal and other cephalopods such as *Octopus* there are feedback circuits involving microneurons with some similarities to K cells. The importance of the mushroom bodies in memory formation in bees has been suggested by several behavioural experiments (Menzel *et al.* 1974; Martin *et al.* 1978; Erber *et al.* 1980) and also by anatomical differences in the volumes and structure of the hymenopteran calyces compared with those of other insects (Howse 1974).

Vowles (1964) suggested that the long-lasting after-effects that he recorded in response to momentary stimulation resulted from reverberatory connections between the bees' mushroom bodies and sensory centres. Erber (1978) in a detailed study of bee mushroom body extrinsic neurons found after-effects of up to several minutes duration following stimulation with scent, light or sugar-water. There is still insufficient electrophysiological information to explain how such after-effects are produced. However, the numerous looped pathways suggest that the after-effects may be the result of feedback excitation or inhibition.

4.4. *Delay and timing functions for intrinsic and extrinsic neurons*

Schürmann (1974), on the basis of Maynard's (1967) estimate of K cell conduction velocity (0.2 mm/ms, in *Periplaneta*), derived a value of 3.5 ms for the delay imposed by the K cell path length in crickets and bees. Schürmann (1973) made an interesting comparison of the neuronal arrangement of the mushroom bodies with that of the vertebrate cerebellum. He suggested that the mushroom bodies are a system for the transposition of distances into the sequential activation or inhibition of the extrinsic nerve fibres.

In Schürmann's model the Kenyon cells are acting as a clock in the millisecond range. If the structure does form the basis of a millisecond clock then it may act in a fashion analogous to that suggested for the cerebellum by Braitenburg (1977), in the coordination of rapid movements making up simple behaviour. In insects, however, the coordination of simple movements appears to be a function of the thoracic ganglia rather than the brain. In the millisecond range it is perhaps more likely that the mushroom bodies act as a system for the comparison of temporally disparate sensory inputs.

The possibilities for timing and delay functions in the mushroom bodies are greatly extended by the presence of feedback loops (see figure 76). Activity looped via a single K cell layer could be required to decay to a given threshold value which would be achieved only after a given number of cycles. Alternatively activity could be looped in several arrays of K cells, and individual extrinsic neurons or groups of such neurons could be set to detect the simultaneous arrival of patterns of excitation at different points about the loops. A prerequisite of the latter system is that the loops should have different cycle times so that significant delays may be achieved.

In a multiple-channel system within which information is reverberating and a number of extrinsic cells are used to look for the coincidence of signals at several points along the delay lines, the time to incidence (τ) is best expressed in terms of the probability (P) of the arrival of a signal within a dendritic field in each line. The probability of the arrival of a signal within an extrinsic neuron dendritic field can simply be considered as the decimal fraction of the loop's entire length that the field represents. The time to incidence in the system can be expressed as

$$\tau = t_s/P_1 P_2 P_3 \ldots P_N,$$

where t_s is the shortest cycle time.

A system capable of detecting the beating of signals within a multi-channel system could also, by following the phase angle of signals within each loop, provide a measure of elapsed time following the establishment of a particular pattern of activity within several channels. An arrangement in which delays are established by the comparison of the relative phase angles of signals in parallel circuits would be resistant to disruptive influences such as temperature changes.

4.5. *Experiments suggested by the anatomy*

A number of well defined lesioning and stimulation experiments are suggested by the anatomy. The feedback loops involve a number of cells whose activity can be readily recorded intracellularly (Homberg & Erber 1979; K. Schildberger, personal communication), and, although the minute size of the Kenyon neurons precludes intracellular recording at present,

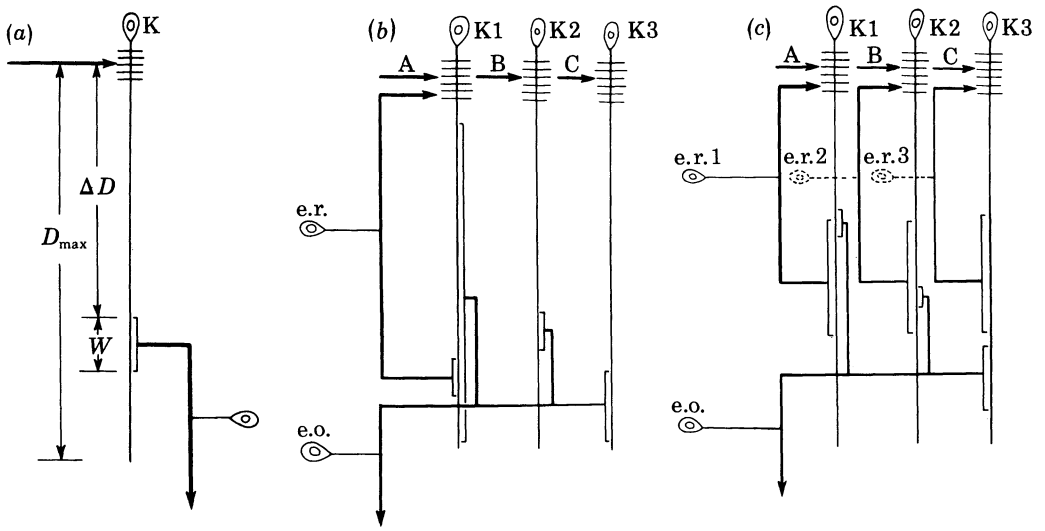

FIGURE 76. Diagrams to illustrate the timing capabilities of the mushroom body neuropil.

(*a*) K cells as simple delay lines. The maximum possible delay of about 3 ms represents the entire length of the K cell fibre (D_{max}). An extrinsic neuron can take output from the K cell at any point along its length, representing a delay *D*. Extrinsic neurons have bands of dendrites that can extend over varying lengths of K cell. The width of the extrinsic cell dendritic field (*W*) can be considered as a window that limits the resolution of the system.

(*b*) K cells as part of a delay line extended by feedback. Three Kenyon neuron delay lines K 1–3 are shown, each representing many parallel pathways, each of which receives a different input (A, B, C). One K cell line is shown looped back upon itself by an extrinsic reafferent neuron (e.r.). An extrinsic output neuron (e.o.) is shown with a dendritic field in each of the three lines. It is suggested that the feedback loop stores information for periods greater than the maximum of 3 ms represented by the length of the K cell fibre alone. The extrinsic output receives continued excitation from the line K1 but only responds when additional inputs arrive simultaneously within the dendritic fields in lines K2 and K3. The extrinsic output's dendritic window in the line K1 is large as it simply detects continued activity.

(*c*) K cell delay lines as part of a reverberatory clock. The three lines K1–3 are looped by three extrinsic reafferent cells (e.r. 1–3). A single extrinsic neuron is shown with a narrow dendritic window in each line. It is suggested that the cell responds to the simultaneous arrival of a signal within each window, a coincidence that may require several cycles within the loops before it occurs.

much may be learnt from extracellular recordings of field potentials (Kaulen 1981). A major objective of future electrophysiological experiments must be to establish the role of feedback loops in the production of the long-lasting after-effects recorded in the extrinsic neurons of the mushroom bodies. The protocerebro-calycal tract and other major feedback connections are of sufficient size to allow selective stimulation or destruction. Subsequent analysis of the insect's behaviour by the techniques perfected by Huber may elucidate the function of these curious reafferent pathways.

4.6. *The evolution of the mushroom bodies*

In most insects the mushroom bodies are concerned with the analysis of information from the antennal lobes. In the Hymenoptera, however, a major visual input is found in addition to olfactory, mechanosensory and gustatory ones. It is of interest to consider why what is apparently a primarily olfactory neuropil should have become associated with visual functions. As Sherrington (1906) and Herrick (1933) point out, the sense of olfaction has a severely restricted ability to localize the origin of a stimulus. Localization is effected by seeking behaviour or, its antithesis, avoidance. For either of these two behaviours the minimal requirement is to be able to move and to compare the concentration of a chemical at two points sufficiently distant to produce a measurable change. More complex mechanisms would, as Herrick suggests, almost certainly involve other senses with sharper localization both physiologically and anatomically. A comparable system might use a loop in which to store and compare changing features of the olfactory surround. A more demanding olfactory localization might require a chemotopic map related to the visual surround. Olfactory memory involves not only the localization of the stimulus but also the recognition of what the stimulus is. The association of individual flower patterns and colours with their scent will also require the development of pathways between the olfactory and visual system. The demonstration of such a course of insect olfactory evolution will require the patient and detailed study of fibre pathways in many insects. It is interesting to note that in the locust (unpublished observations) protocerebro-calycal feedback pathways exist and, as Honnegger & Schürmann (1975) have shown, there are pathways, if only few in number, from the optic neuropils to the calyces. The evolution of the mushroom bodies and their potential associations with memory in Hymenoptera warrant further attention.

This research was supported by a grant from the Science Research Council and the award of a Research Fellowship by the Centre for Overseas Pest Research. I am greatly indebted to Dr L. J. Goodman and Professor I. Percival, of Queen Mary College, Professor R. Menzel, Professor J. Erber and Mr P. Kaulen, of Berlin Freie Universität, Professor F. Huber of M.P.I. Seeweisen and Dr J. Patterson of St Bartholomew's Hospital Medical School for their helpful suggestions. In particular I gratefully acknowledge the help of Dr J. Altman for her work on the manuscript.

References

Braitenberg, V. 1977 *On the texture of brains.* Berlin, Heidelberg and New York: Springer-Verlag.

Colonnier, M. 1964 The tangential organisation of the visual cortex. *J. Anat.* **98**, 327–344.

Drongelen, W. van., Holley, A. & Døving, K. B. 1978 Convergence in the olfactory system: quantitative aspects of odour sensitivity. *J. theor. Biol.* **71**, 39–48.

Dujardin, F. 1850 Mémoire sur le système nerveux des insects. *Annls Sci. nat.* B **14**, 195–206.

Elsner, N. & Huber, F. 1969 Die Organisation des Werbegesunges der Heuschreche *Gomphocerippus rafus* L. in Abhängigkeit von zentral und peripheren Bedingungen. *Z. vergl. Physiol.* **65**, 389–423.

Erber, J. 1978 Response characteristics and after effects of multimodal neurons in the mushroom body area of the honey bee. *Physiol. Ent.* **3**, 77–89.

Erber, J., Masuhr, T. H. & Menzel, R. 1980 Localisation of short-term memory in the brain of the bee, *Apis mellifera. Physiol. Ent.* **5**, 343–358.

Ernst, K.-D., Boeckh, J. & Boeckh, V. 1977 A neuroanatomical study of the organisation of the central antennal pathways in insects. II. Deutocerebral connections in *Locusta migratoria* and *Periplaneta americana. Cell Tiss. Res.* **176**, 285–308.

Goll, W. 1967 Strukturuntersuchungen am Gehirn von *Formica. Z. Morph. Ökol. Tiere* **59**, 143–210.

Goss, G. C., Brandon, J. G. & Globus, A. 1980 Changes in morphology of dendritic spines on honeybee calycal interneurons associated with cumulative nursing and foraging experiences. *Brain Res.* **192**, 49–59.

Gregory, G. E. 1970 Silver staining of insect central nervous systems by the Bodian protargol method. *Acta Zool., Stockh.* **51**, 169–178.

Gregory, G. E. 1980 Alcoholic Bouin fixation of insect nervous systems for Bodian silver staining. I. Composition of 'aged' fixative. *Stain Technol.* **55**, 143–149.

Herrick, C. J. 1933 The functions of the olfactory parts of the cerebral cortex. *Proc. natn. Acad. Sci. U.S.A.* **19**, 7–14.

Homberg, U. & Erber, J. 1979 Response characteristics and identification of extrinsic mushroom body neurons of the bee. *Z. Naturforsch.* **34c**, 612–615.

Honnegger, H. W. & Schürmann, F. W. 1975 Cobalt sulphide staining of optic fibres in the brain of the cricket, *Gryllus campestris. Cell Tiss. Res.* **159**, 213–225.

Howse, P. E. 1974 Design and function in the insect brain. In *Experimental analysis of insect behaviour* (ed. L. Barton Browne), pp. 180–195. Berlin, Heidelberg and New York: Springer-Verlag.

Howse, P. E. & Williams, J. L. D. 1969 The brains of social insects in relation to behaviour. *Proc. VI Congr. IUSSI, Bern*, pp. 59–64.

Huber, F. 1955 Über die Funktion der Pilzkörper (corpora pedunculata) beim Gesang der Keulenheuschreche *Gomphocerus rufus* L. (Acridiidae). *Naturwissenschaften* **42**, 566–567.

Huber, F. 1959 Auslösung von Bewegungsmustern durch elektrische Reizung des Oberschlundganglions bei Orthopteren (Saltatoria: Gryllidae, Acridiidae). *Zool. Anz.* **23** (suppl.), 248–269.

Huber, F. 1960 Untersuchungen über die Funktion des Zentralnervensystems und insbesondere des Gehirnes bei der Fortbewegung und der Lauterzeugung der Grillen. *Z. vergl. Physiol.* **44**, 60–132.

Jawlowski, H. 1958 Nerve tracts in the bee (*Apis mellifera*) running from the sight and antennal organs to the brain. *Annls Univ. Mariae Curie-Sklodowska* **C12**, 307–323.

Jonescu, C. N. 1909 Vergleichende Untersuchungen über das Gehirn der Honigbien. *Z. Naturw.* **45**, 11–180.

Kaissling, K. E. 1971 Insect olfaction. In *Handbook of sensory physiology*, vol. 4(1), pp. 331–342. Berlin, Heidelberg and New York: Springer-Verlag.

Kaulen, P. 1981 M.Sc. thesis, Freie Universität, Berlin.

Kenyon, F. C. 1896 The brain of the bee. A preliminary contribution to the morphology of the nervous system of the arthropoda. *J. comp. Neurol.* **6**, 133–210.

Kopsch, F. 1896 Erfahrungen über die Verwendung der Formaldehyde bei der Chromsilber-Imprägnation. *Anat. Anz.* **11**, 727–729.

Mancini, G. & Frontali, N. 1967 Fine structure of the mushroom body neuropile of the brain of the roach *Periplaneta americana. Z. Zellforsch. mikrosk. Anat.* **83**, 334–343

Martin, U., Martin, H. & Lindauer, M. 1978 Transplantation of a time-signal in honeybees. *J. comp. Physiol.* **124**, 193–201.

Maynard, D. M. 1967 Organization of central ganglia. In *Invertebrate nervous systems* (ed. C. A. G. Wiersma), pp. 231–255. Chicago University Press.

Menzel, R., Erber, J. & Masuhr, T. H. 1974 Learning and memory in the honeybee. In *Experimental analysis o insect behaviour* (ed. L. Barton Browne), pp. 195–218. Berlin, Heidelberg and New York: Springer-Verlag.

Mobbs, P. G. 1978 Some aspects of the structure and development of the locust ocellus. Ph.D. thesis, University of London.

Otto, D. 1971 Untersuchungen zur zentralnervösen Kontrolle der Lauterzeugung von Grillen. *Z. vergl. Physiol.* **74**, 227–271.

Pareto, A. 1972 Die zentrale Verteiling der Fühlerafferenz bei Arbeiterinnen der Honigbiene (*Apis mellifera*). *Z. Zellforsch. mikrosk. Anat.* **131**, 109–140.

Pearson, L. 1971 The corpora pedunculata of *Sphinx ligustri* L. and other Lepidoptera: an anatomical study. *Phil. Trans. R. Soc. Lond.* B **259**, 477–516.

Ribi, W. 1976 A Golgi–electron microscope method for insect nervous tissue. *Stain Technol.* **51**, 13–16.

Rowell, C. H. F. 1963*a* A method for chronically implanting stimulating electrodes into the brains of locusts, and some results of stimulation. *J. exp. Biol.* **40**, 271–284.

Rowell, C. H. F. 1963*b* A general method for silvering invertebrate central nervous systems. *Q. Jl microsc. Sci.* **104**, 81–87.

Satzinger, H. 1980 M.Sc. thesis, Freie Universität, Berlin.

Schürmann, F. W. 1970 Über die Struktur der Pilzkörper des Insektengehirns. I. Synapsen im Pedunculus. *Z. Zellforsch. mikrosk. Anat.* **103**, 365–381.

Schürmann, F. W. 1972 Über die Struktur der Pilzkörper des Insektengehirns. II. Synaptische Schaltungen im Alpha-Lobus des Heimschens *Acheta domestica* L. *Z. Zellforsch. mikrosk. Anat.* **127**, 240–257.

Schürmann, F. W. 1973 Über die Struktur der Pilzkörper des Insektengehirns. III. Die Anatomie der Nervenfasern in der Corpora Pedunculata bei *Acheta domesticus* L. (Orthoptera): eine Golgi-Studie. *Z. Zellforsch. mikrosk. Anat.* **145**, 247–285.

Schürmann, F. W. 1974 Bemerkungen zur Funktion der Corpora pedunculata im Gehirn der Insekten aus morphologischer Sicht. *Expl Brain Res.* **19**, 406–432.

Schürmann, F. W. & Weschler, W. 1970 Synapsen im Antennenhügel von *Locusta migratoria* (Orthoptera, Insecta). *Z. Zellforsch. mikrosk. Anat.* **108**, 563–581.

Sherrington, C. S. 1906 *Integrative action of the nervous system.* New York: Scribner.
Steedman, H. F. 1947 Ester wax: a new embedding medium. *Q. Jl microsc. Sci.* **88**, 123–133.
Strausfeld, N. J. 1970 Variations and invariants of cell arrangements in the nervous system of insects. (A review of neural arrangements in the visual system and corpora pedunculata.) *Dt. Zool. Ges.* **64**, 97–107.
Strausfeld, N. J. 1976 *Atlas of an insect brain.* Berlin, Heidelberg and New York: Springer-Verlag.
Suzuki, H. 1975 Antennal movements induced by odour and central projection of the antennal neurons in the honeybee. *J. Insect Physiol.* **21**, 831–847.
Trujillo-Cenoz, O. & Melamed, J. 1962 Electron microscope observations on the calyces of the insect brain. *J. Ultrastruct. Res.* **7**, 389–398.
Vowles, D. M. 1954 The function of the corpora pedunculata in bees and ants. *Br. J. Anim. Behav.* **2**, 116.
Vowles, D. M. 1955 The structure and connections of the corpora pedunculata in bees and ants. *Q. Jl microsc. Sci.* **96**, 239–255.
Vowles, D. M. 1964 Models and the insect brain. In *Neural theory and modelling* (ed. R. F. Reiss), pp. 377–399. Stanford University Press.
Wadepuhl, M. 1980 Kontrolle des akustichen Verhaltens einheimescher Feldheufschrecken durch das Gehiren. Ph.D. thesis, University of Munich, F.R.G.
Wadepuhl, M. & Huber, F. 1979 Elicitation of singing and courtship movements by electrical stimulation of the brain of the grasshopper. *Naturwissenschaften* **66**, S.320.
Weiss, M. J. 1972 A reduced silver staining method applicable to dense neuropiles, neuroendocrine organs, and other structures in insects. *Brain Res.* **39**, 268–273.
Weiss, M. J. 1974 Neuronal connections and the function of the corpora pedunculata in the brain of the American cockroach, *Periplaneta americana* (L). *J. Morph.* **142**, 21–69.
Wigglesworth, V. B. 1957 The use of osmium in the fixation of tissues. *Proc. R. Soc. Lond.* B **147**, 185–199.
Williams, J. L. D. 1972 Some observations on the neuronal organisation of the supra-oesophageal ganglion in *Schistocerca gregaria* (Förskal) with particular reference to the central complex. Ph.D. thesis University of Wales.
Witthöft, W. 1967 Absolute Anzahl und Verteilung der Zellen im Hirn der Honigsbiene. *Z. Morph. Tiere*, **61**, 160–184.
Young, J. Z. 1938 *The Evolution of the nervous system and of the relationship of organism and environment. Essays presented to E. S. Goodrich* (ed. G. R. de Beer), pp. 179–204. Oxford: Clarendon Press.

Explanation of symbols and abbreviations

α	α-lobe
a.c.	anterior commissure
a.d.p.c.	anterior dorsal protocerebral commissure
a.g.t.	antero-glomerular tract
a.l.p.t.	anterior lateral protocerebral tract
a.l.	antennal lobe
a.n.	antennal nerve
A	anterior
a.o.t.	anterior optic tubercle
a.o.t.t.	anterior optic tubercle tract to lobula
a.s.o.t.	anterior superior optic tract
β	β-lobe
β–βt	β-lobe to β-lobe tract
β–c.b.	β-exit to central body tract
b.r.	basal ring neuropil of calyx
c.	calyx
c.αo.t.	tract to optic tubercle from calyx and α exit
c.b.	central body
c.b.(u.)	central body upper division

c.b.(l.)	central body lower division
c.b.(v.n.)	central body ventral noduli
c.f.	central feltwork of antennal lobe
c.t.	central tracheae of dorsal protocerebrum
c.n.	collar neuropil of calyx
D	dorsal
d.l.	dorsal lobe
d.s.	dorsal strand
i.r.t.	inner ring tract of basal ring
i.t.t.	inter-tubercle tract
K cell	Kenyon cell
K I–V	Kenyon cell types I–V
l.	lobula
Ll	left lateral
Lr	right lateral
l.a.g.t.	lateral antenno-glomerular tract
l.c.	lateral calyx
l.p.n.a.	lateral photocerebral neuropil area
l.n.	lip neuropil of calyx
M	median
m.a.g.t.	median antenno-glomerular tract
m.c.	median calyx
m.l.a.g.t.	mediolateral antenno-glomerular tract
oc.	ocellus
o.r.t.	outer ring tract of basal ring
o.t.	ocellar tract
p.	pedunculus
p.c.t.	protocerebro-calycal tract
P	posterior
s.o.g.	suboesophageal ganglion
T 1–6	antennal nerve brain tracts 1–6 (see text)
V	ventral
v.s.	ventral stand of the antennal nerve
v.n.c.	ventral nerve cord

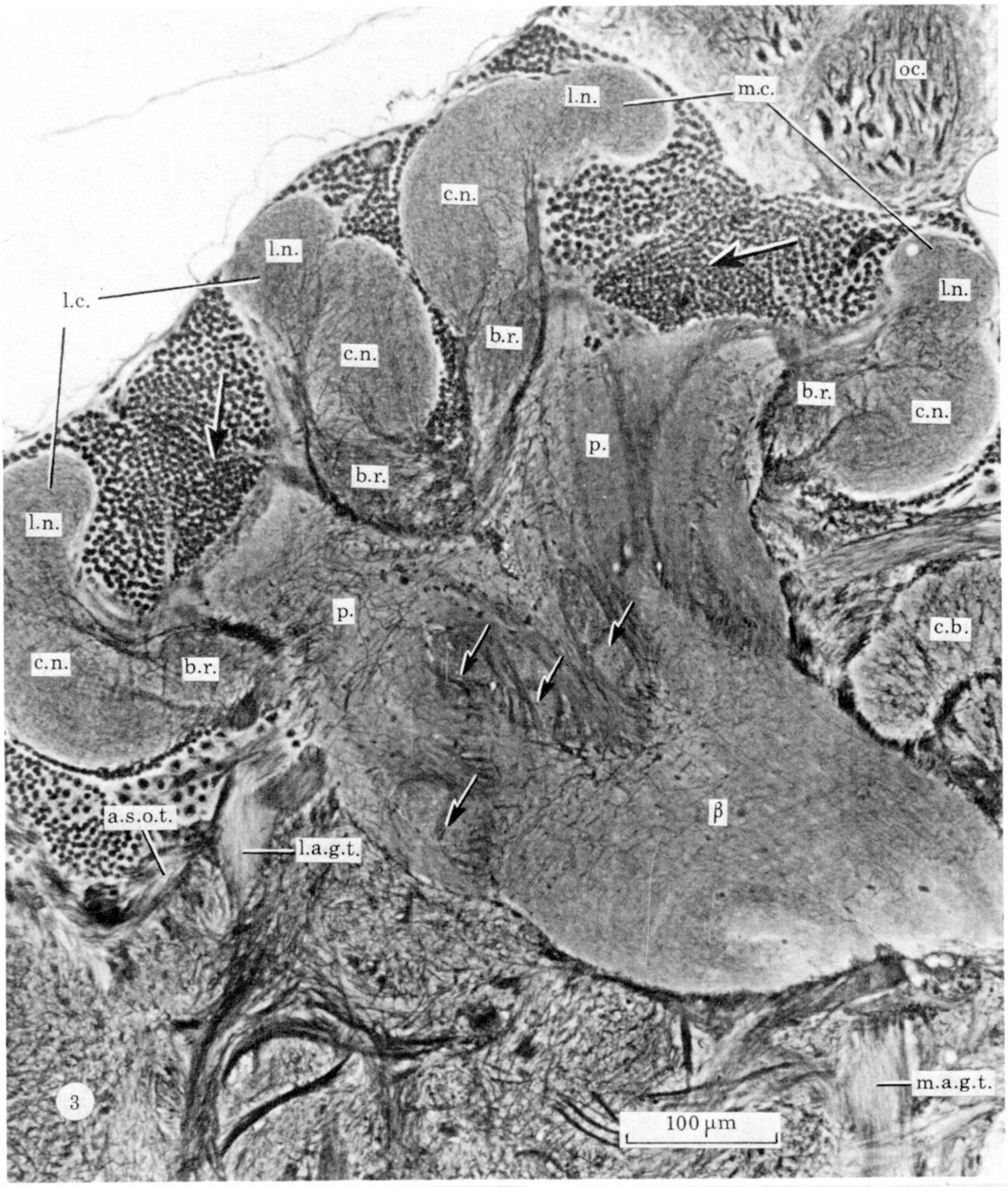
oc.
l.n.
m.c.
c.n.
l.n.
l.c.
l.n.
b.r.
c.n.
b.r.
c.n.
p.
b.r.
l.n.
c.b.
p.
c.n.
b.r.
β
a.s.o.t.
l.a.g.t.
m.a.g.t.
3
100 µm

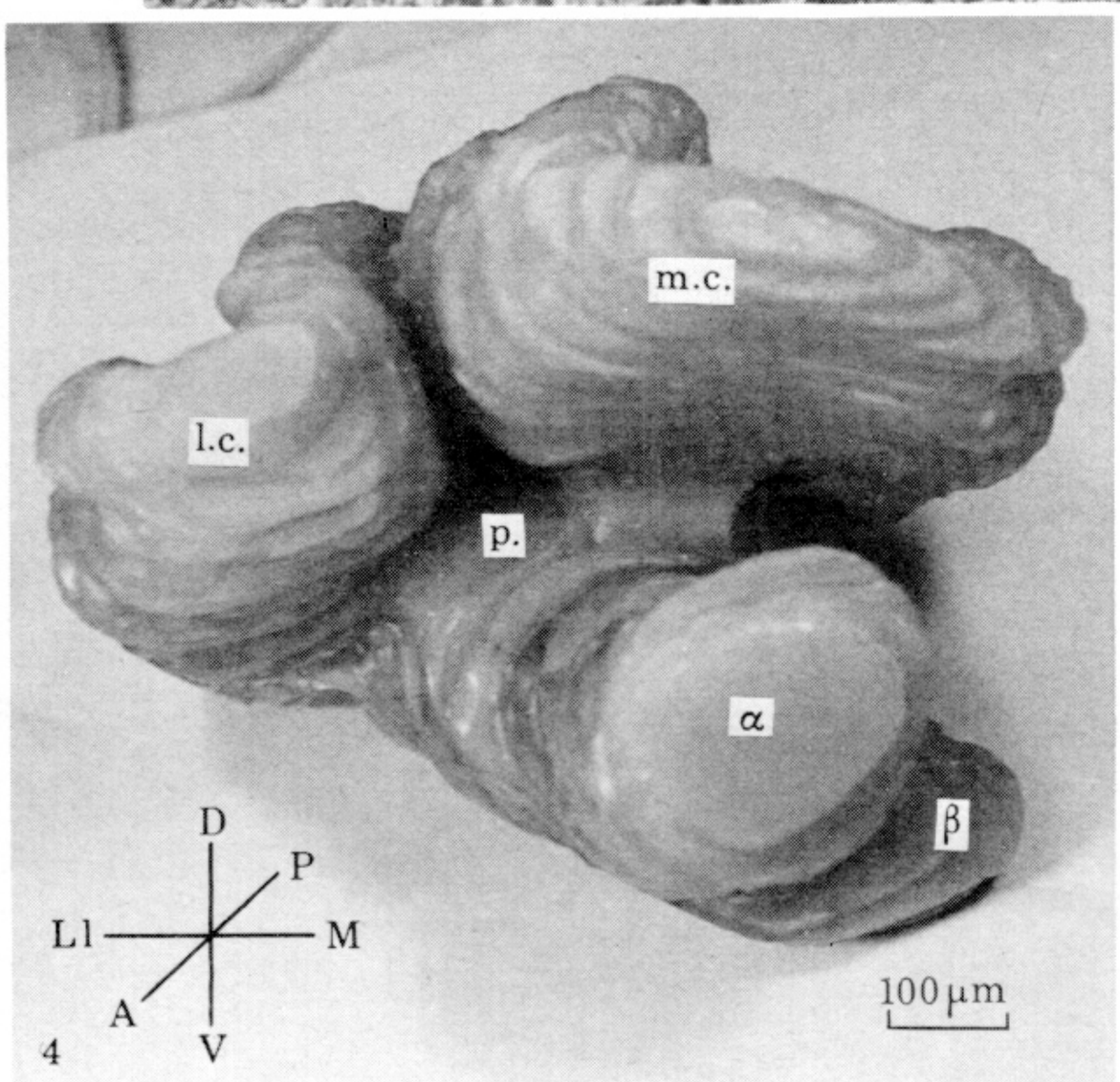
m.c.
l.c.
p.
α
β
D
P
Ll
M
A
V
100 µm
4

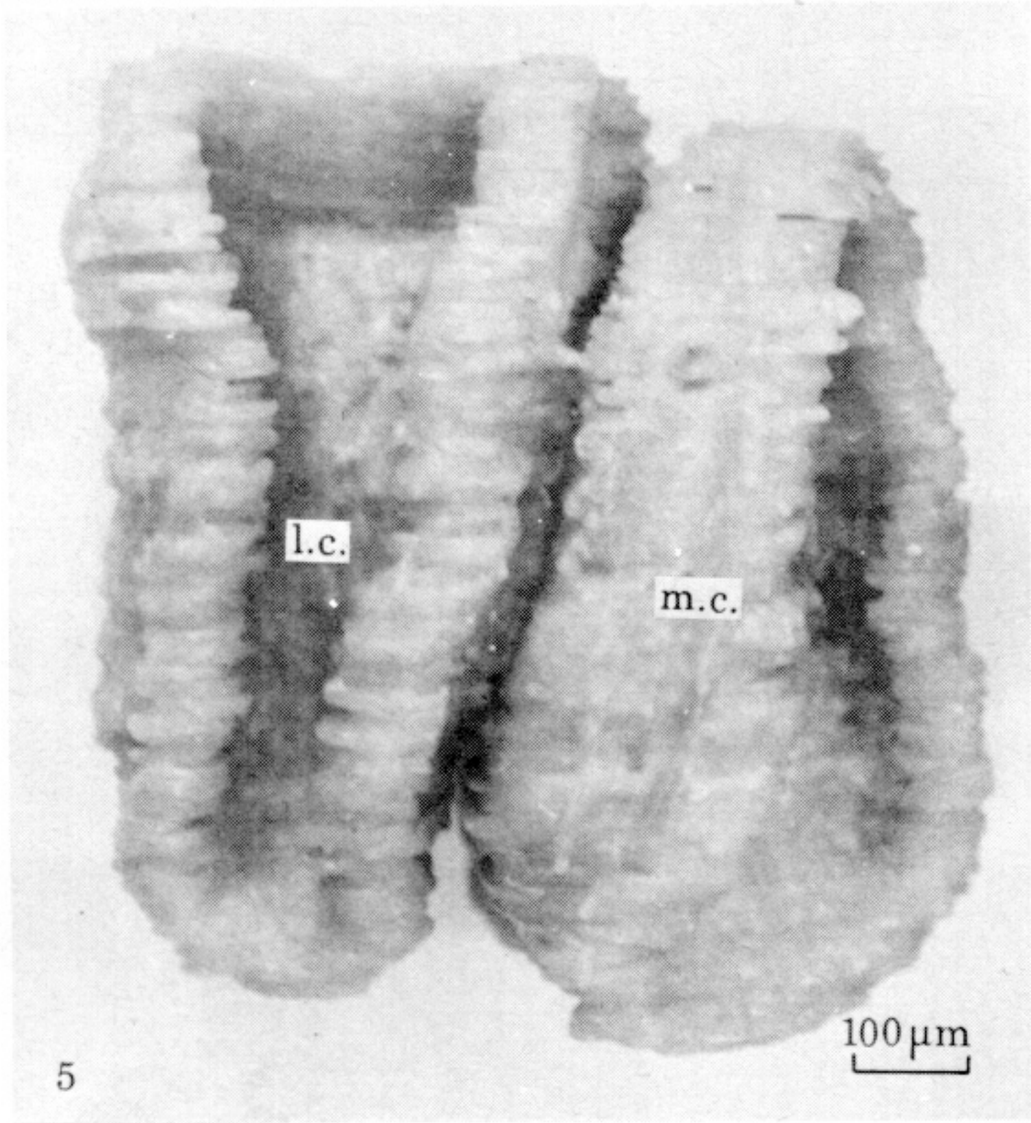
l.c.
m.c.
100 µm
5

6

o.t.

l.n.

p.

m.c.

b.r.

l.n.

c.n.

c.n.

l.n.

l.c.

M

P

A

Lr

100 µm

7

o.t.

c.n.

m.c.

1

2

3

p.

b.r.

l.n.

l.n.

c.n.

b.r.

c.n.

l.c.

100 µm

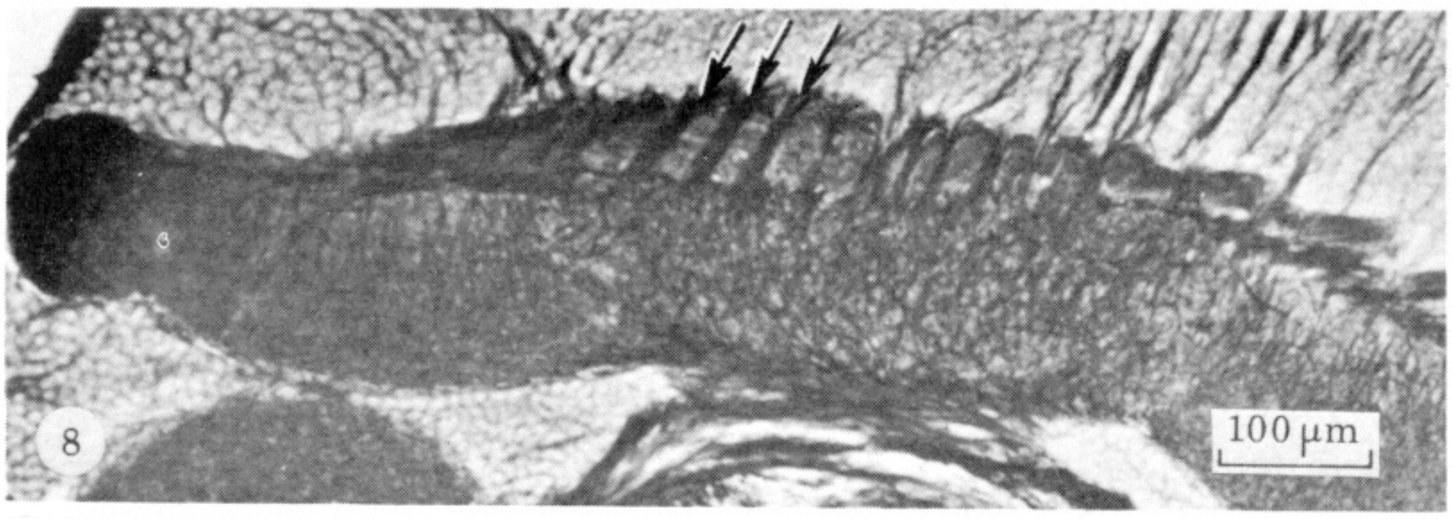
8
100 µm

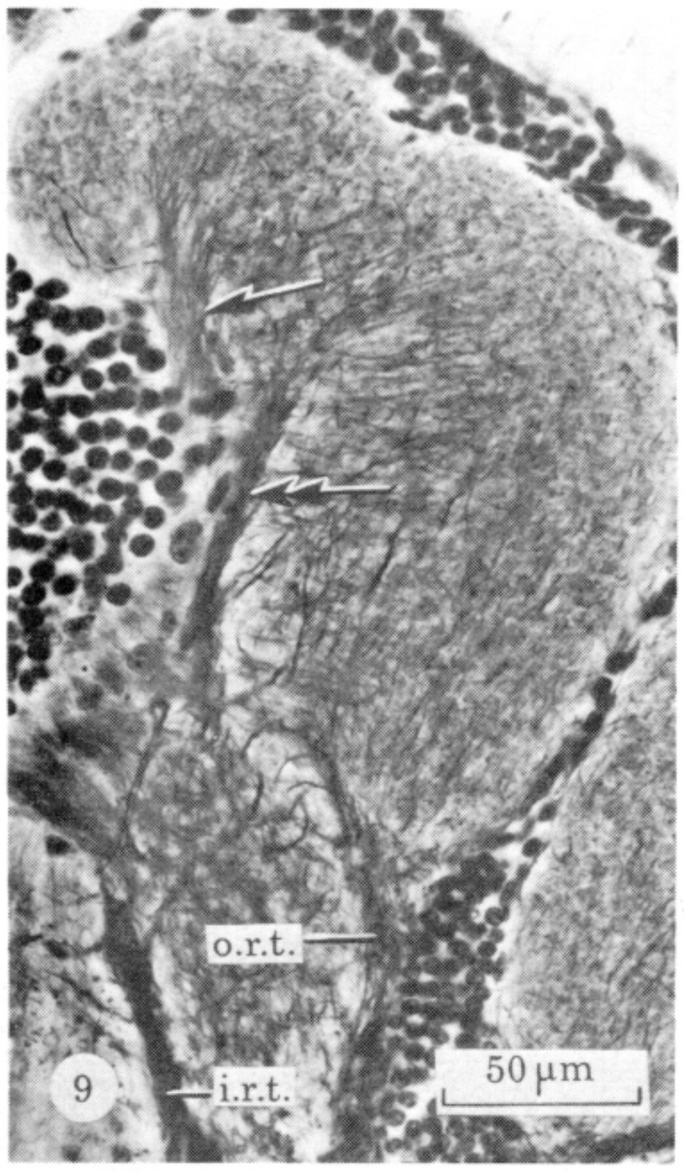
o.r.t.
i.r.t.
9
50 µm

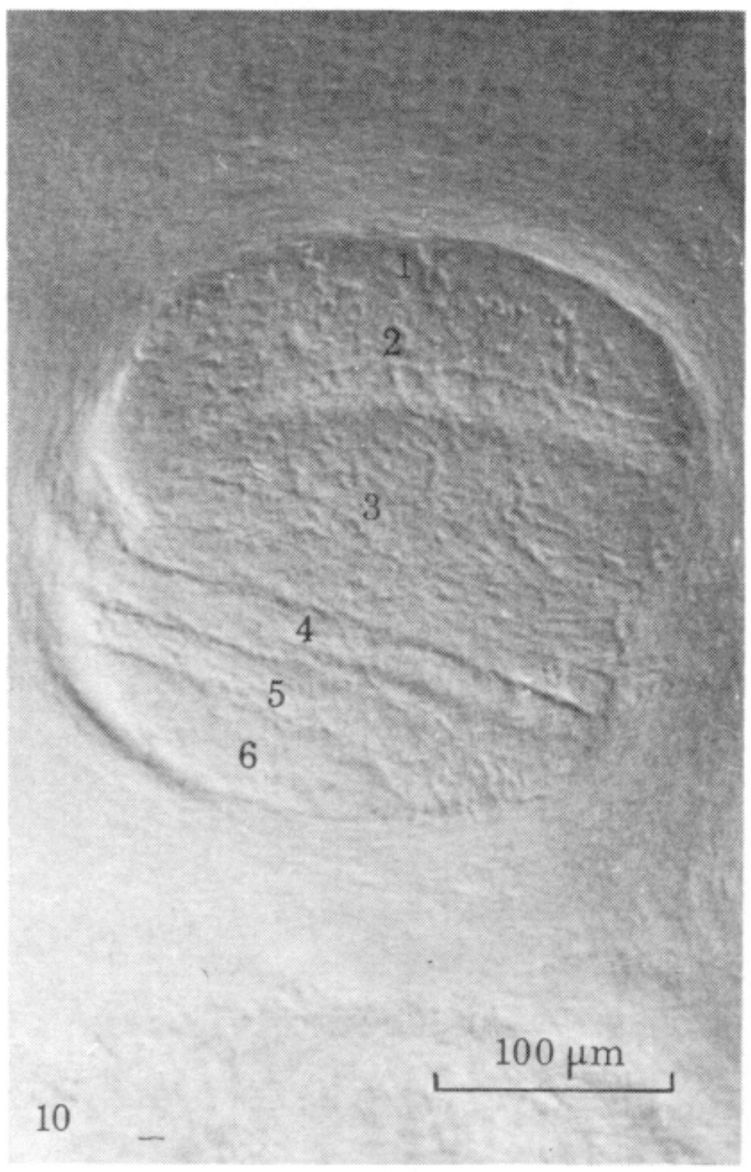
1
2
3
4
5
6
100 µm
10

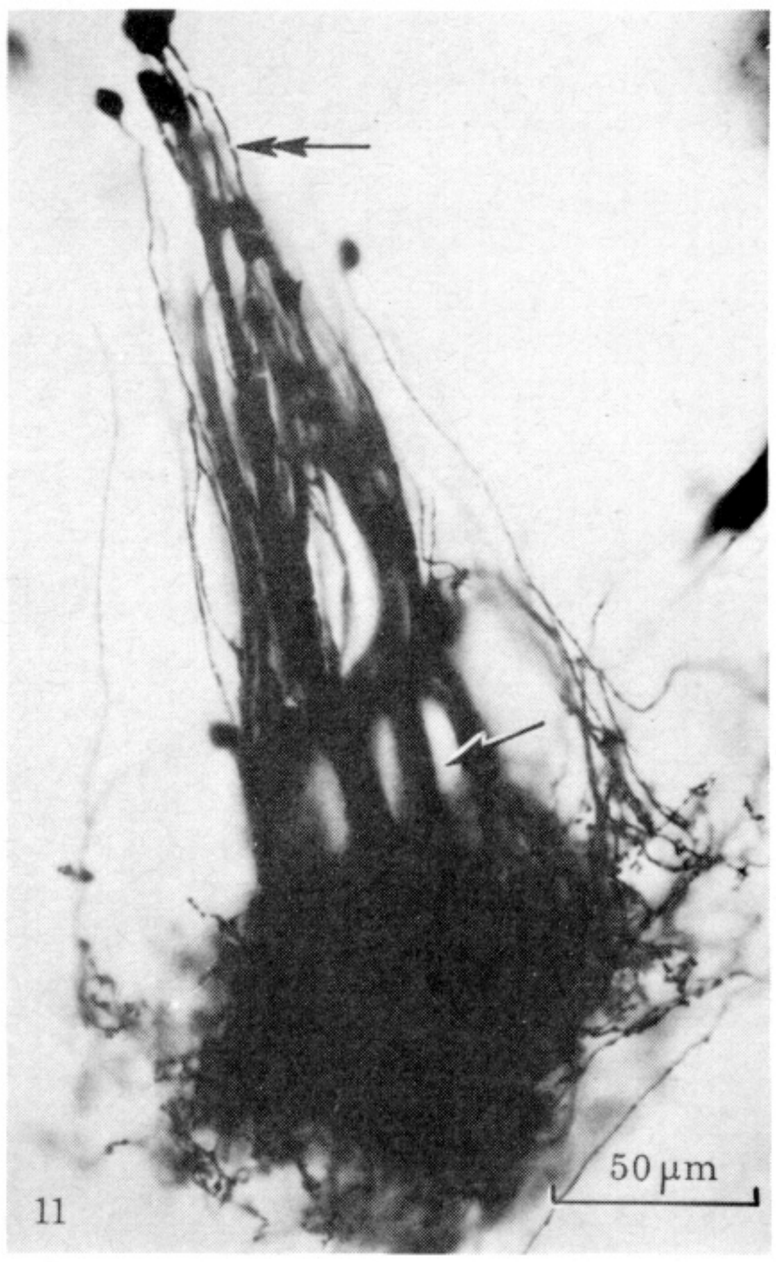
50 µm
11

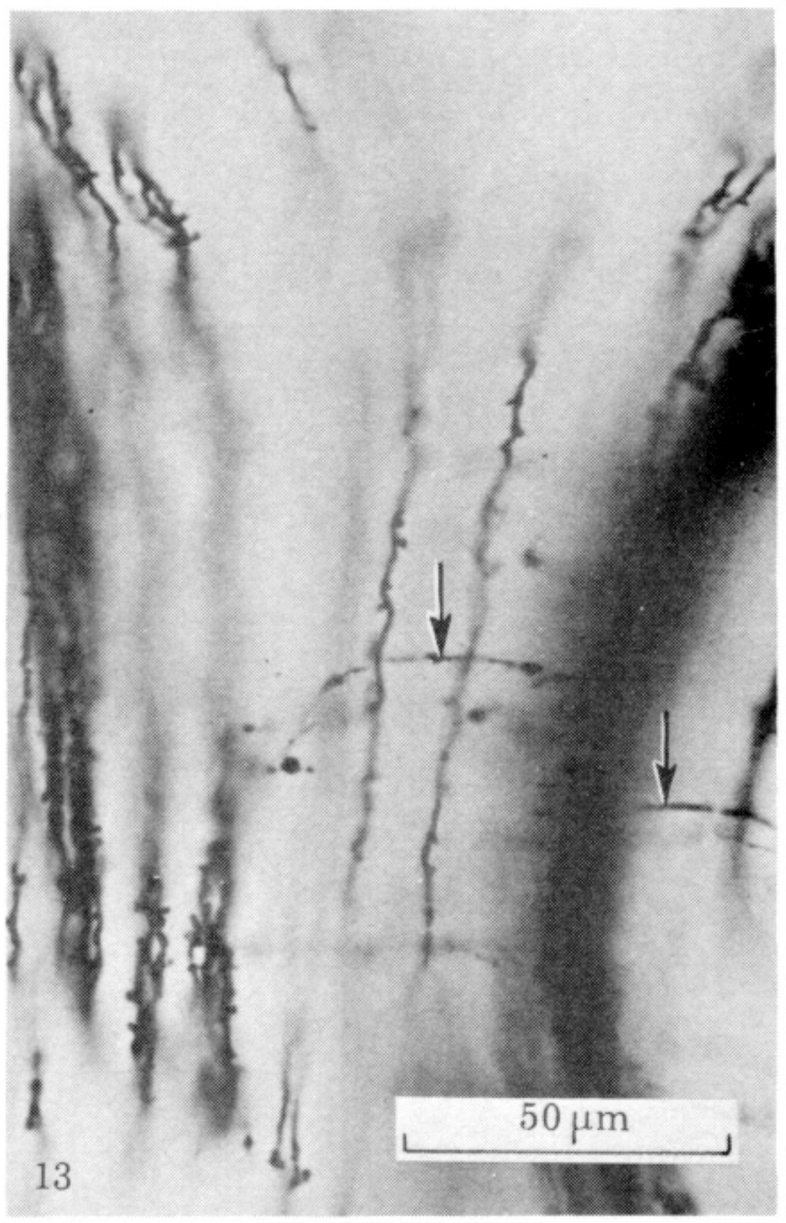
50 µm
13

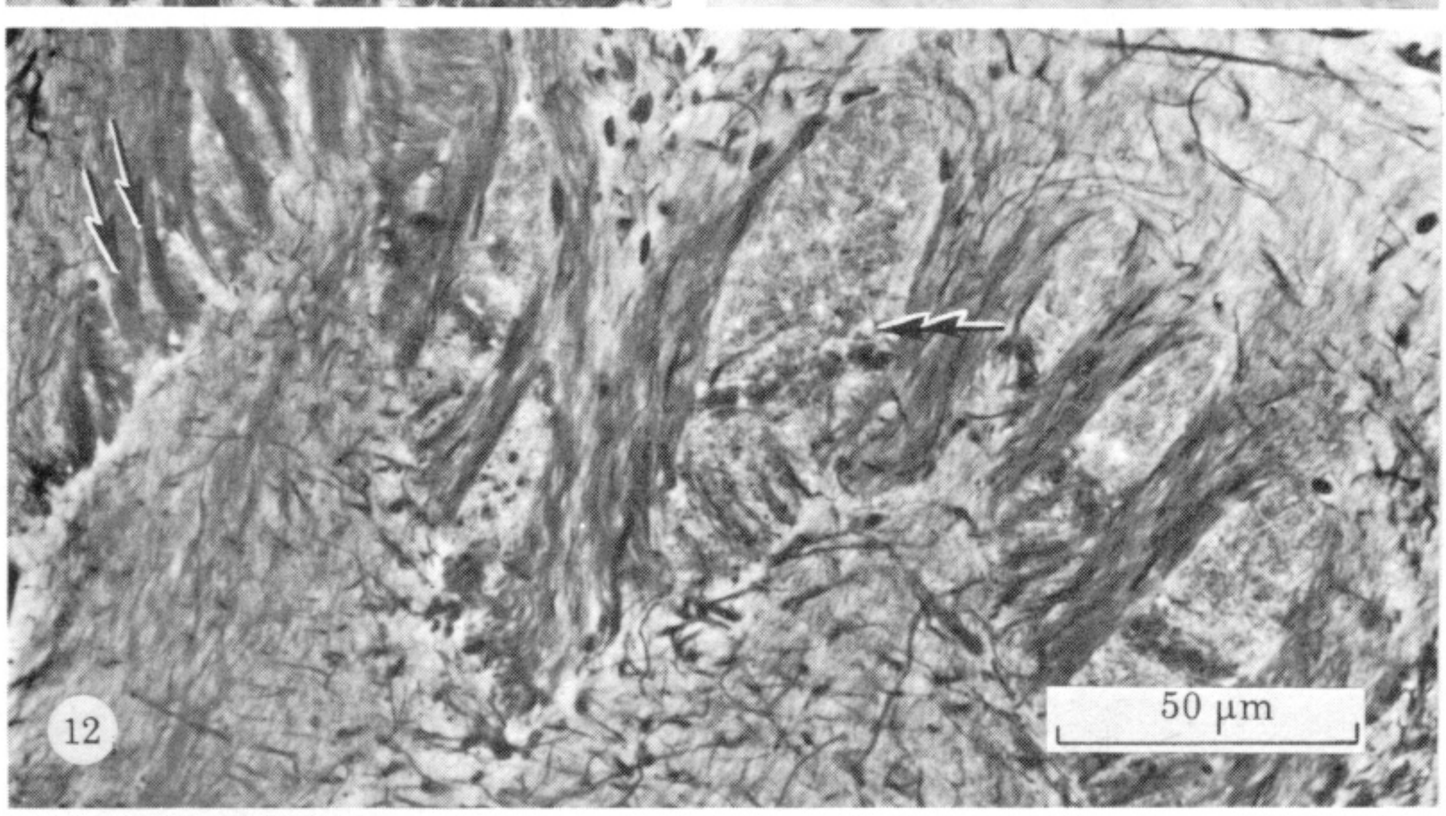
50 µm
12

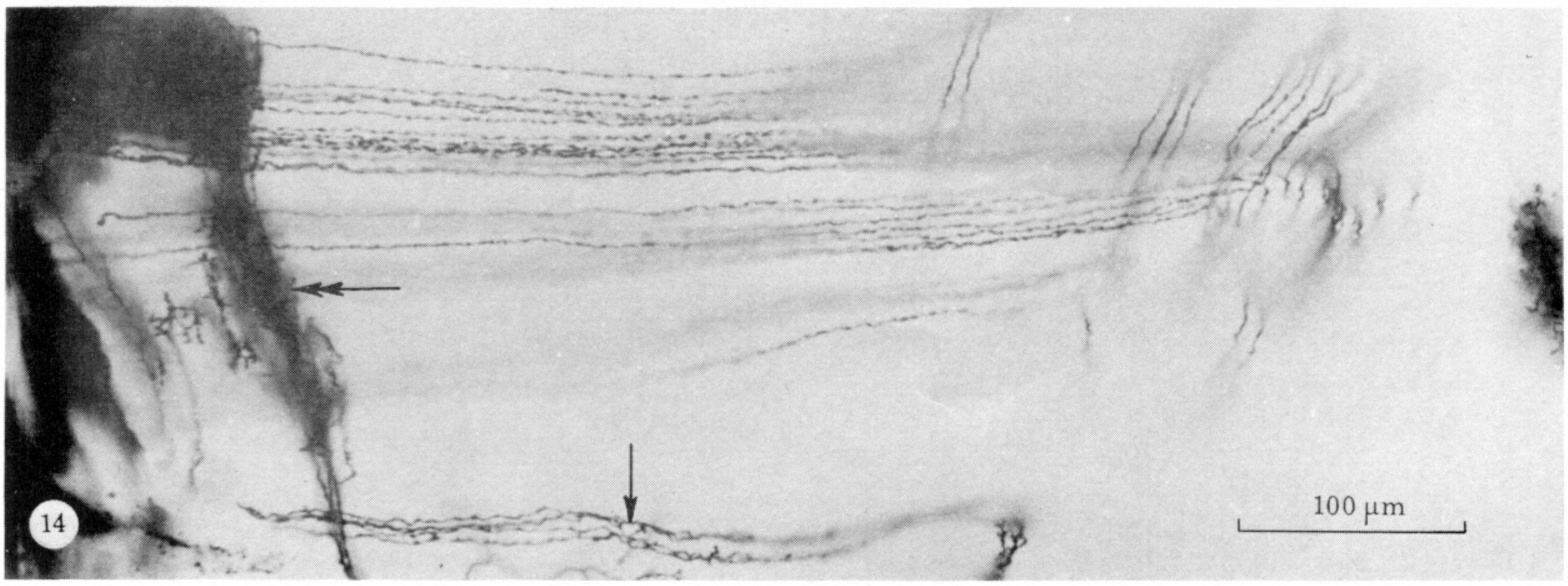
100 µm
14

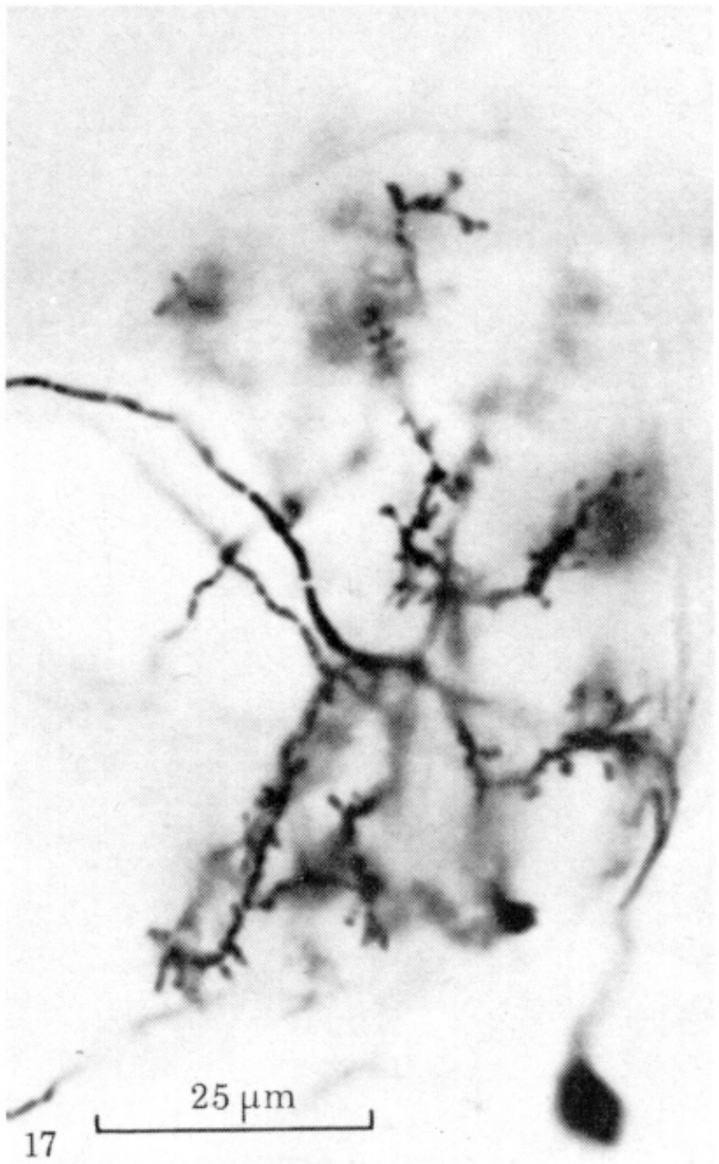

17

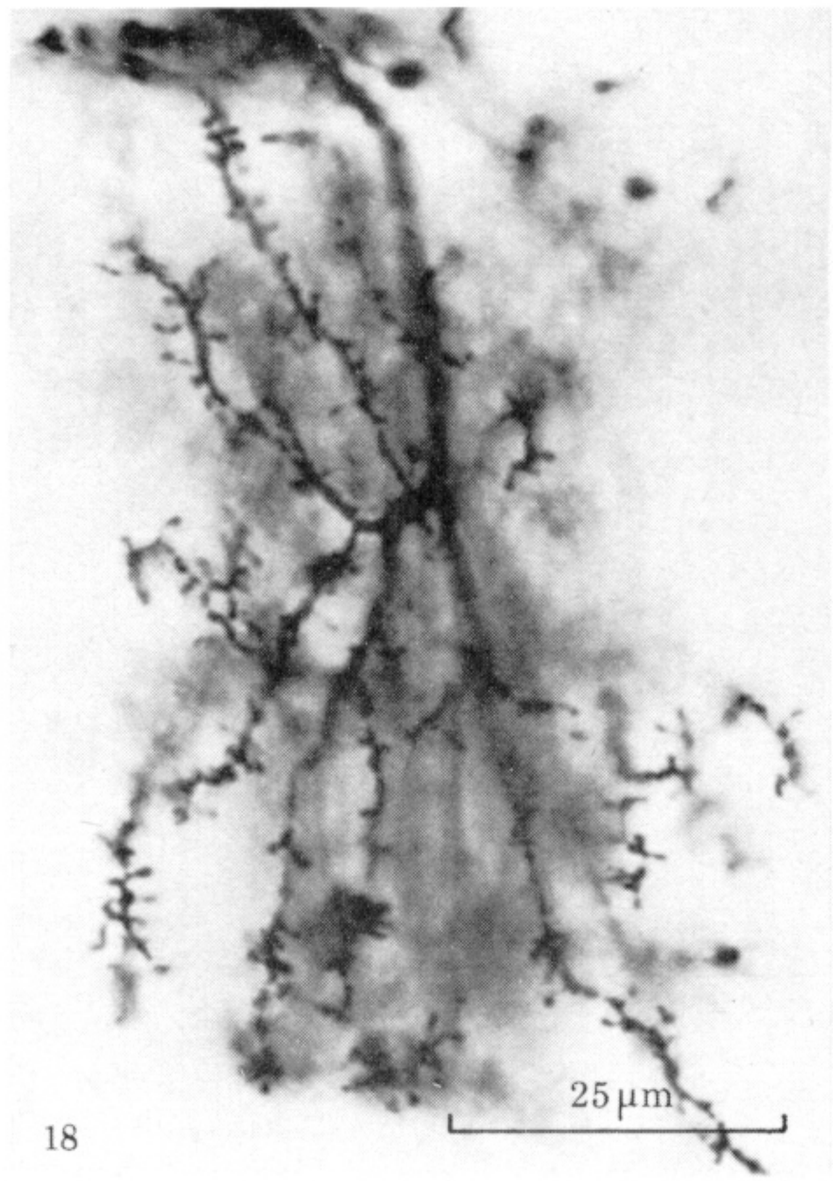

18

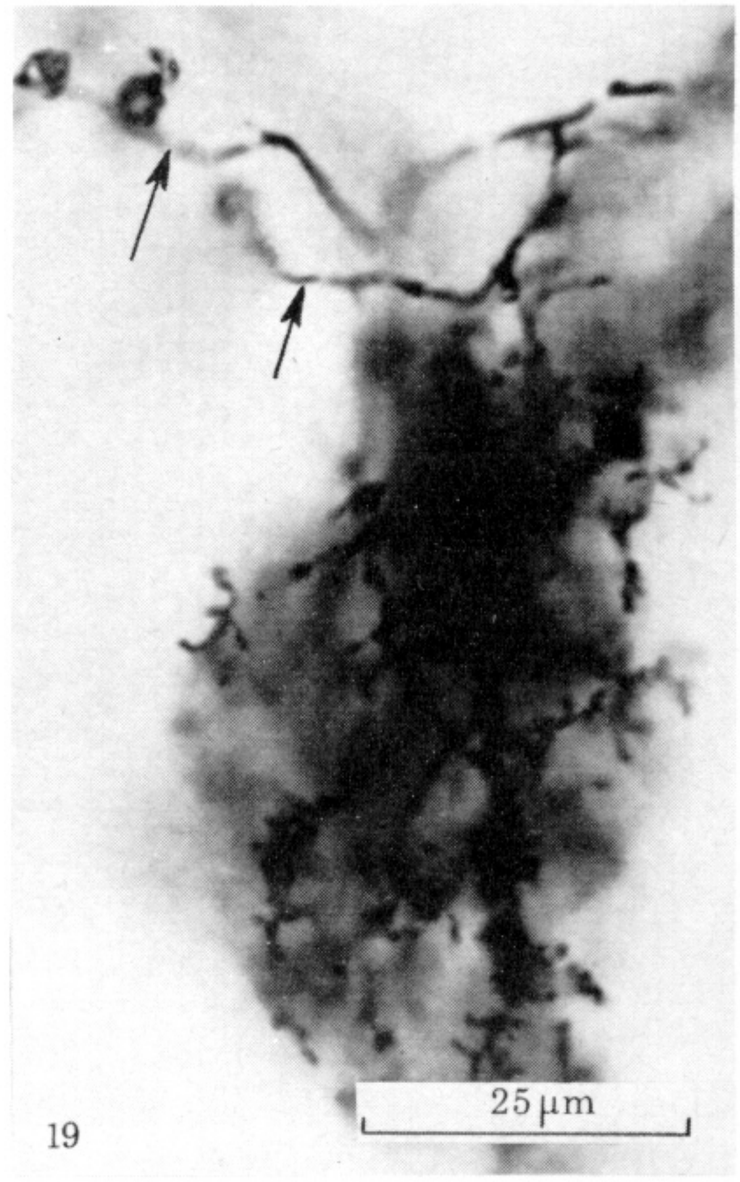

19

20

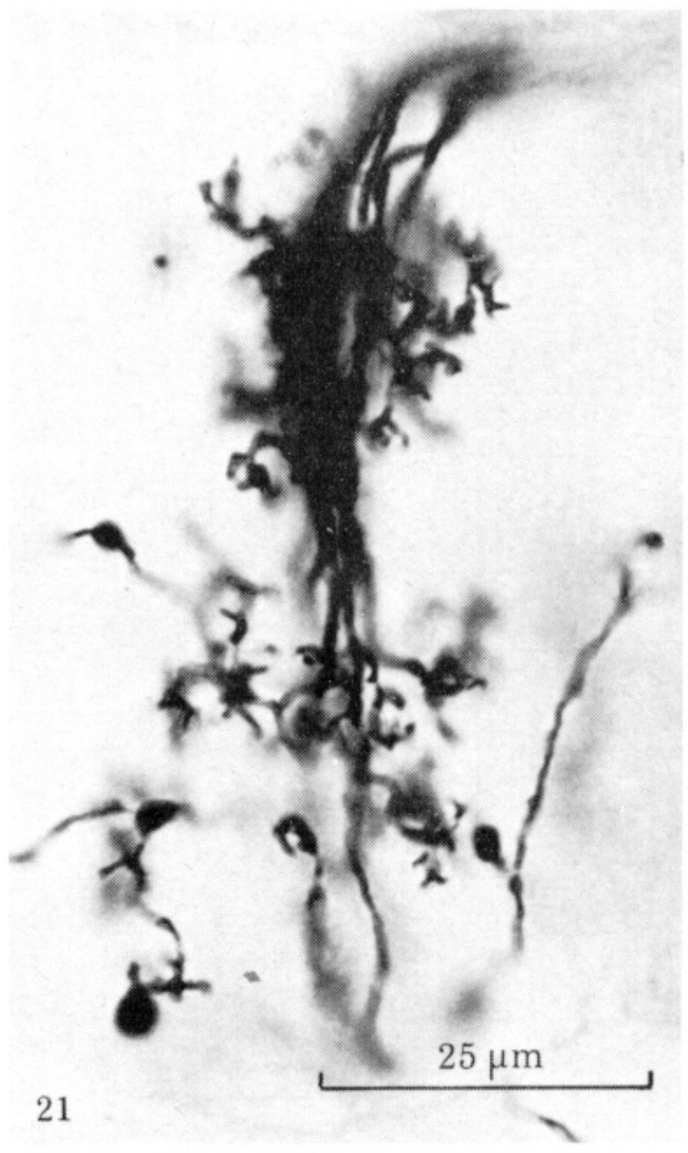

21

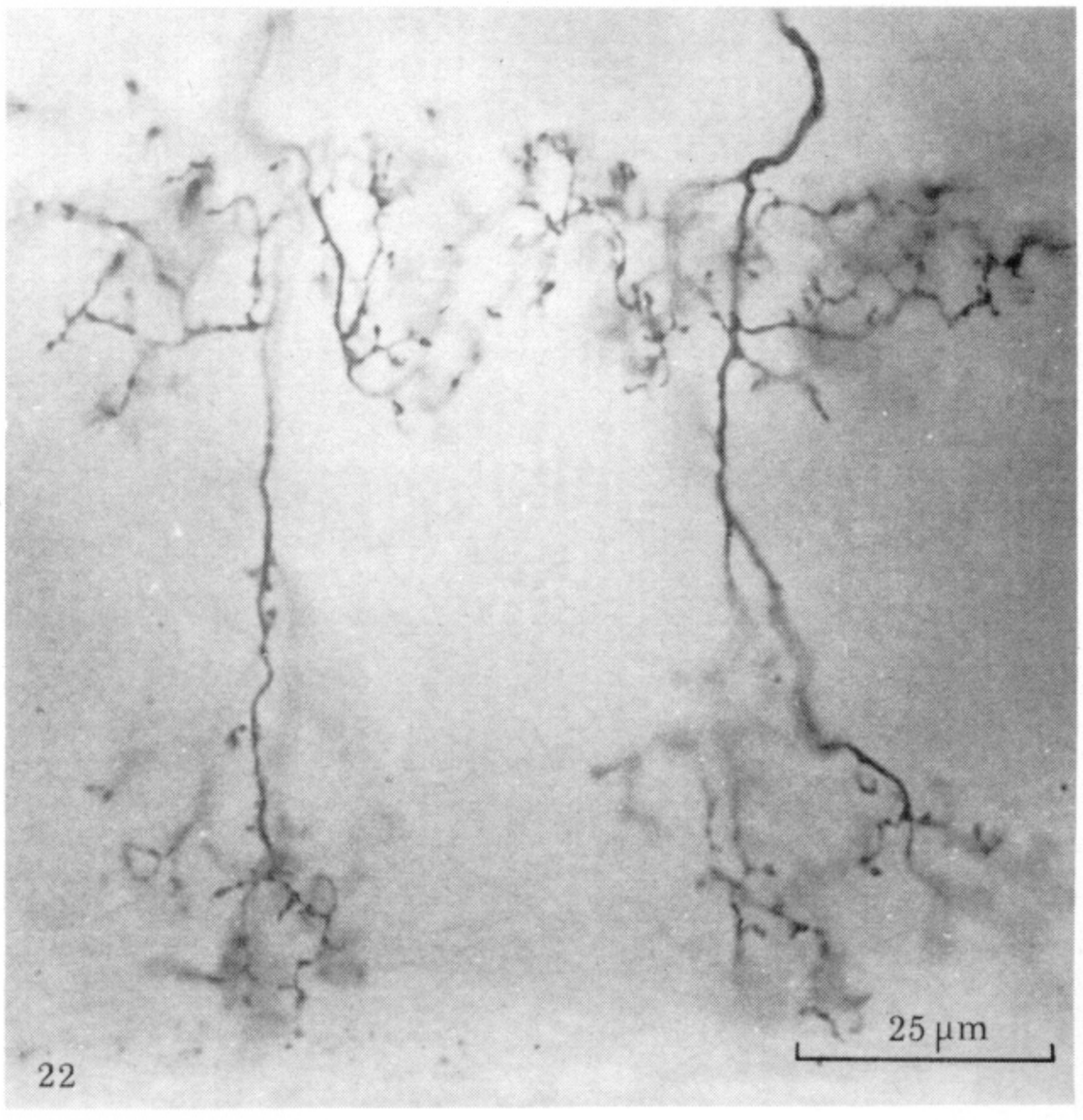

22

23

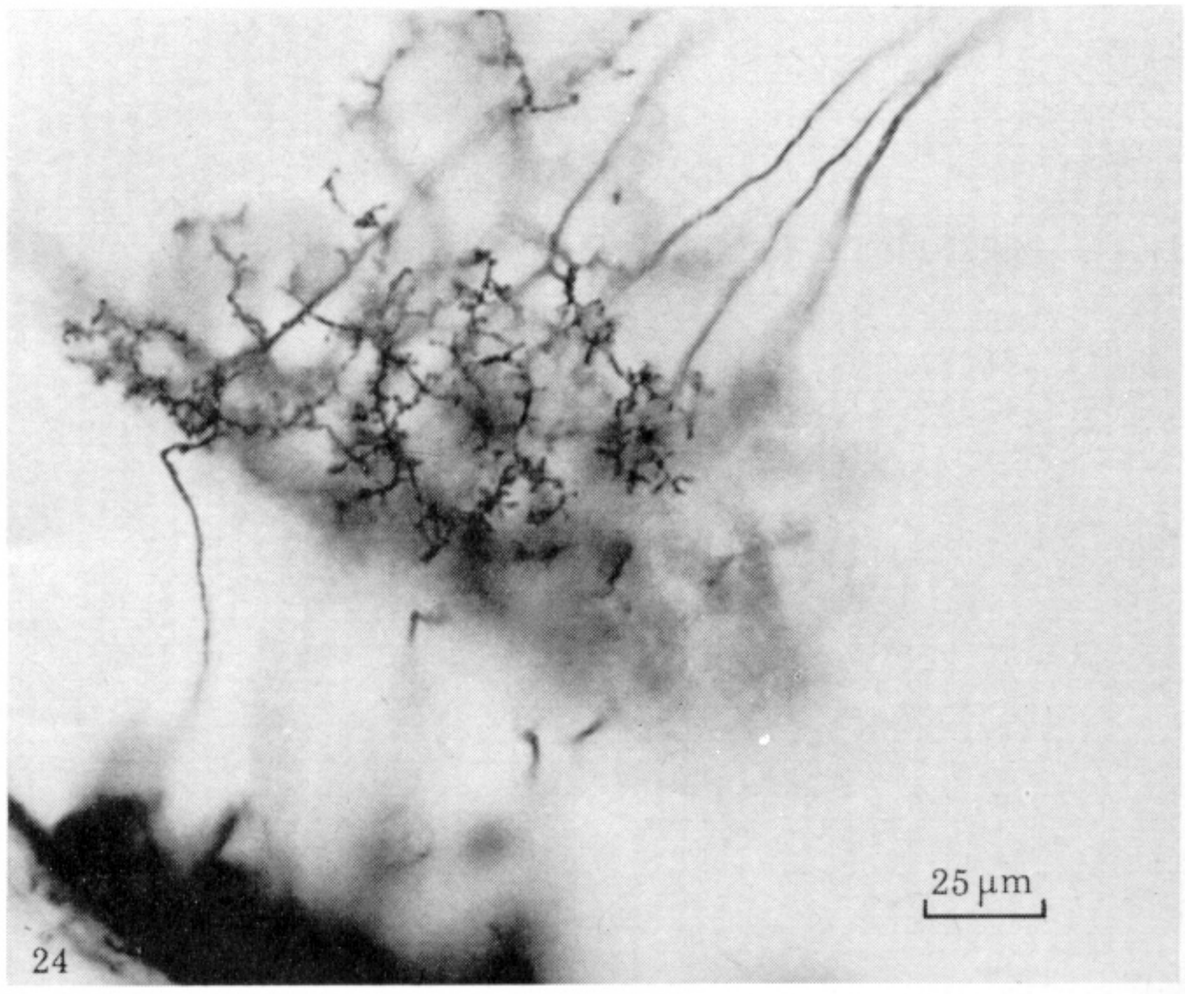

24

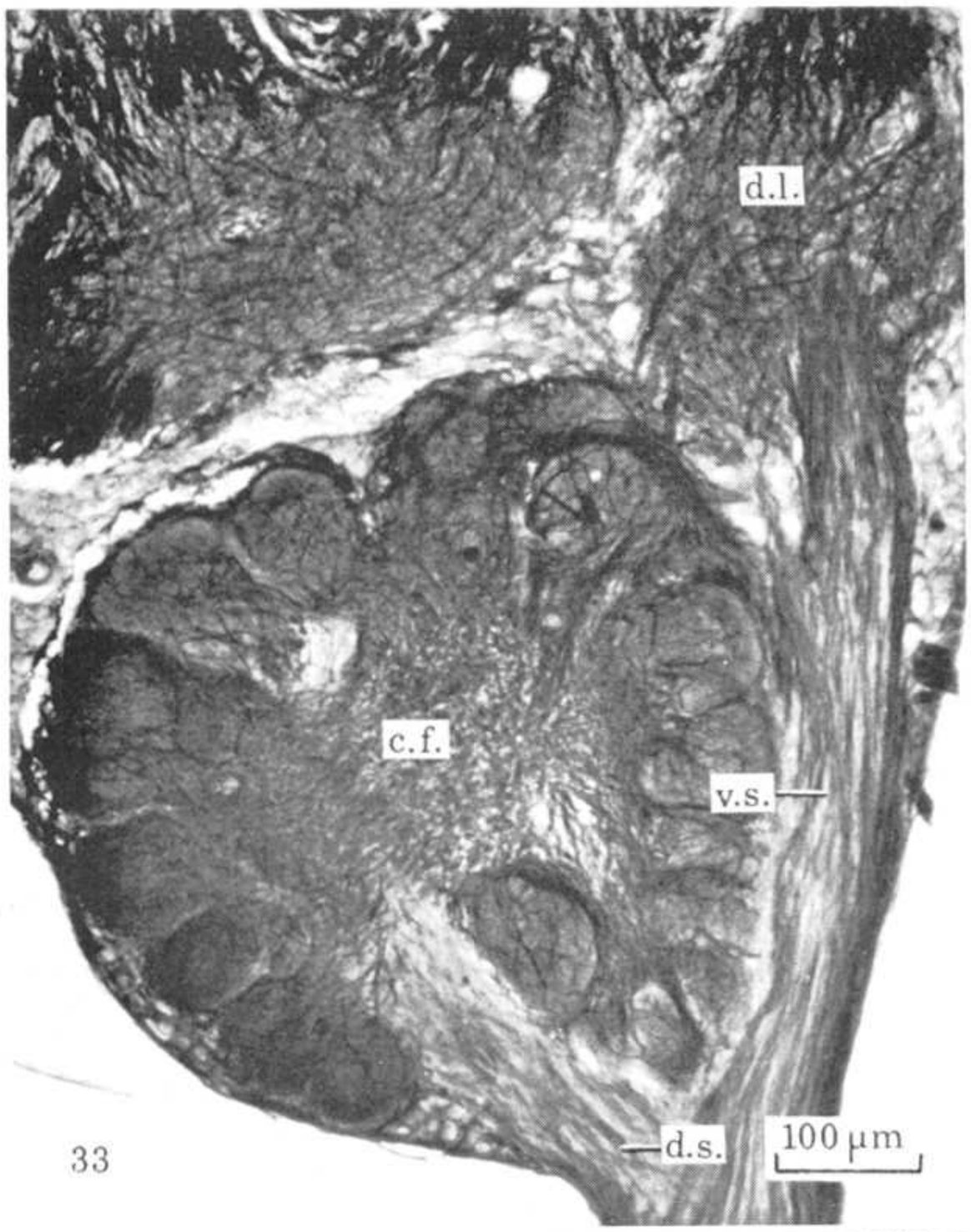

33

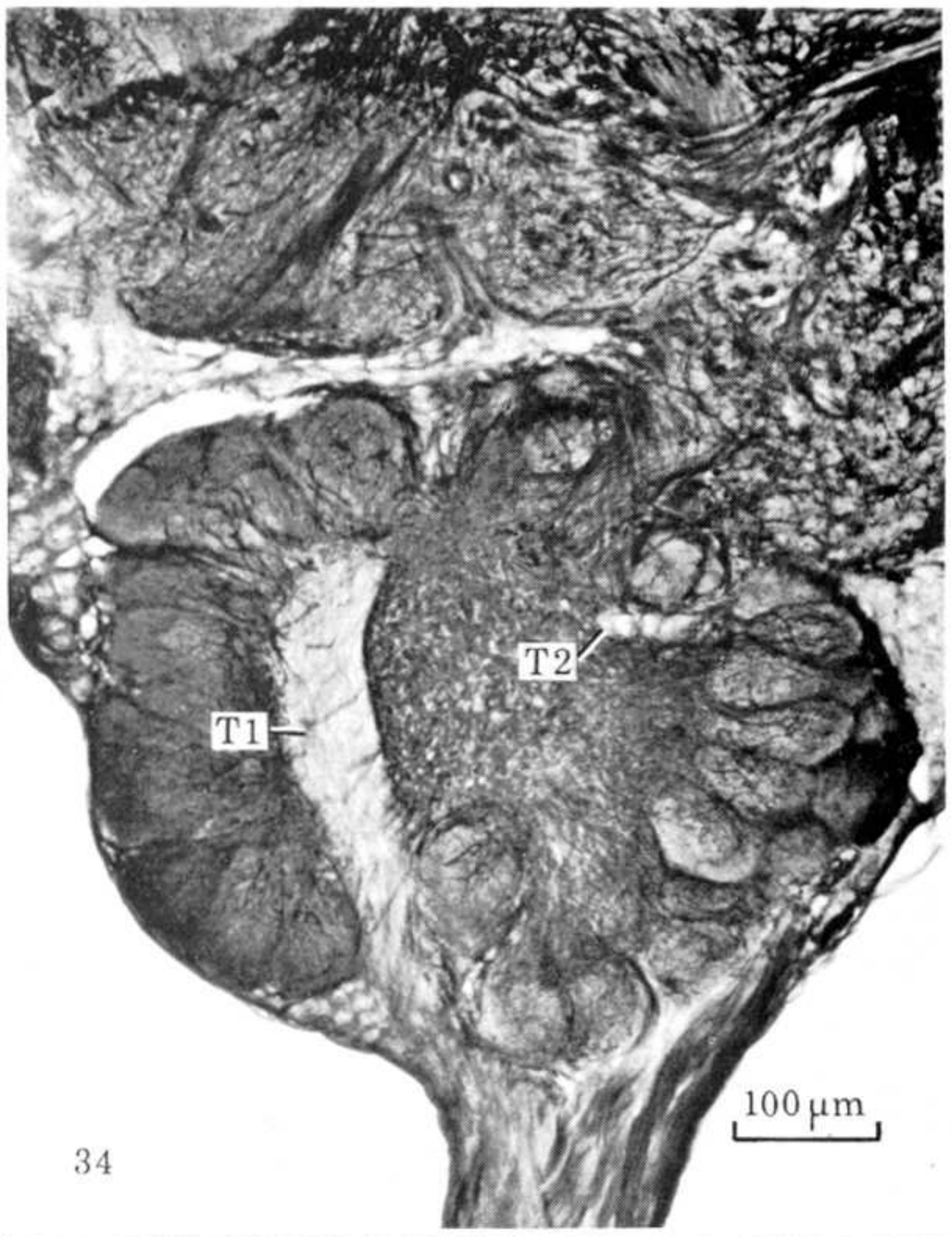

34

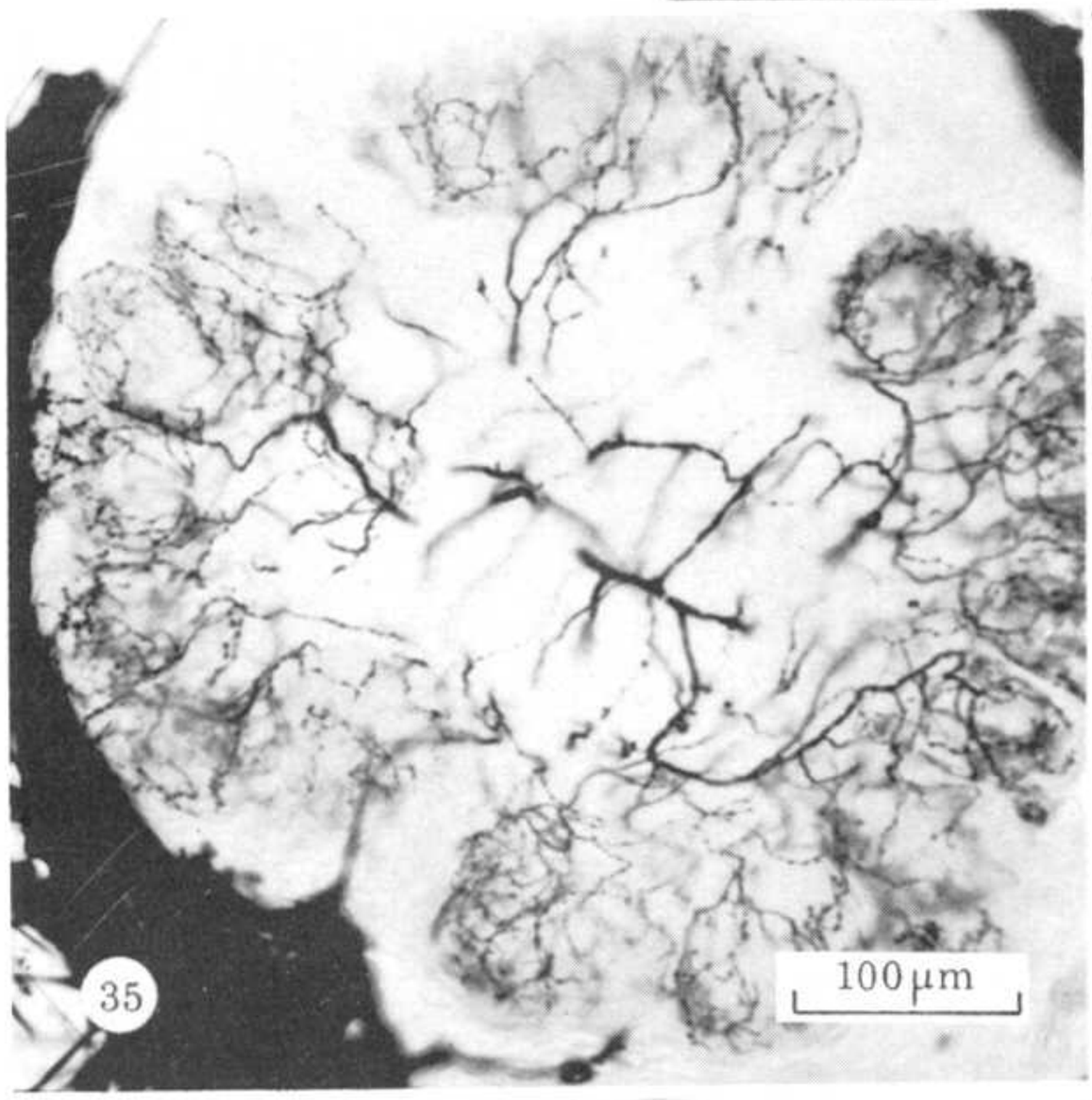

35

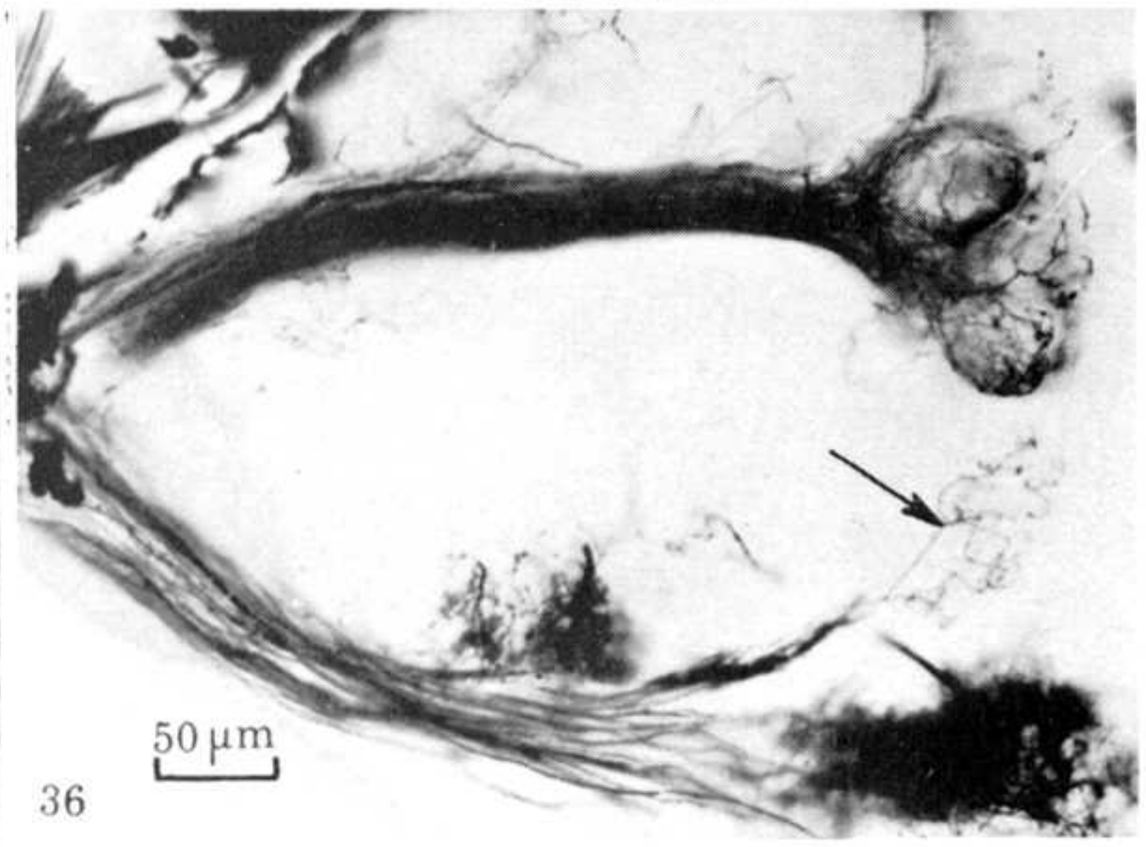

36

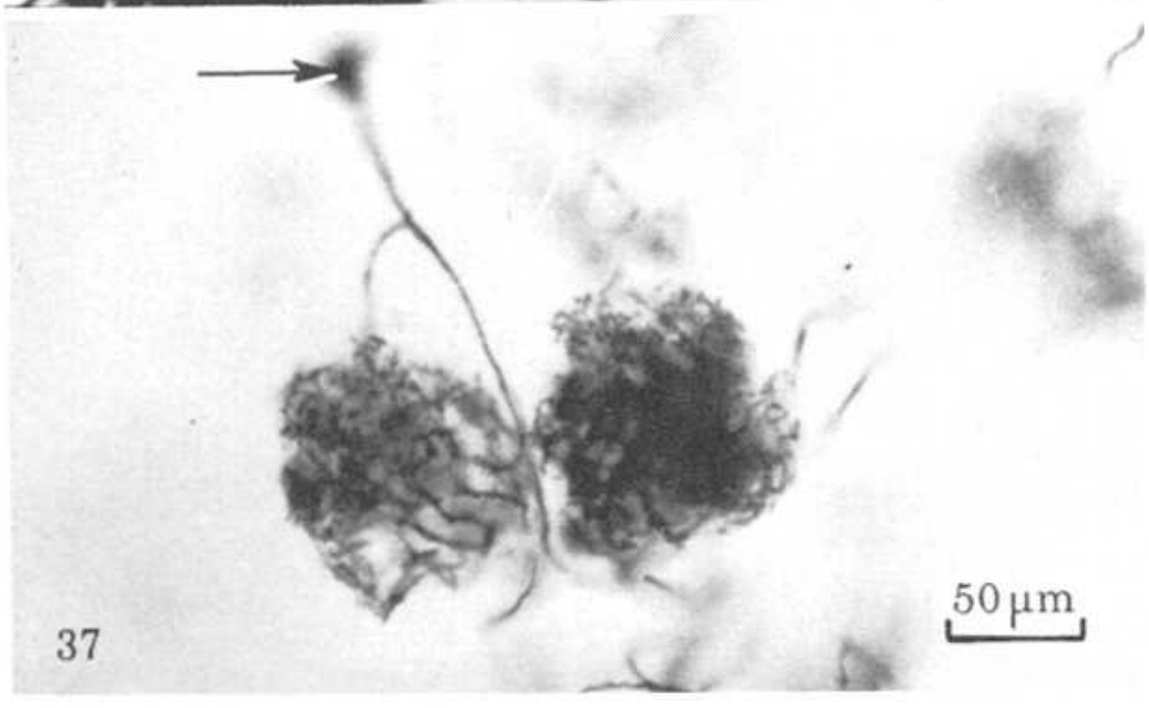

37

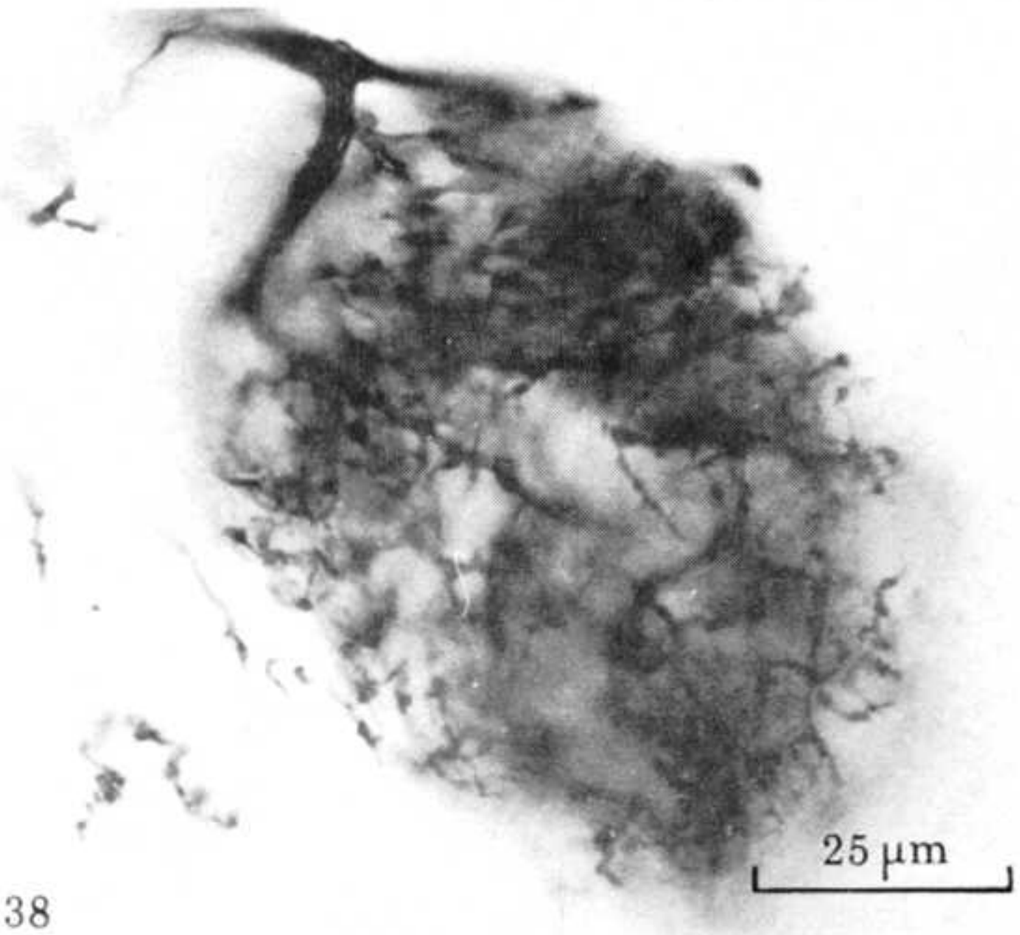

38

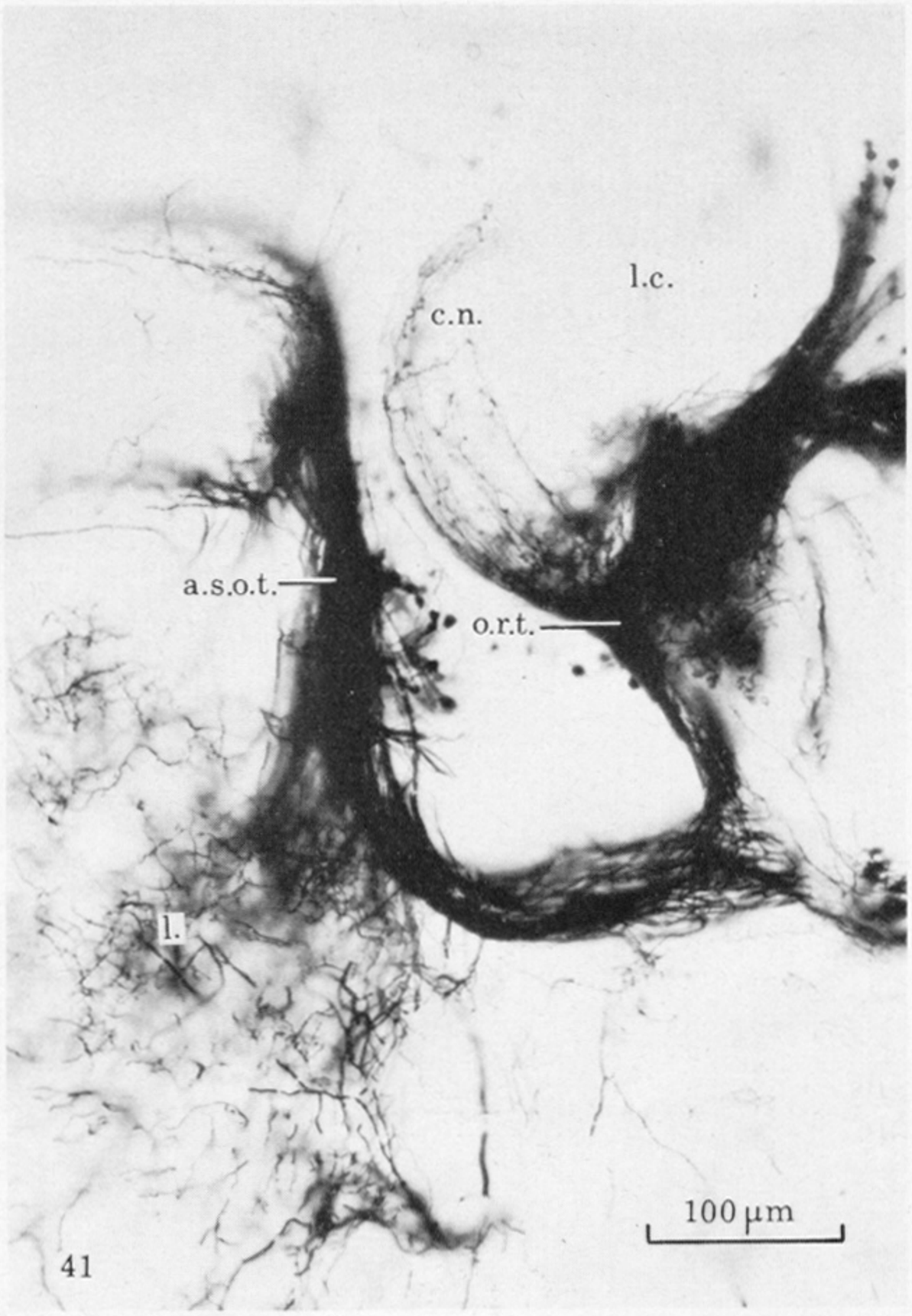
c.n.
l.c.
a.s.o.t.
o.r.t.
l.
100 µm

41

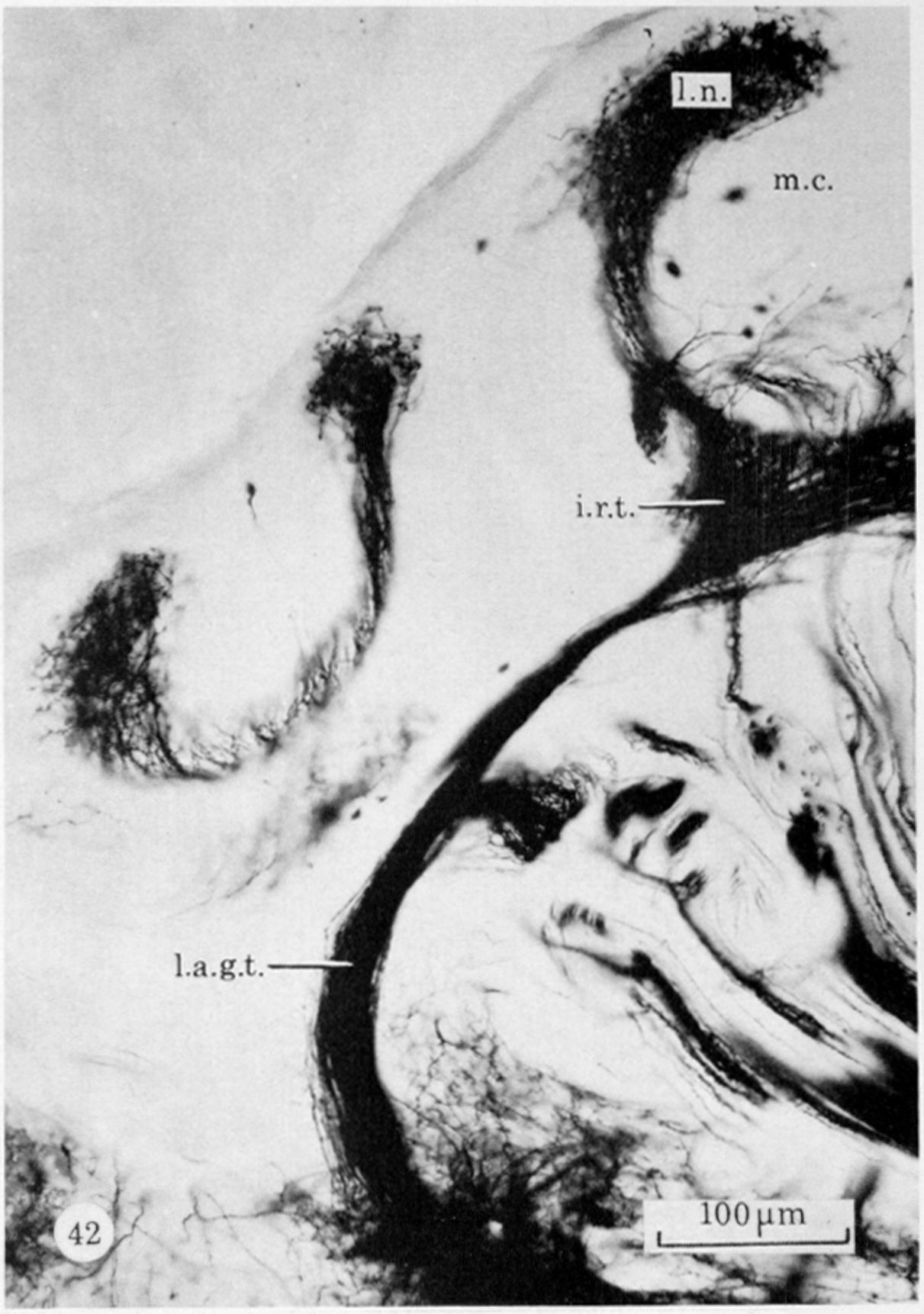
l.n.
m.c.
i.r.t.
l.a.g.t.
100 µm

42

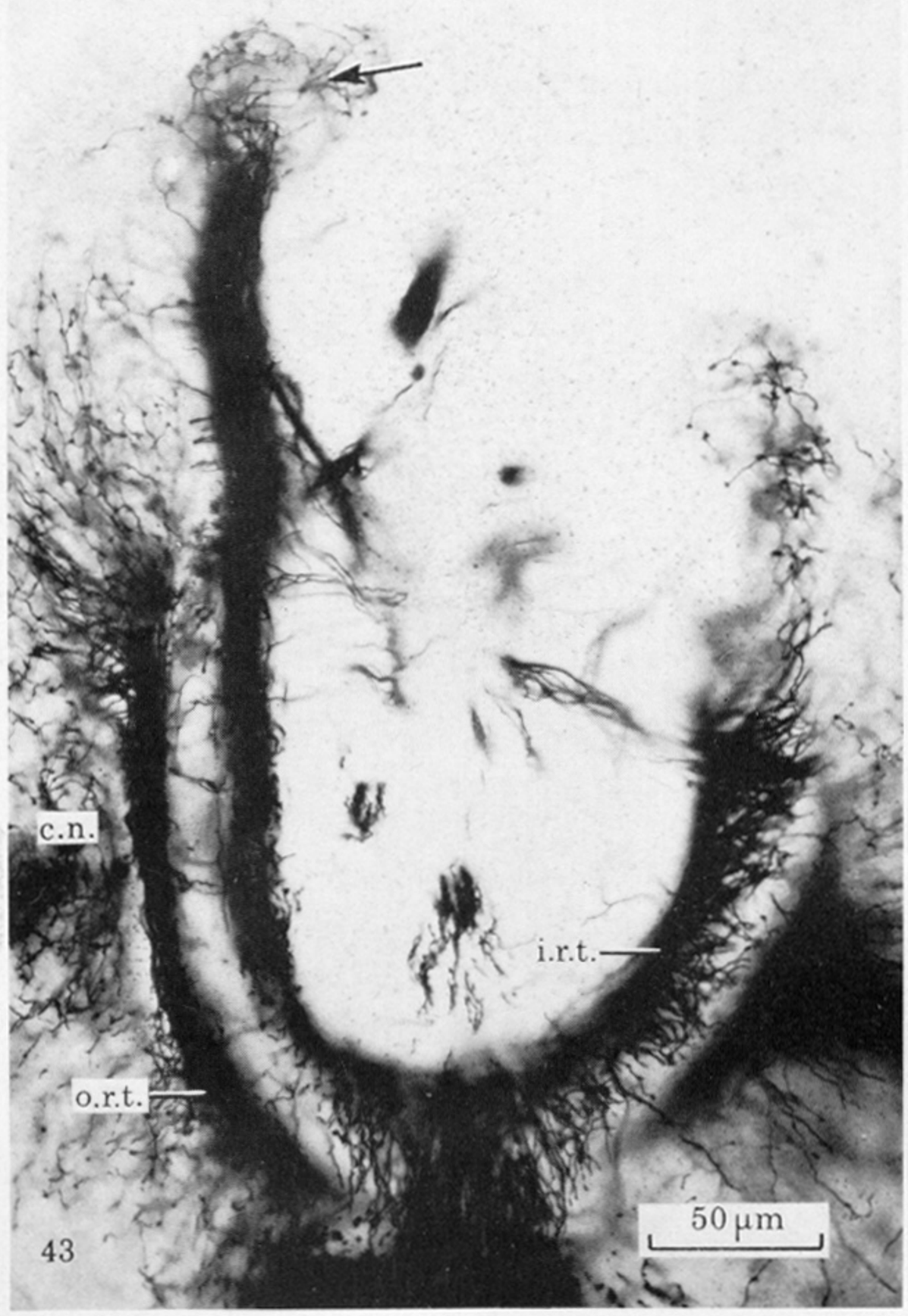
c.n.
i.r.t.
o.r.t.
50 µm

43

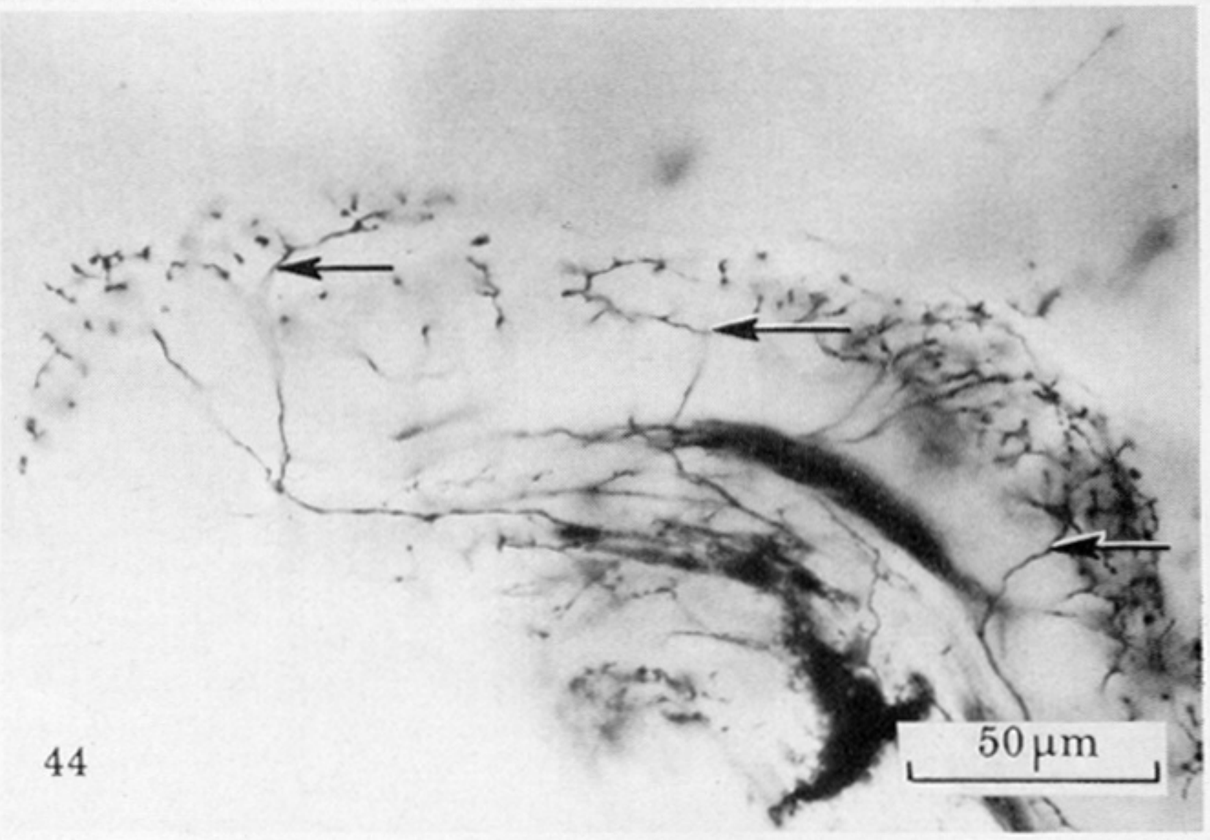
50 µm

44

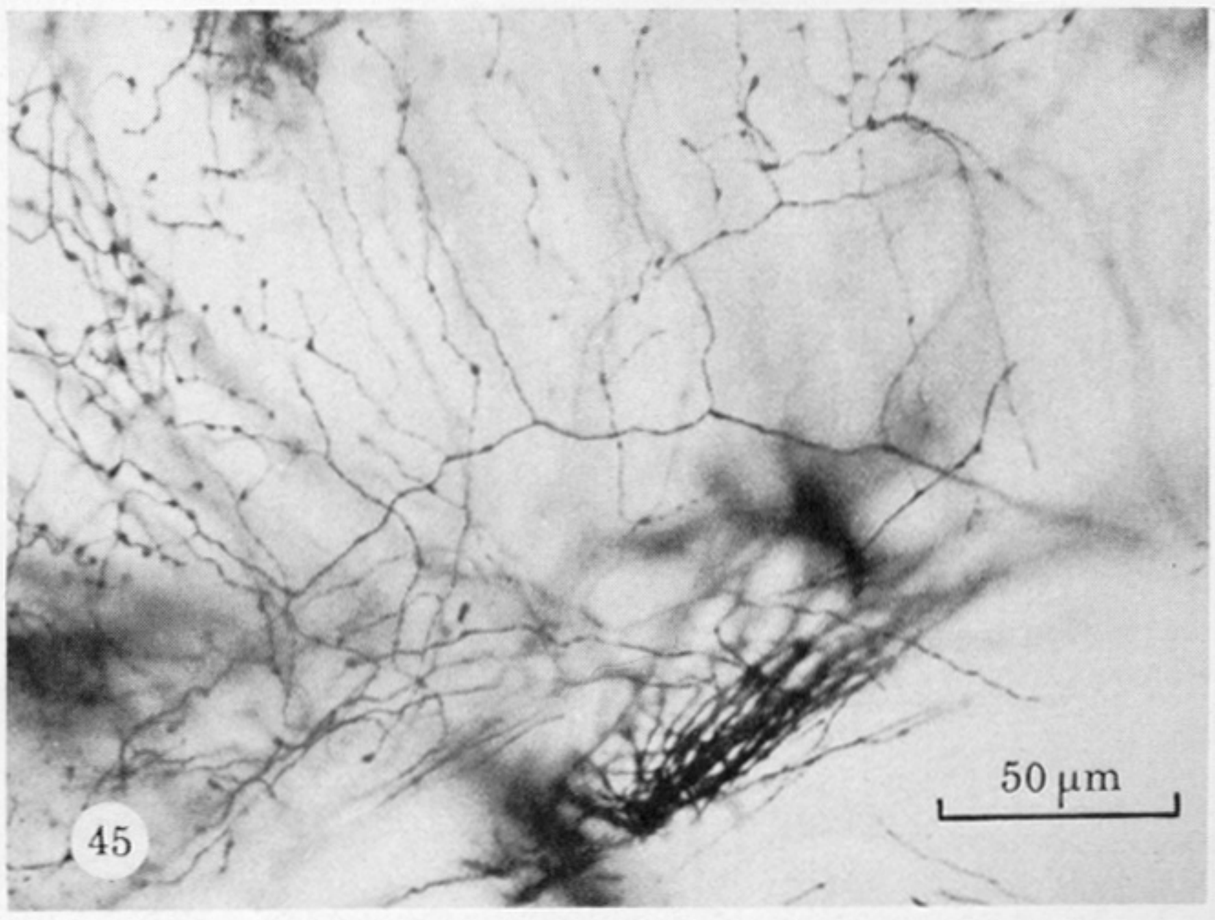
50 µm

45

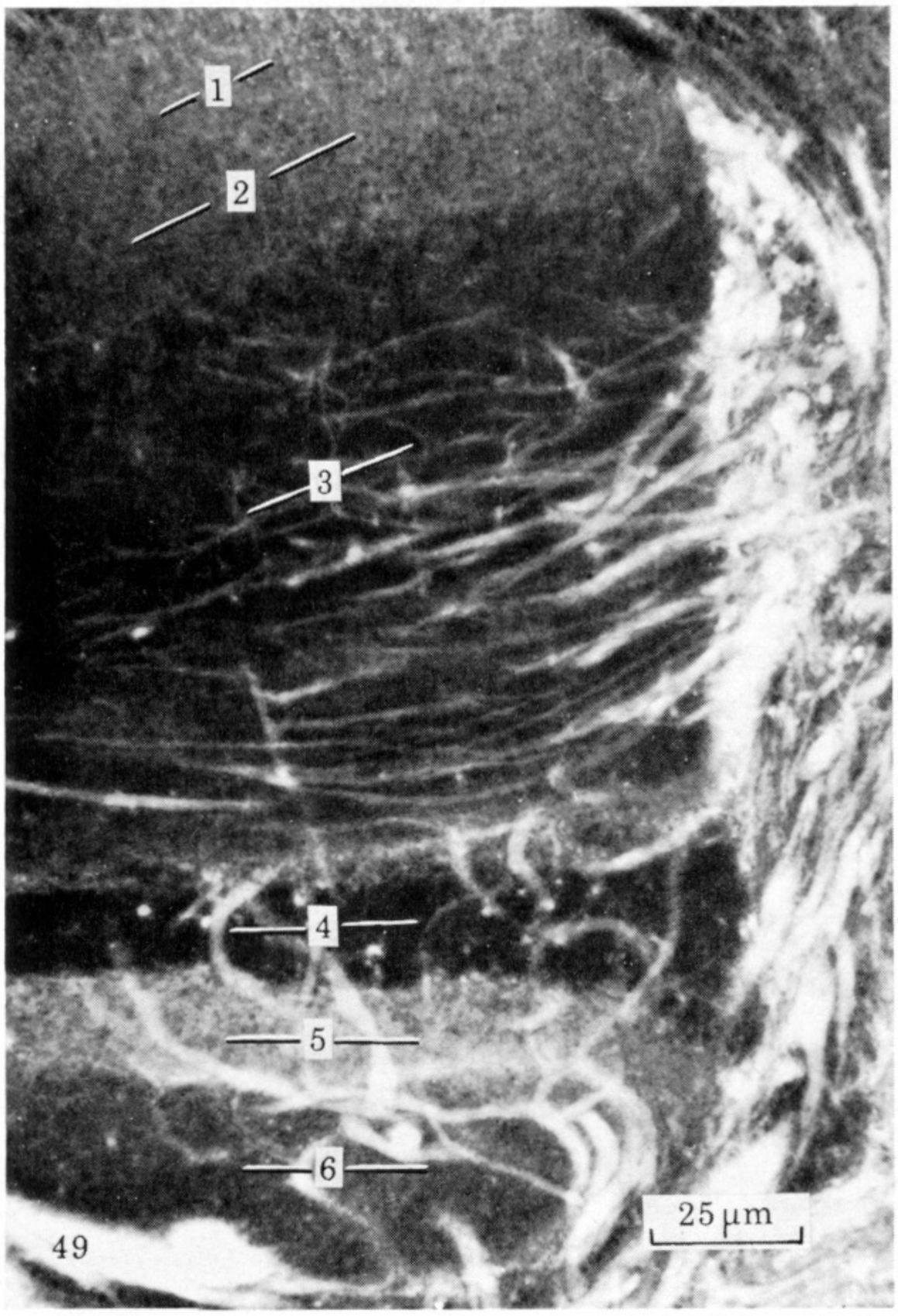

49

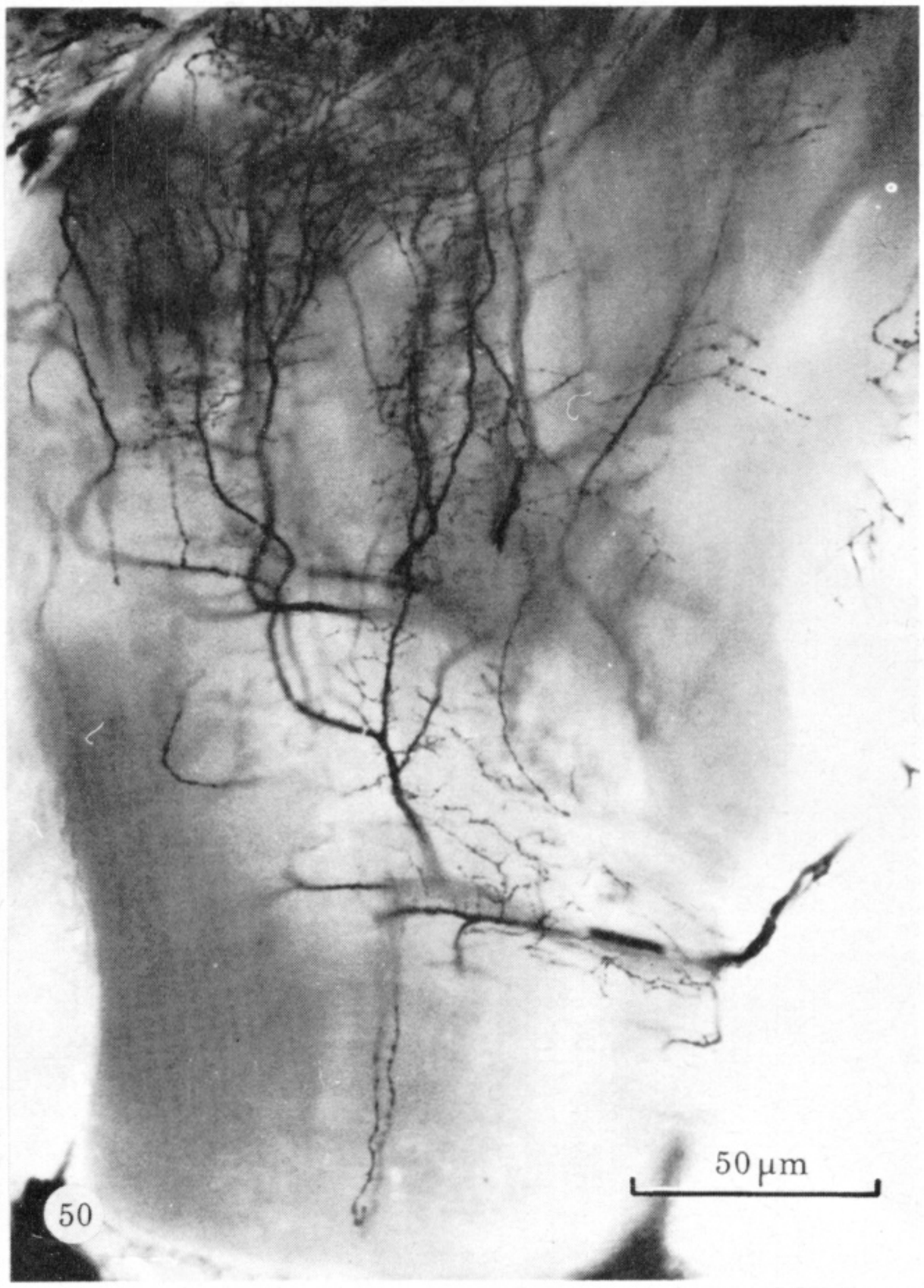

50

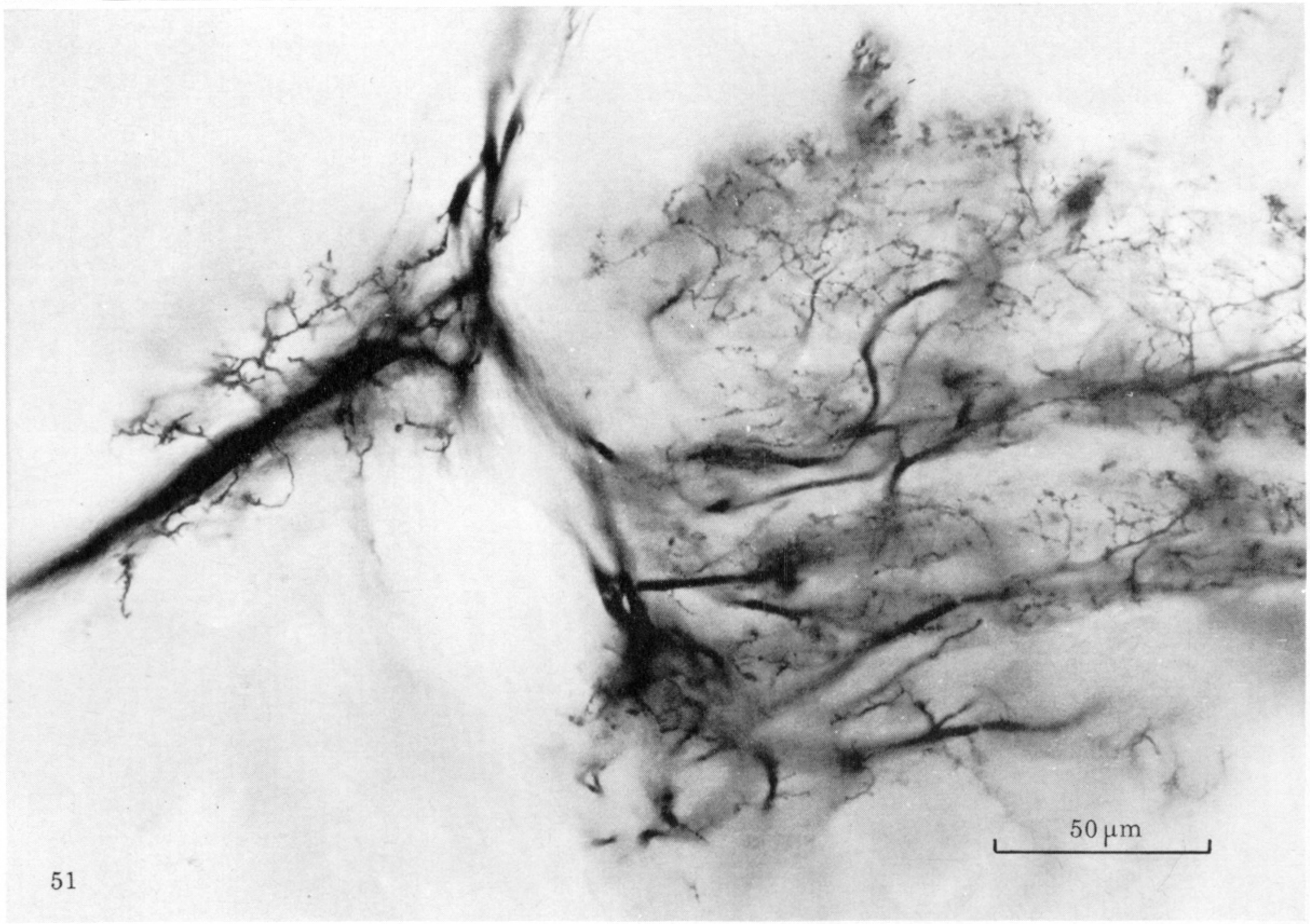

51

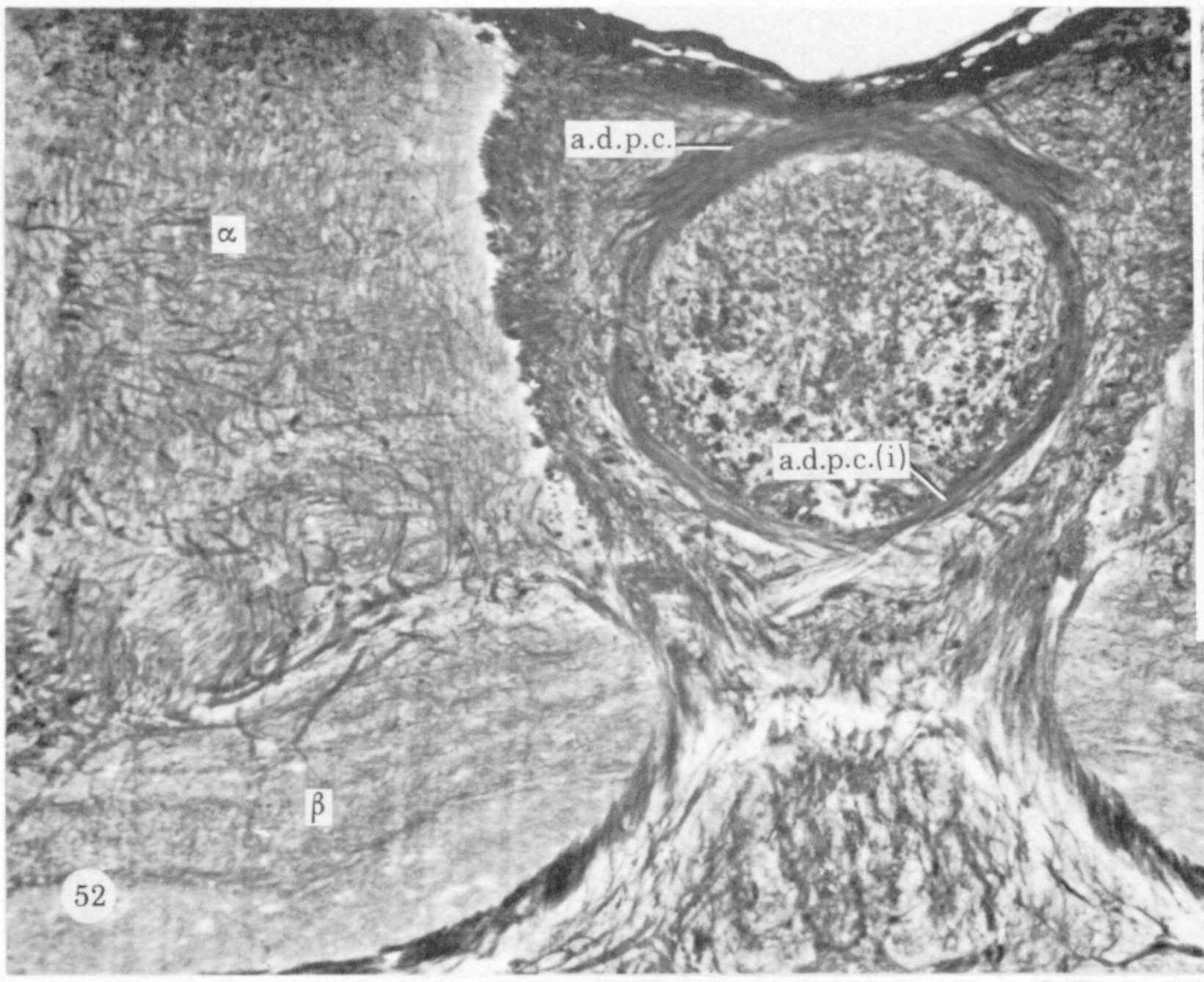
a.d.p.c.
α
a.d.p.c.(i)
β
52

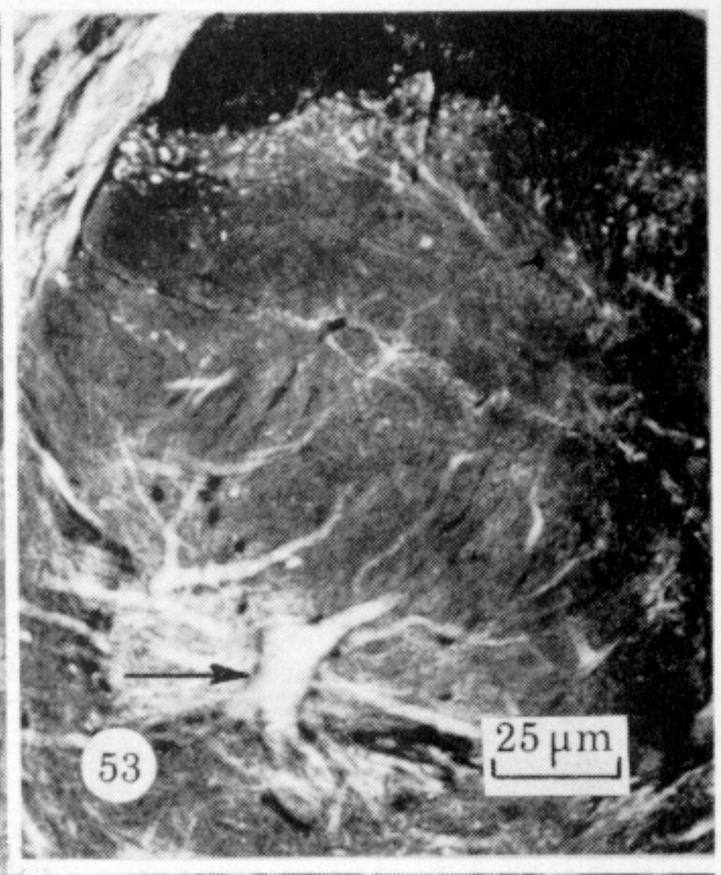
53
25 µm

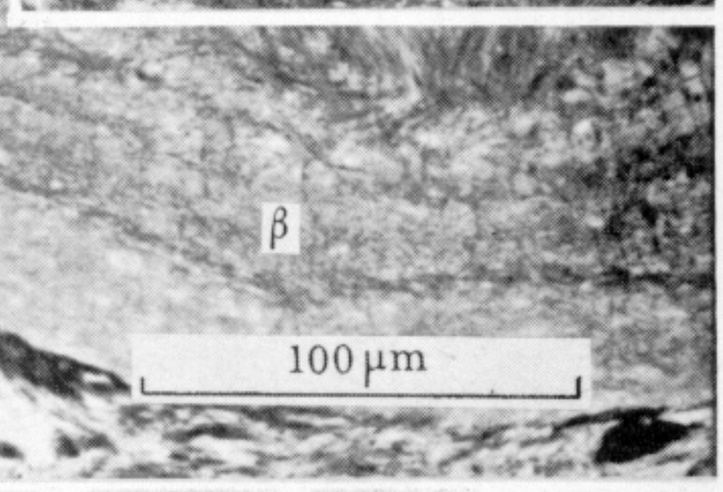
β
100 µm

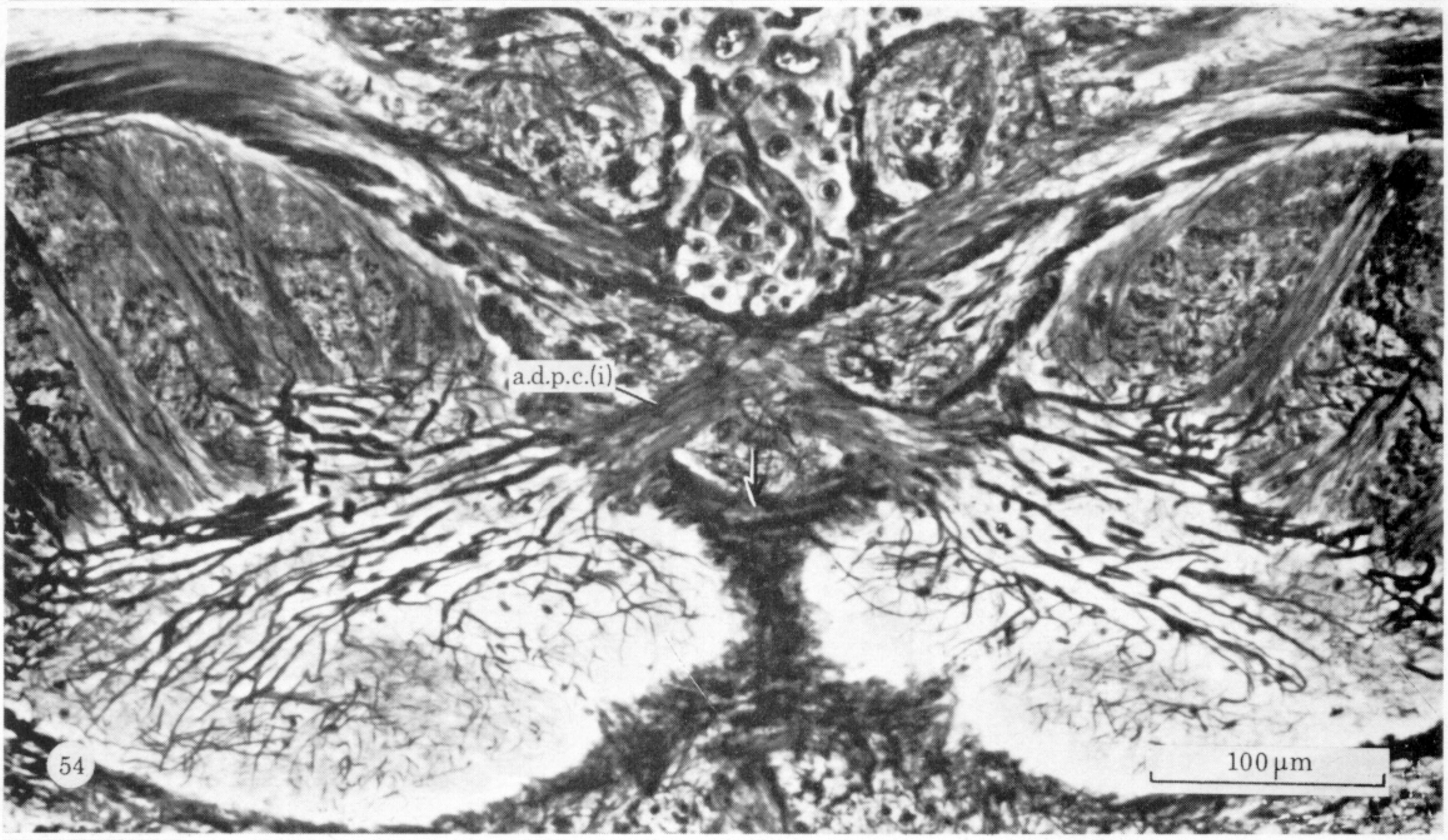
a.d.p.c.(i)
54
100 µm

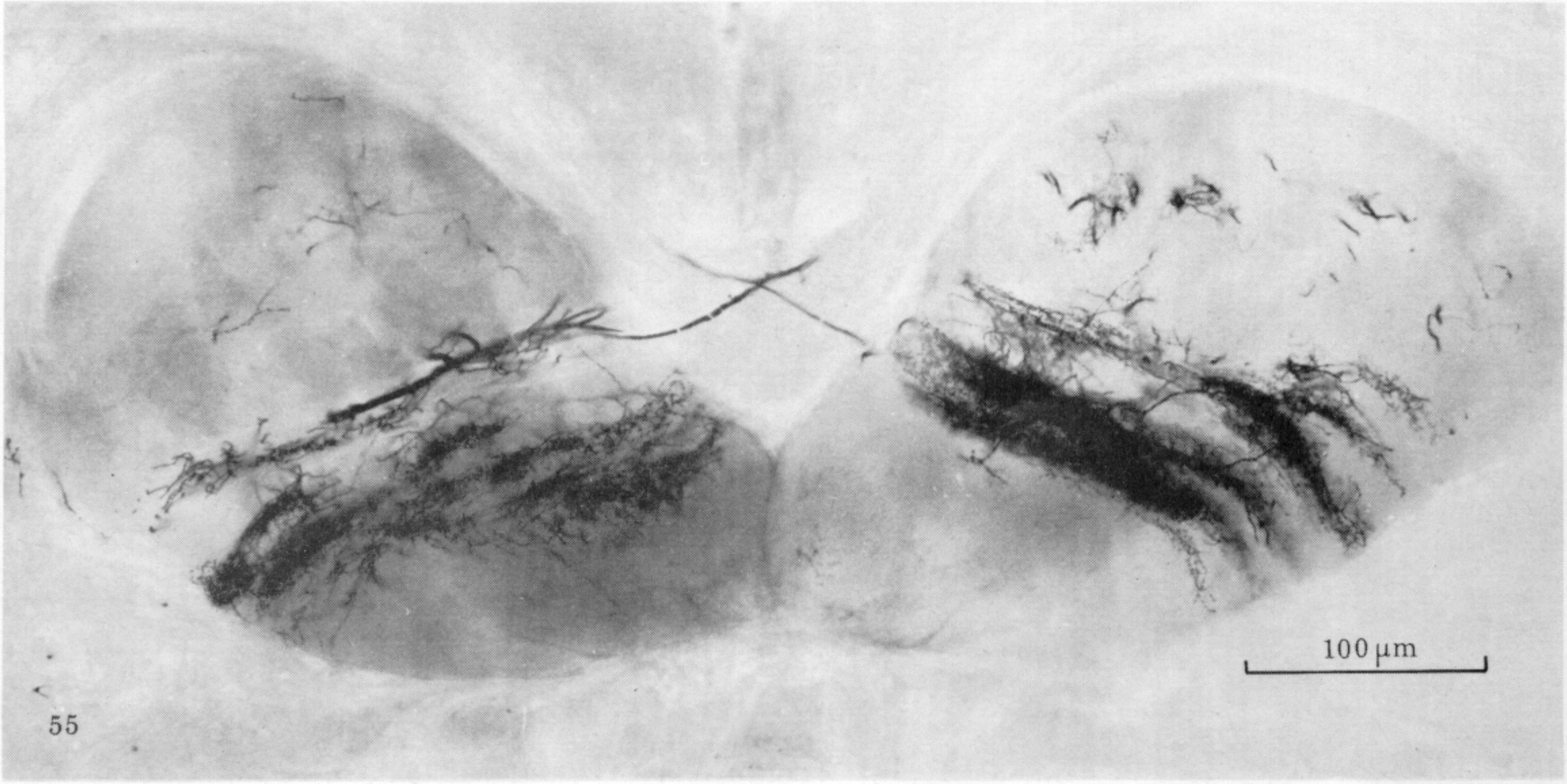
55
100 µm

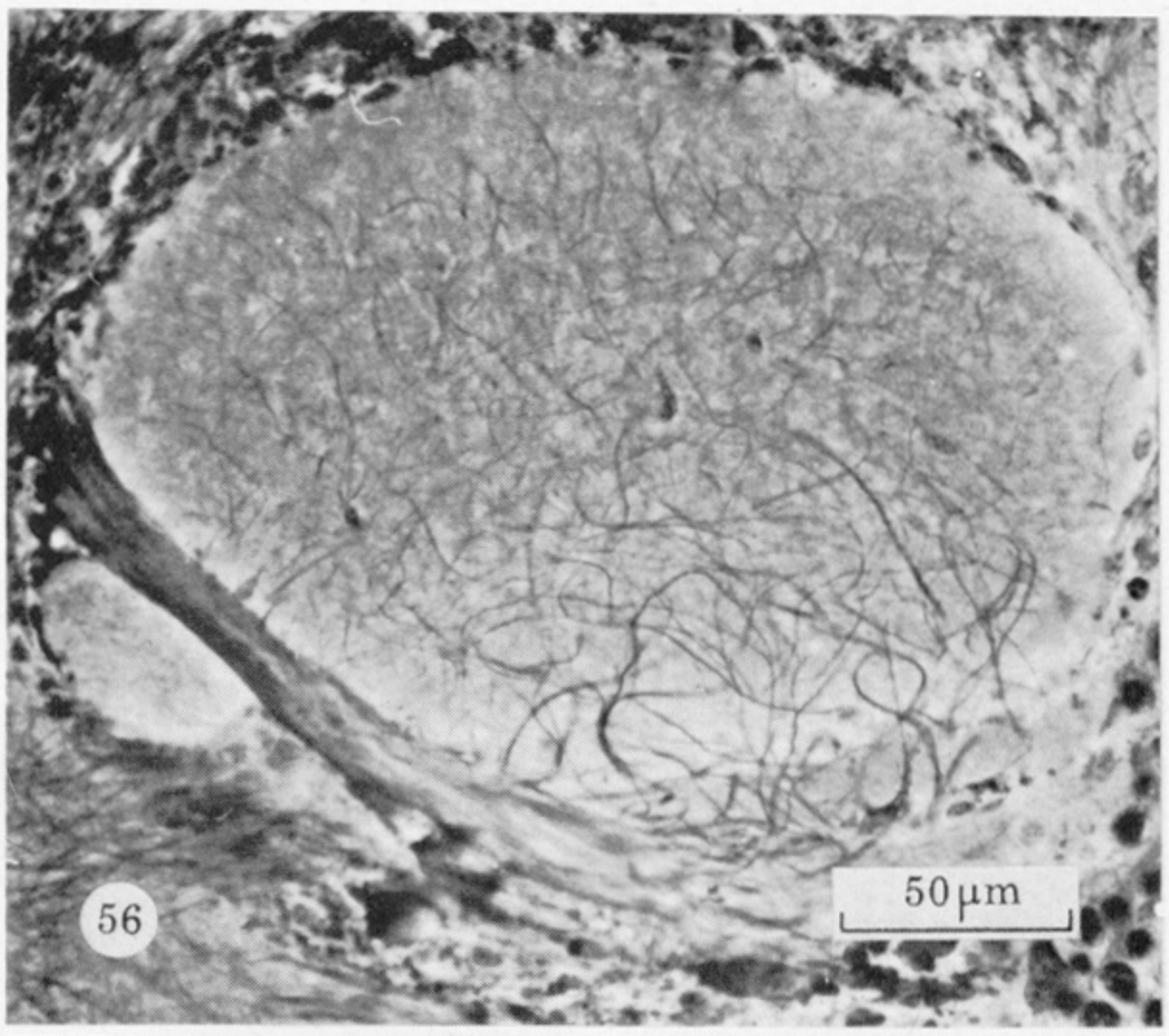
50 µm
56

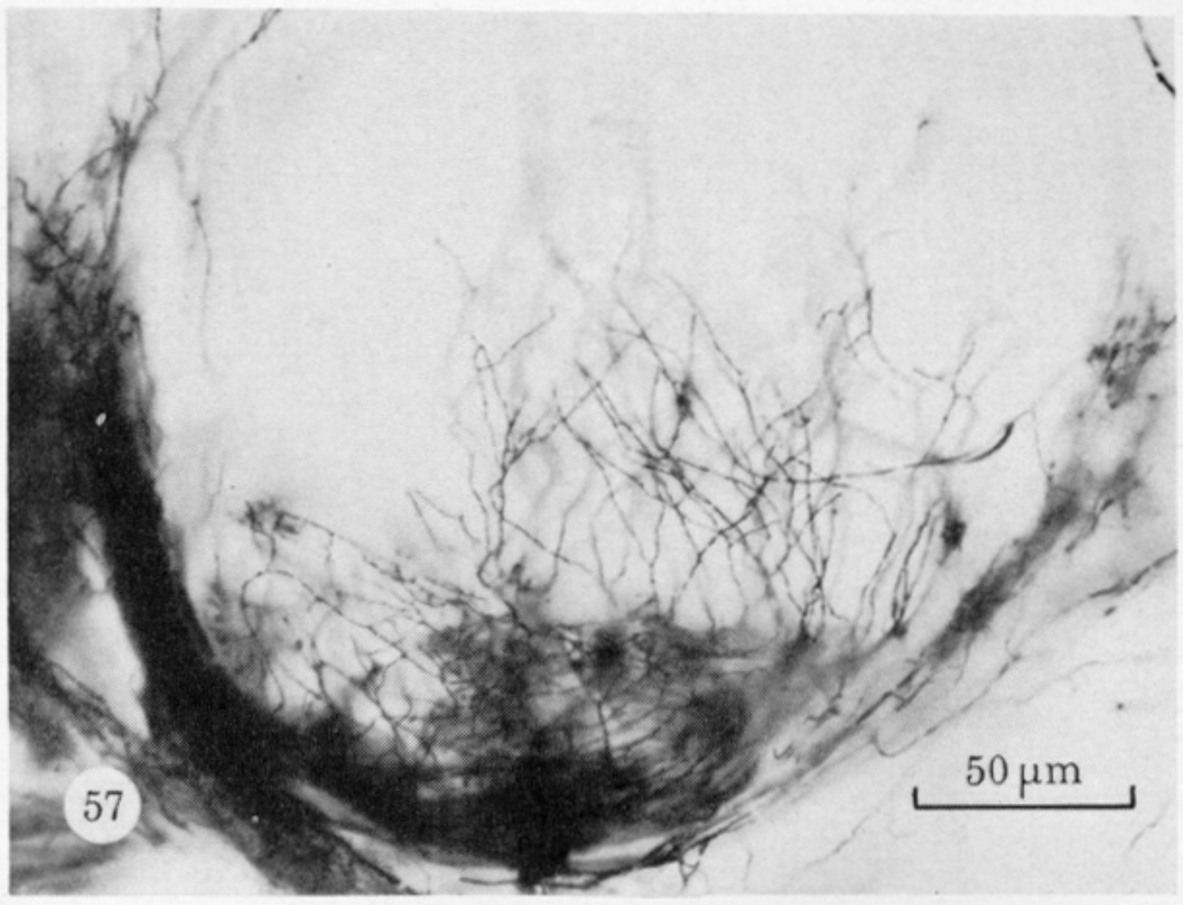
50 µm
57

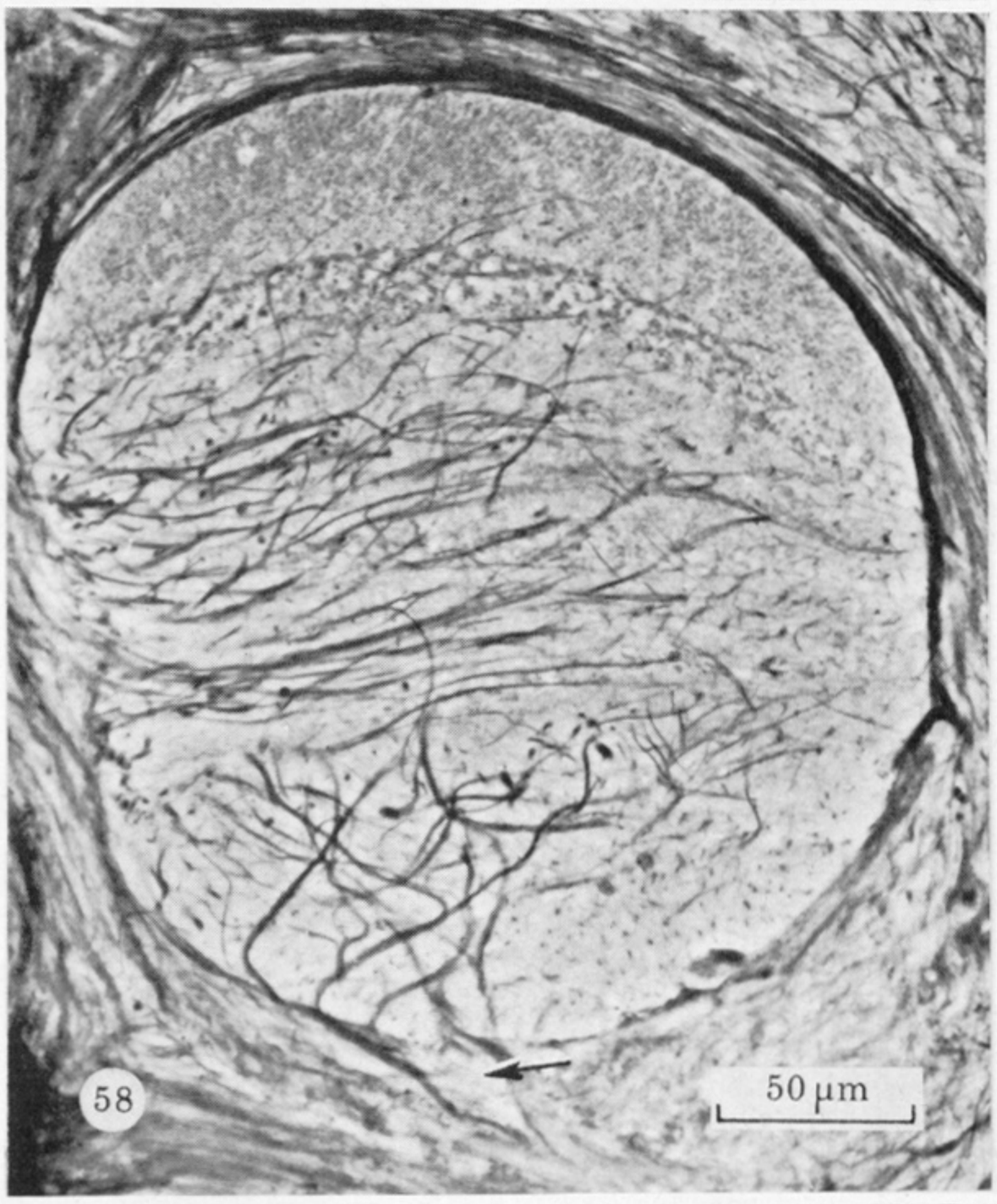
50 µm
58

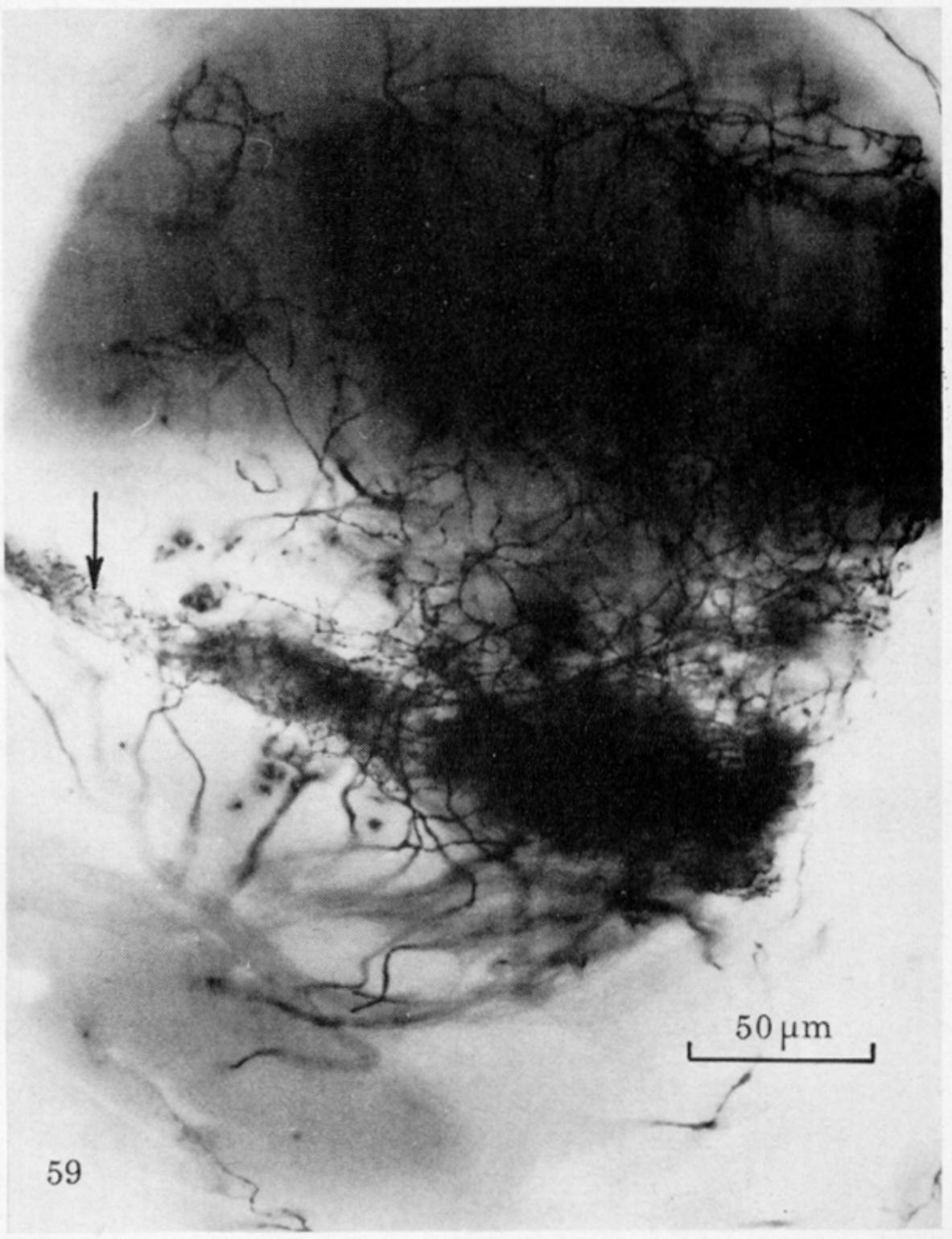
50 µm
59

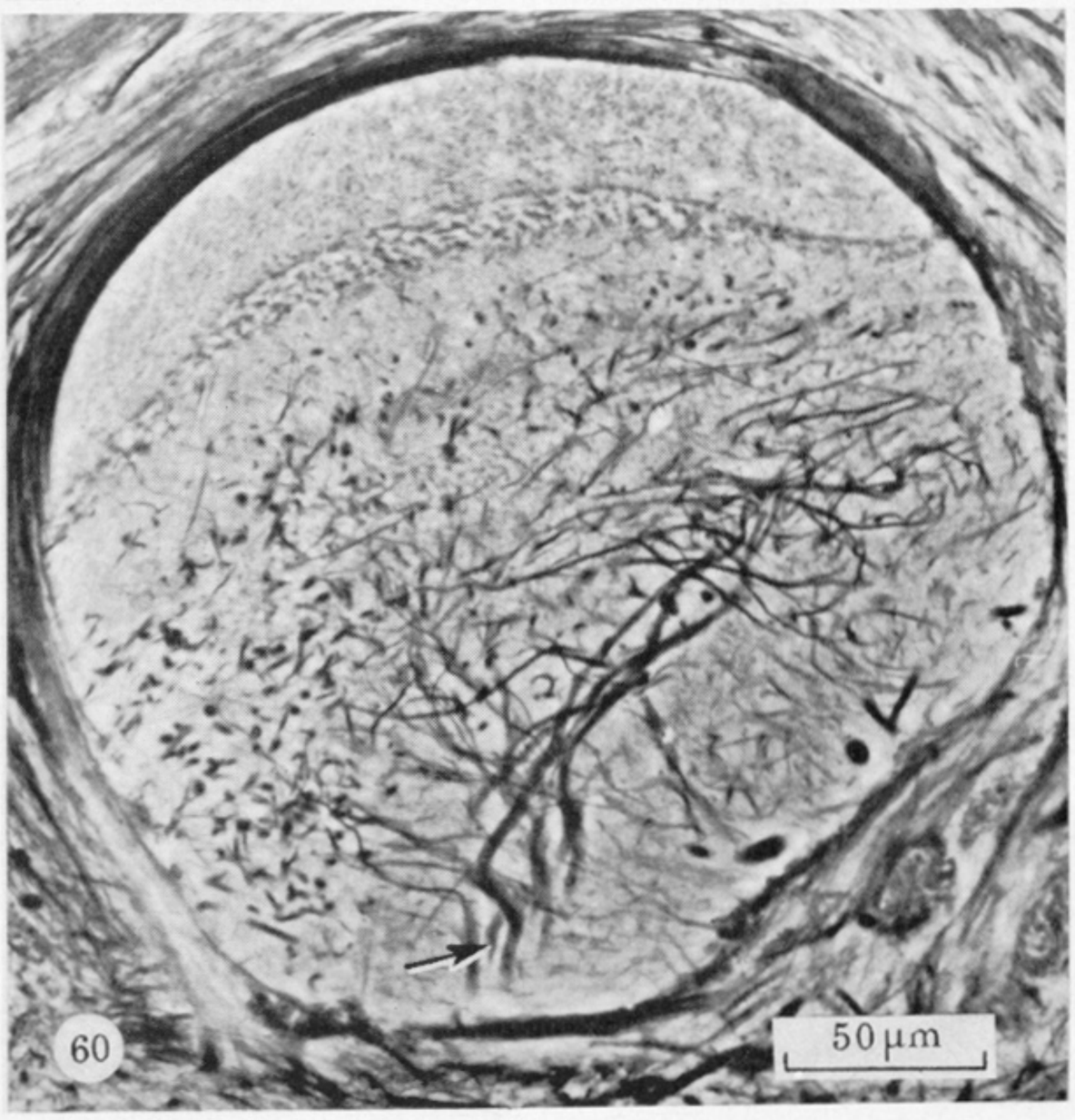
50 µm
60

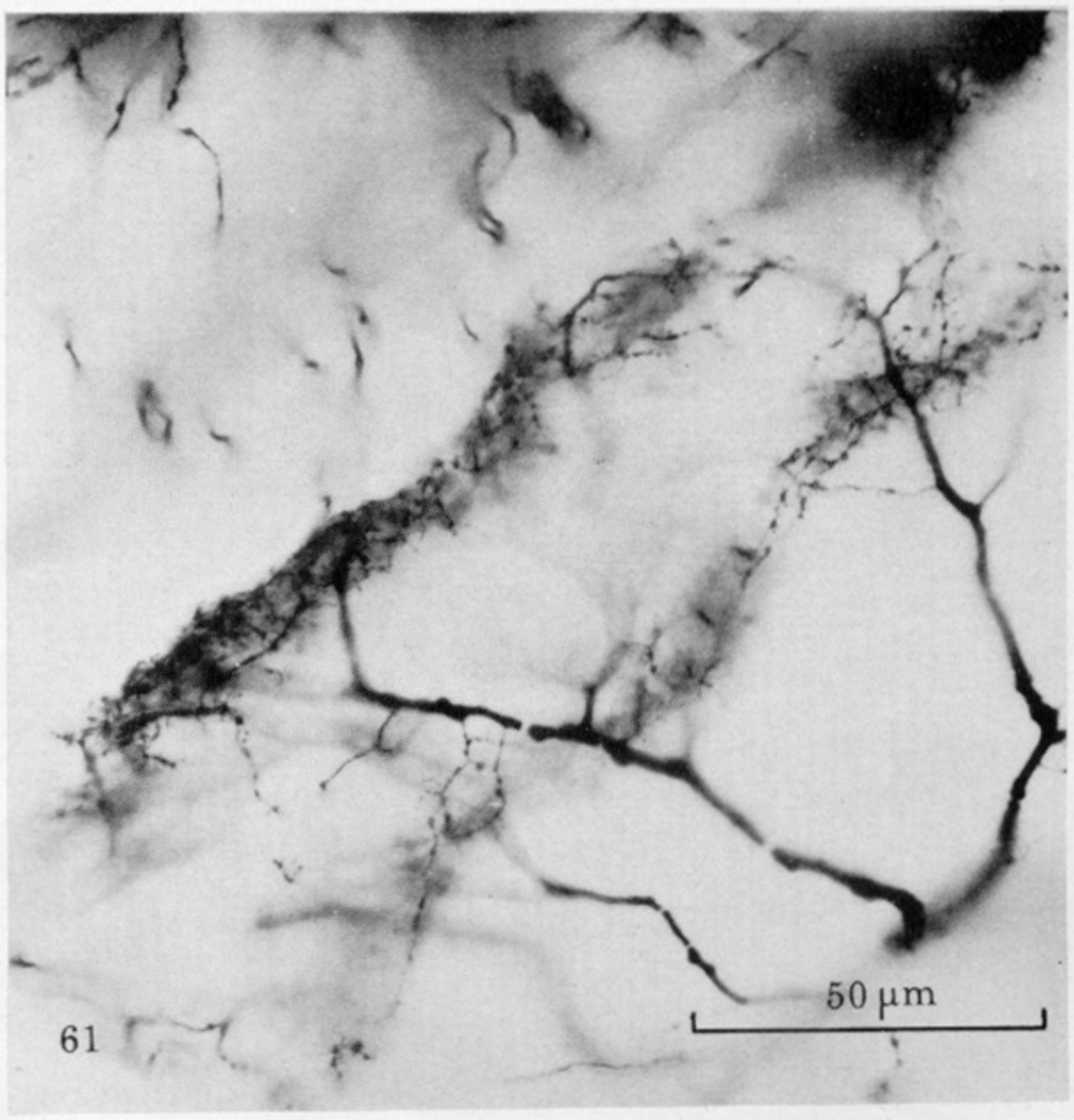
50 µm
61

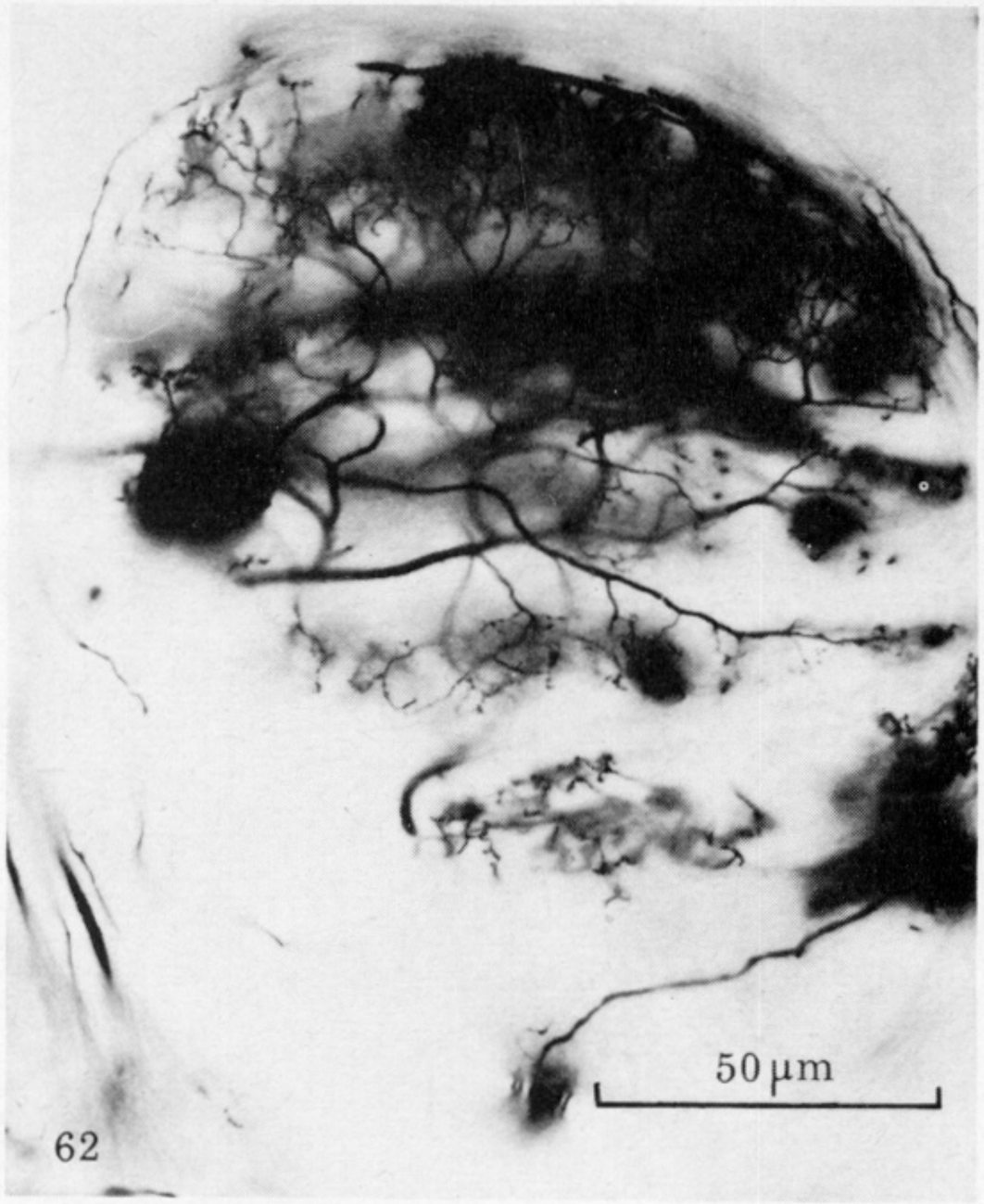

62

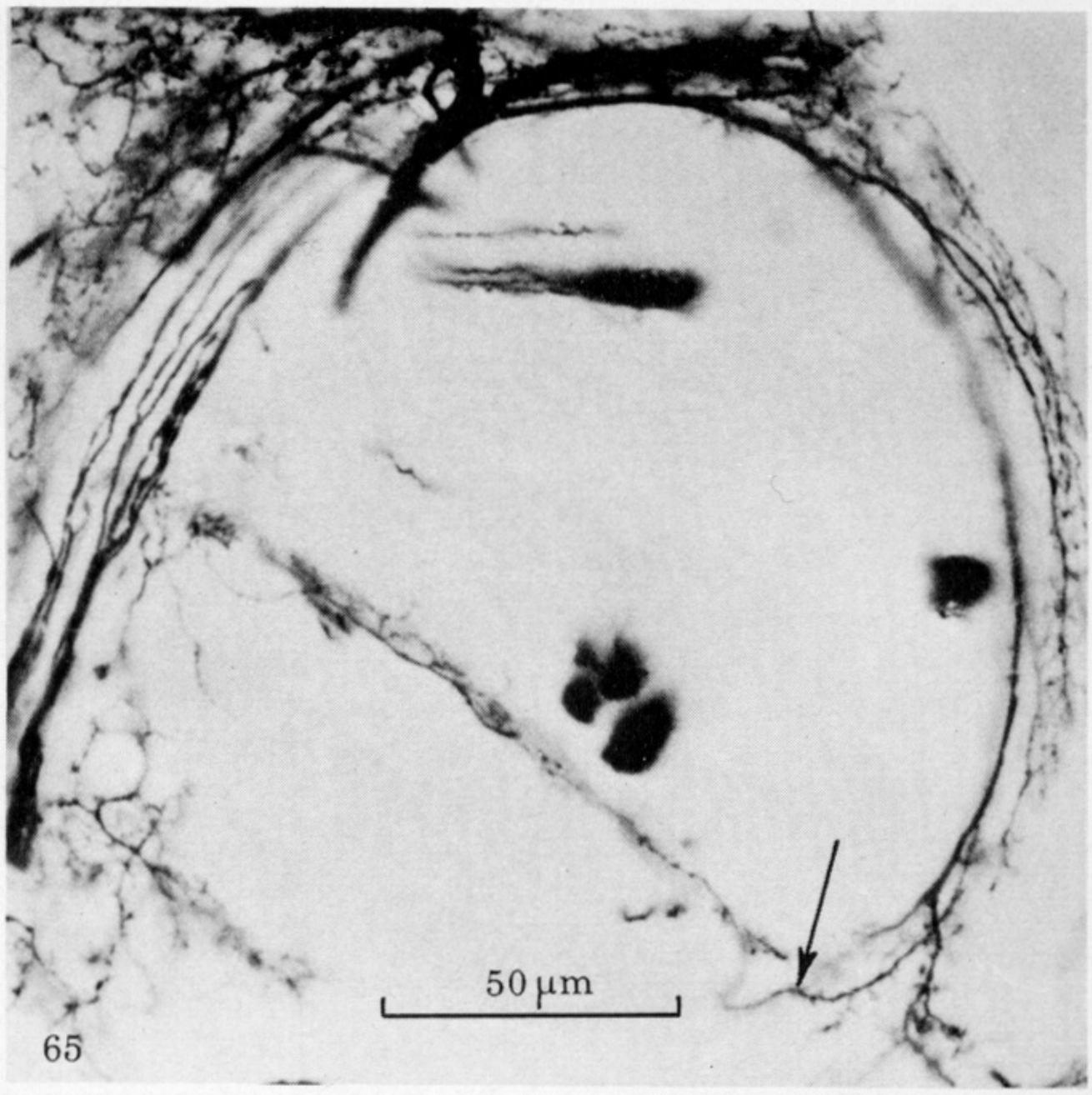

65

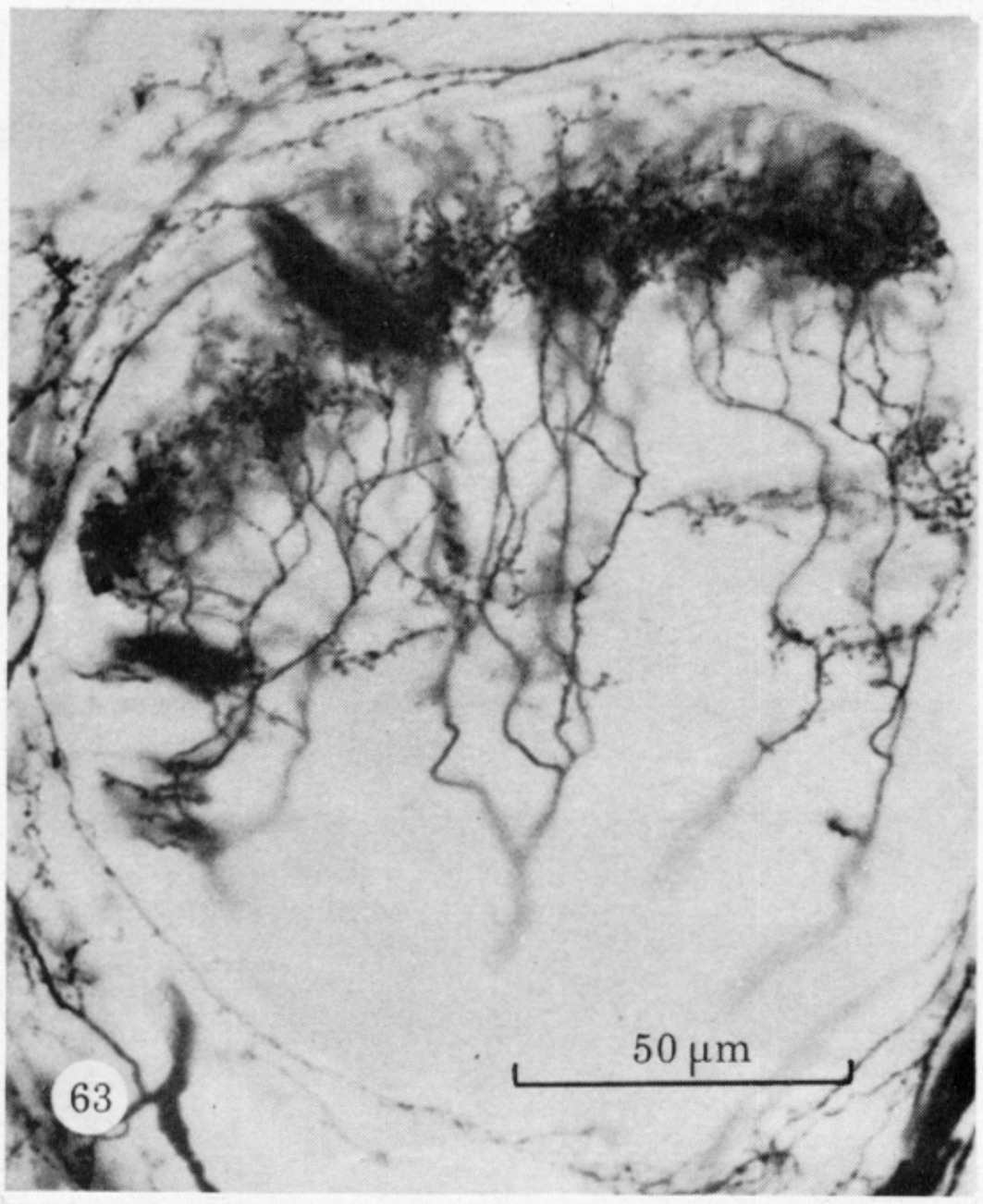

63

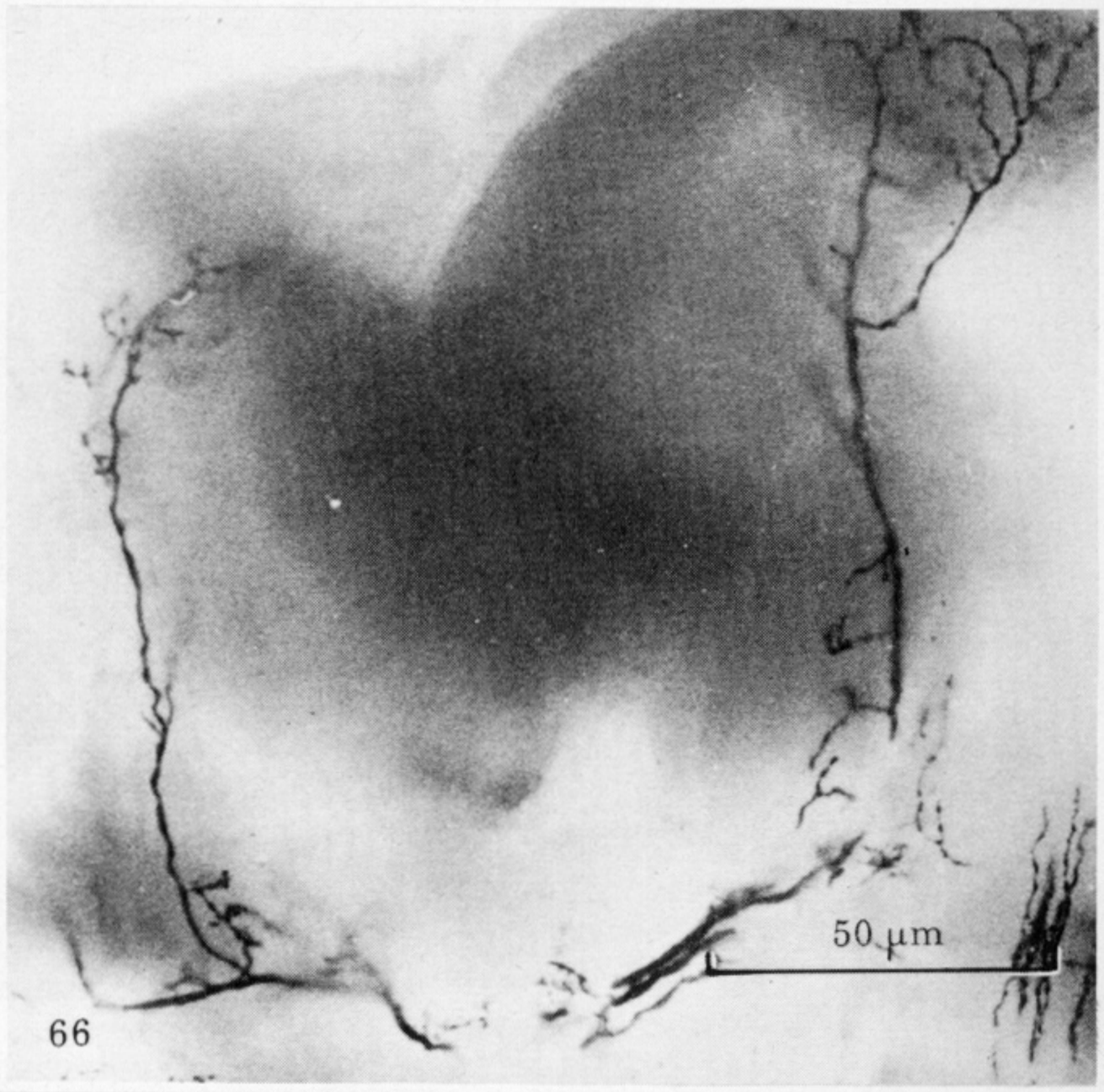

66

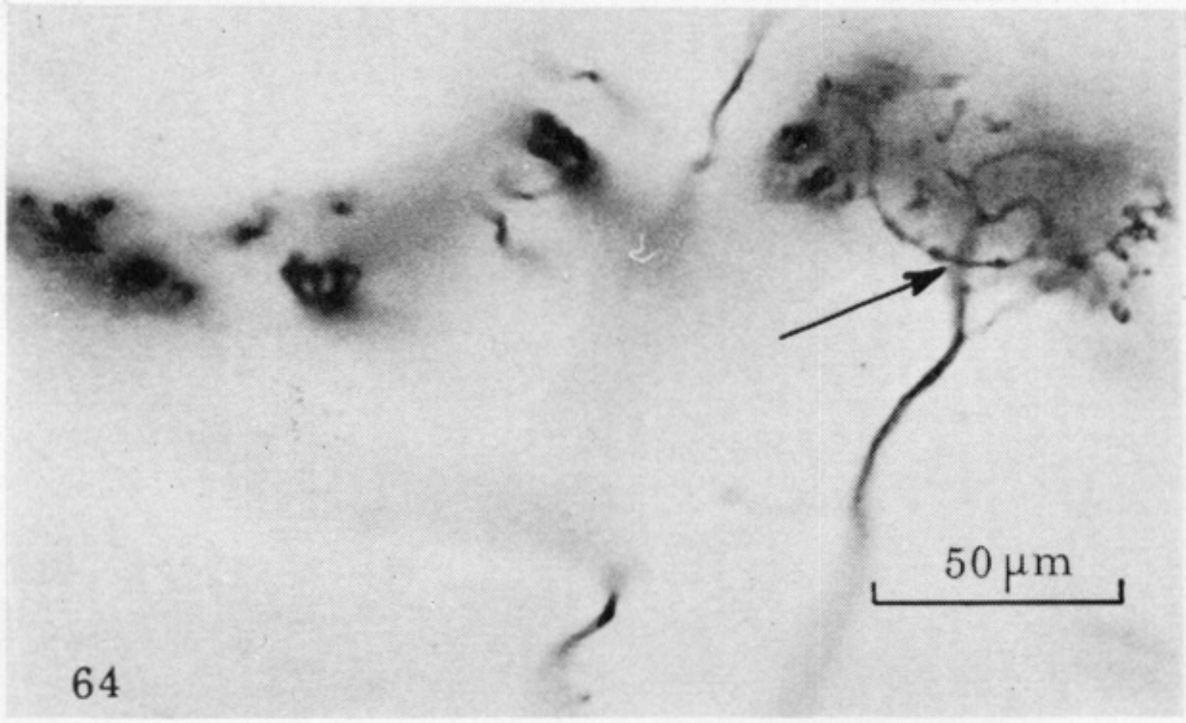

64

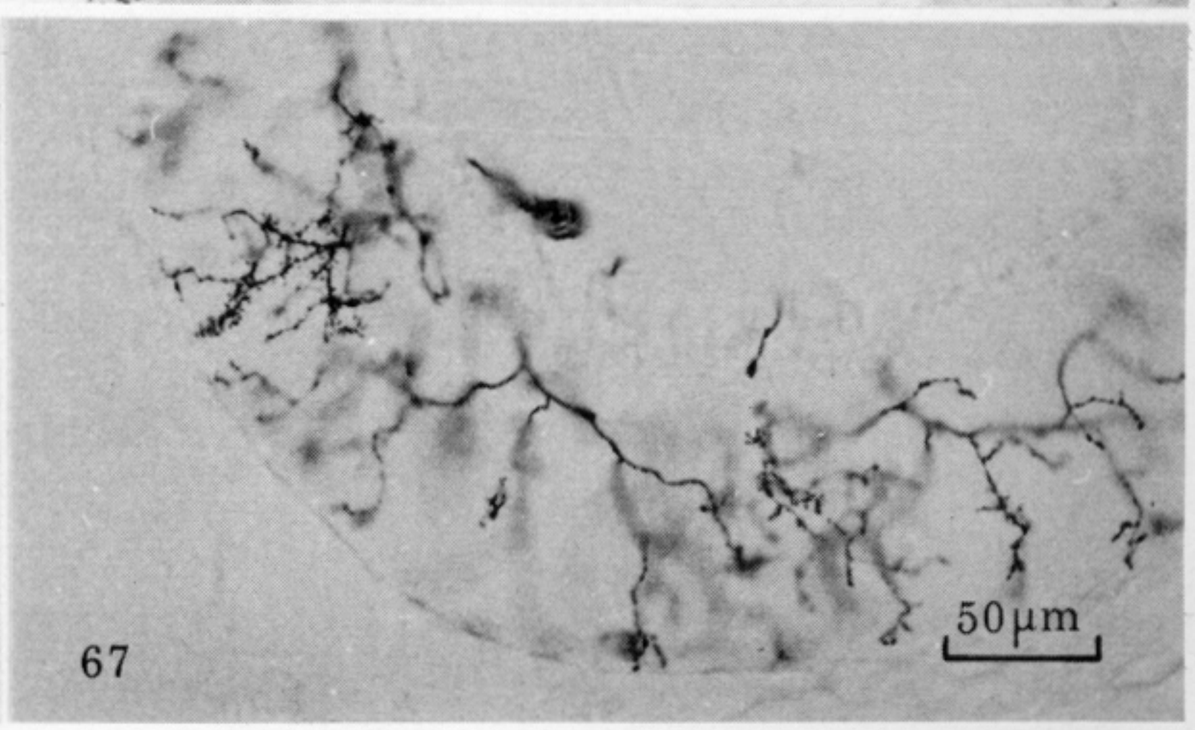

67

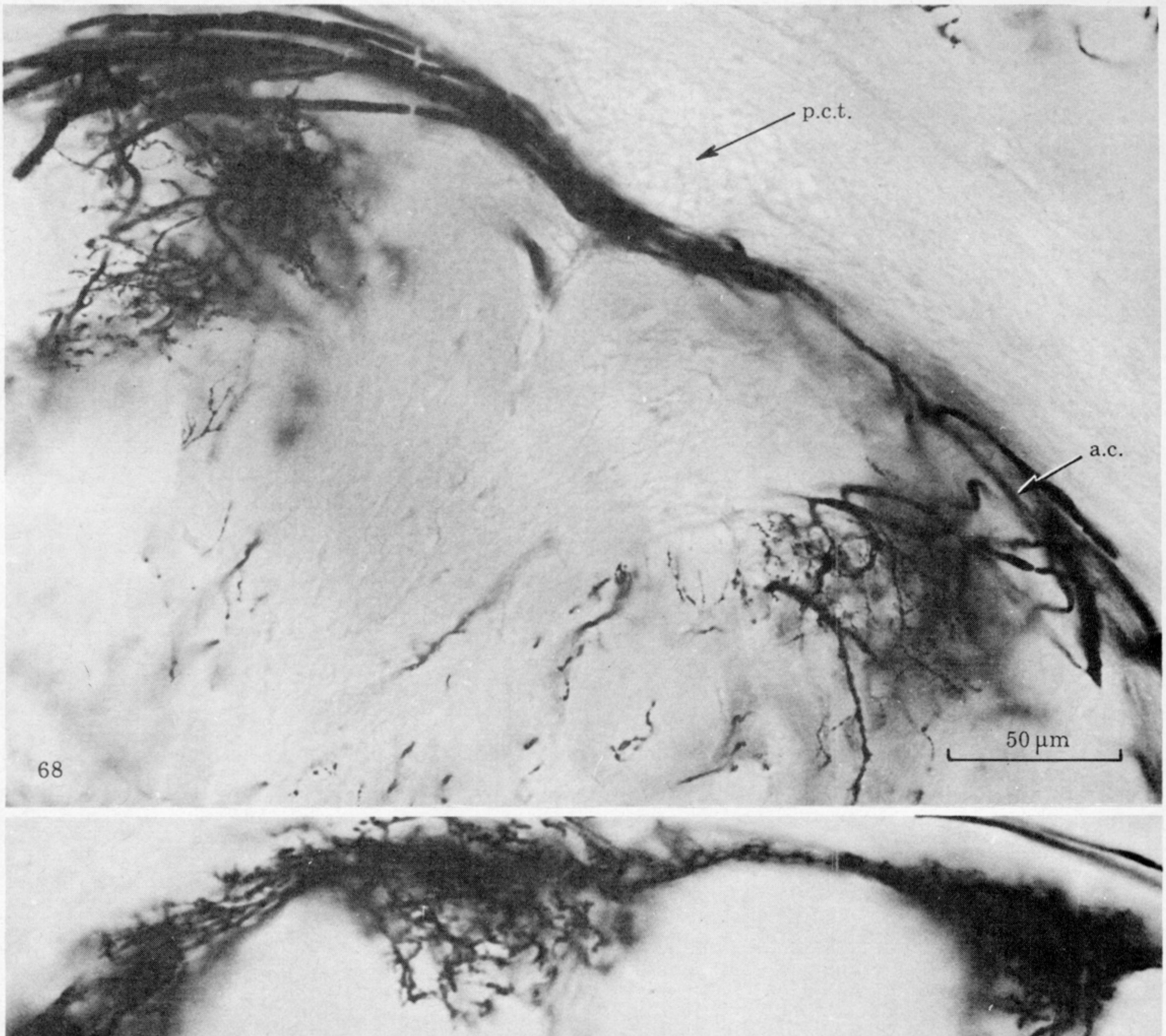

68

69

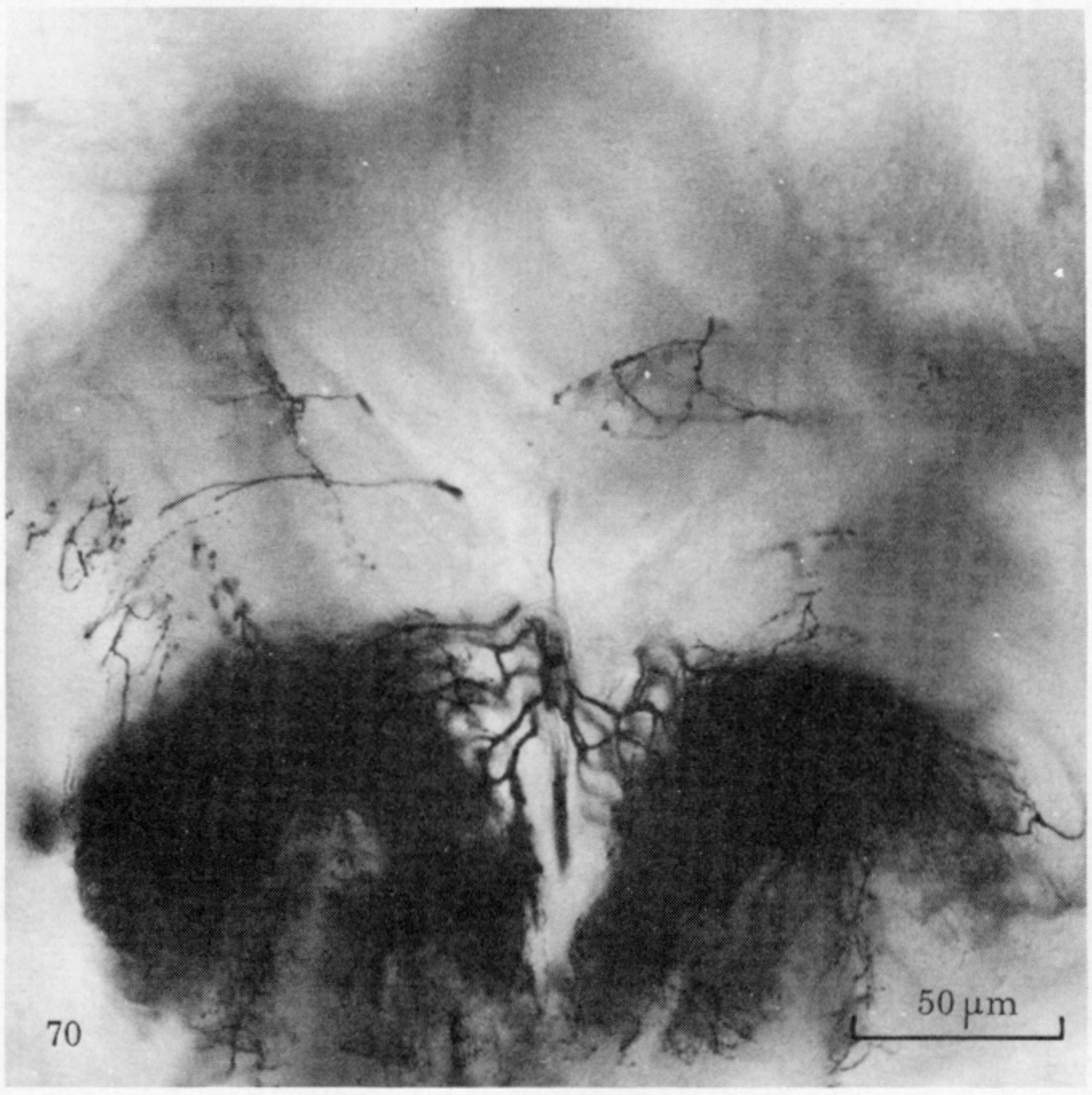

70

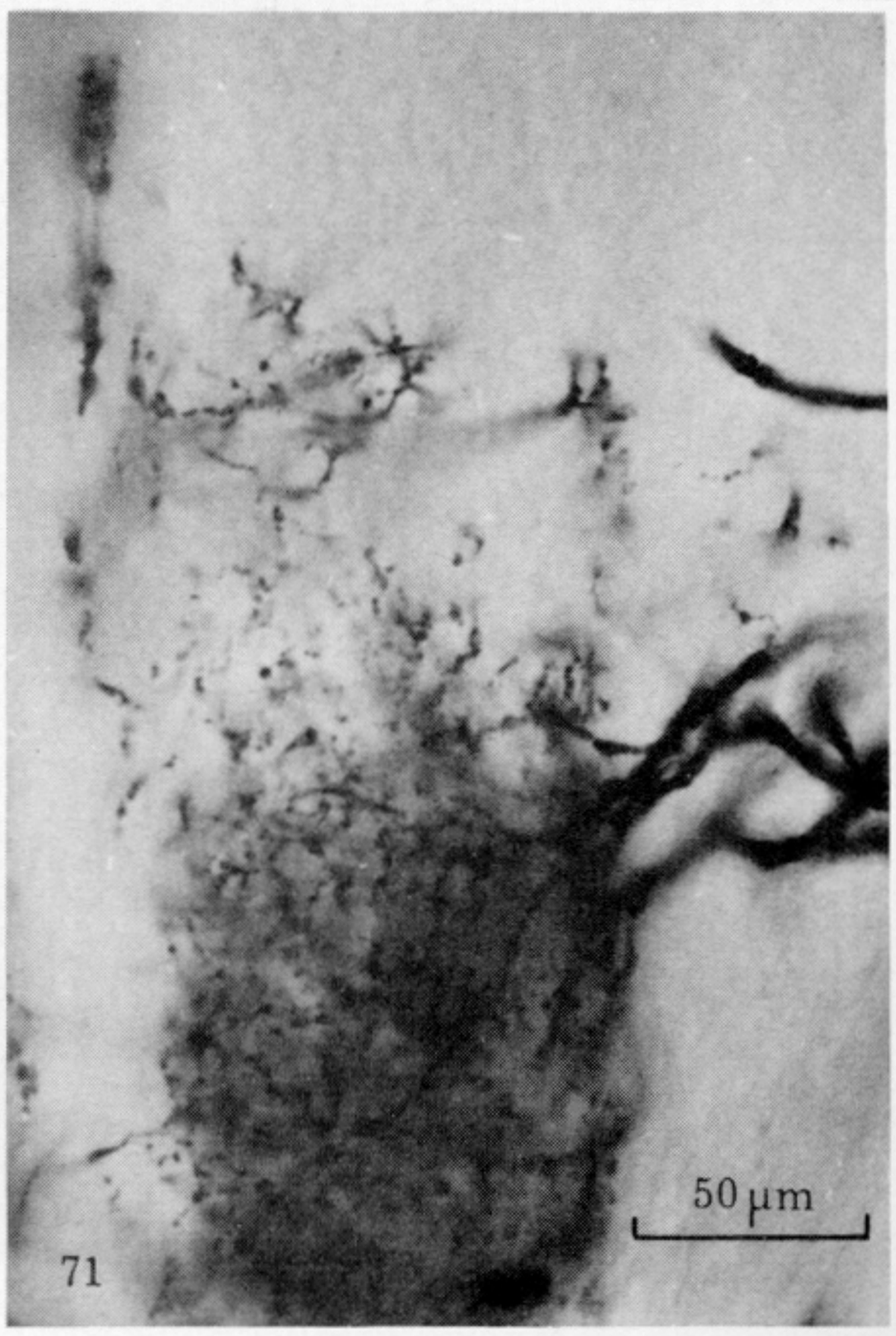

71